THOMAS TAURIS

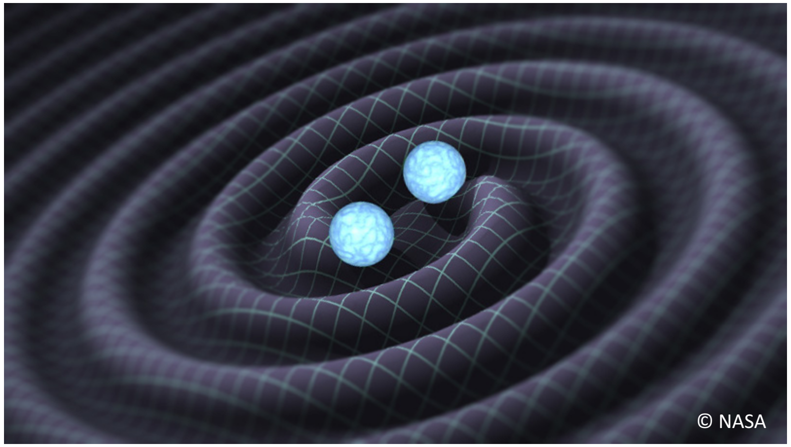

FORMATION AND PROPERTIES OF NEUTRON STAR MERGERS

October 10, 2019   YKIS2019 Kyoto Uni.

AARHUS UNIVERSITY

AARHUS INSTITUTE OF ADVANCED STUDIES

INSTITUT FOR FYSIK OG ASTRONOMI
IFA

INTRODUCTION: my early experience with Japanese culture

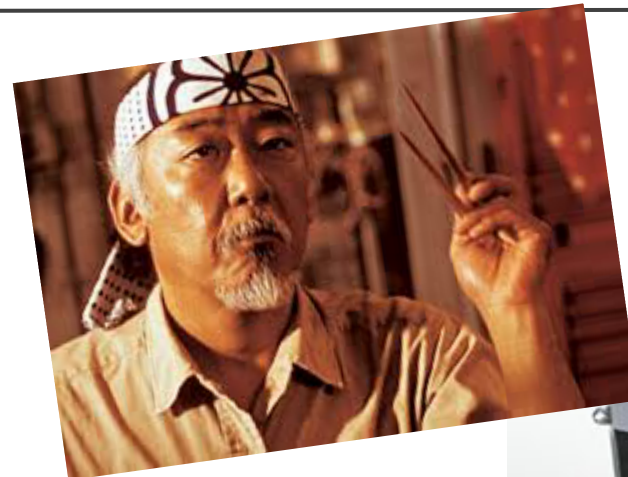

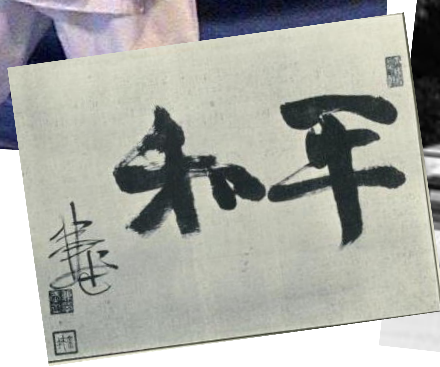

Neutron Stars and Black Holes

Unique **physics labs**.

- Densest matter in obs. Uni.
  (testing supranuclear matter)
- Strongest E/B-fields
  (testing plasma physics)
- Atomic clock precision
- Testing theories of gravity
  (unite quantum theory and gravity)
- Probes of stellar evolution
  and supernovae

Many **astrophysical phenomena** are related to **NSs** and **BHs** in **binaries**:
X-ray sources, radio pulsars, jets, Type Ib/c SNe, GRBs and **GWs and mergers**

Central questions:

How do these NS/BH binaries form ?

And how can we understand their properties (i.e. masses and spins) ?

What are the GW spectra for LISA ?

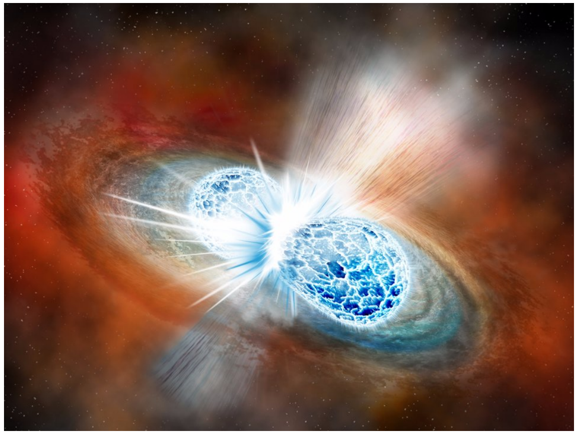

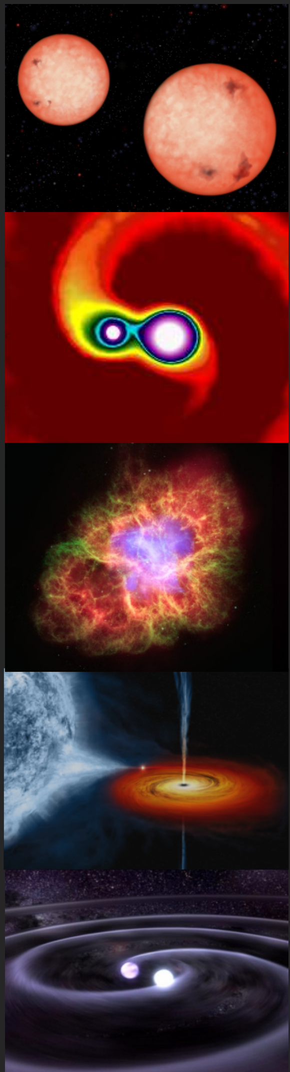

FORMATION AND PROPERTIES OF NS MERGERS

- **Resume of the formation of double NS mergers**
  - **Case BB X-ray binaries / Ultra-stripped SNe**
- **NS masses, spins and B-fields expected in GW sources**
  - **GW170817: properties and merger rates in local Universe**
- **Comments on population synthesis**
- **NS kicks (2nd SN)**
- **LISA GW sources: mass transfer from a white dwarf to a NS**

a personal bias

Tauris et al. (2017), ApJ, 846, 170

Kruckow, Tauris et al. (2018), MNRAS 481, 1908

Tauris (2018), Phys. Rev. Lett. 121, 131105

Sengar, Tauris et al. (2017), MNRAS Letters 470, L6

Tauris & Janka (2019), ApJL, submitted

Great science developments

- Chaty: NS kicks in HMXBs from combining X-ray obs. with GAIA
- Garcia: Modelling low-mass BBHs GW151226 and GW170608
- Chruslinska: Metallicity distribution throughout the Uni.
- Klencki: Donor envelope structure and formation of BH mergers
- Laplace: Residual envelopes after RLO/CE evolution
- Tanikawa: Evolution of massive, extreme metal poor stars

Other people working on double NS formation since 1970's:

van den Heuvel, Bisnovatyi-Kogan, Kalogera, Dewi, Pols, Podsiadlowski, Belczynski, Ivanova, Voss, Piran, Mapelli, Mandel, Vigna-Gomez, Giacobbo, Chruslinska,….

Tauris et al. (2017), ApJ

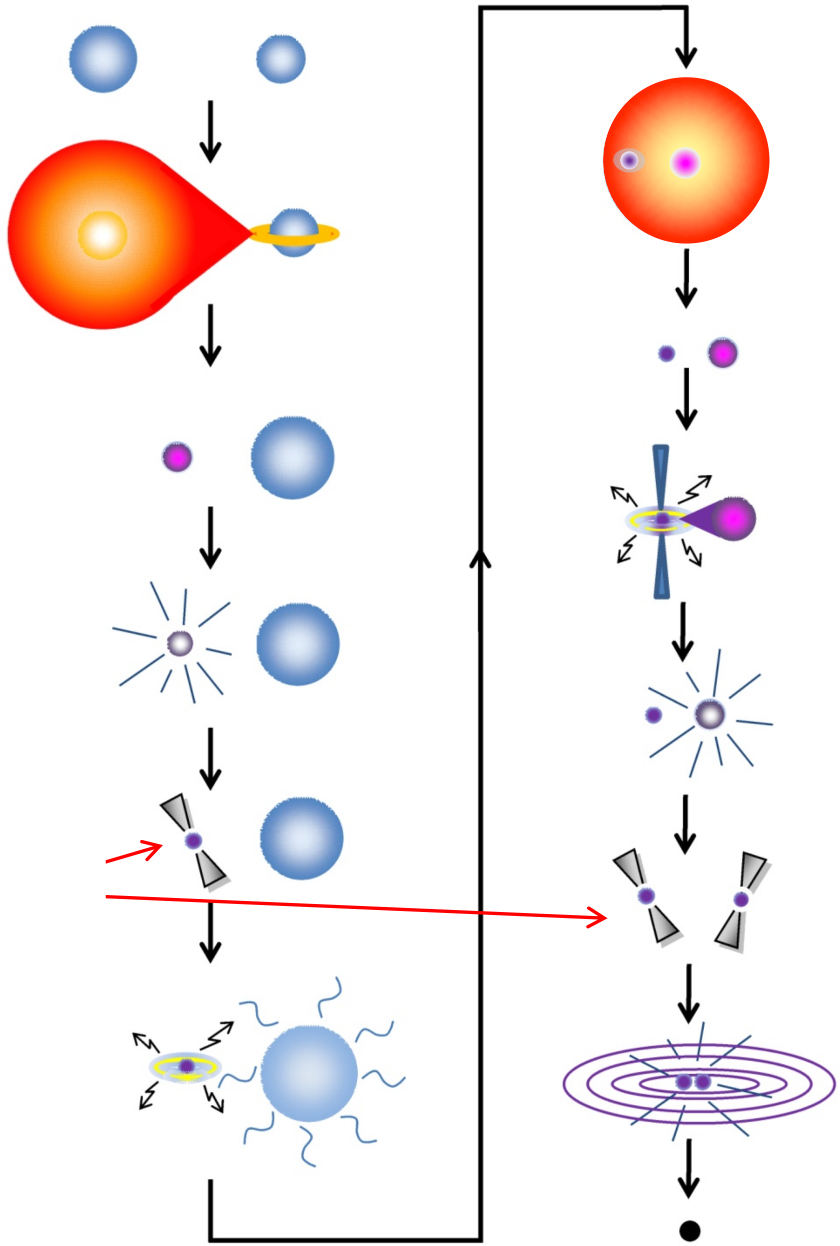

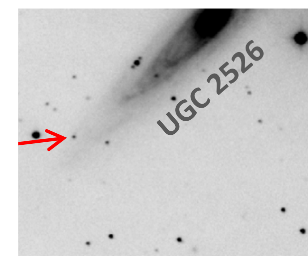

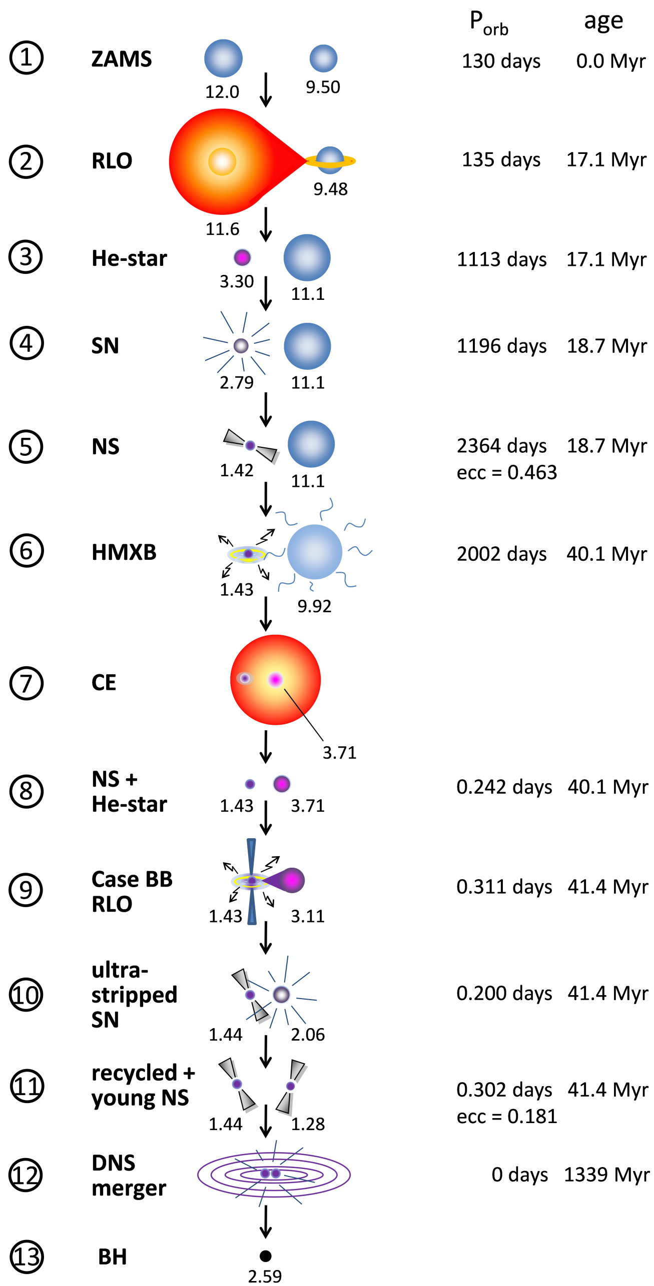

van den Heuvel & Tauris (2020)
Physics of Binary Star Evolution
Princeton University Press

Tauris et al. (2017), ApJ

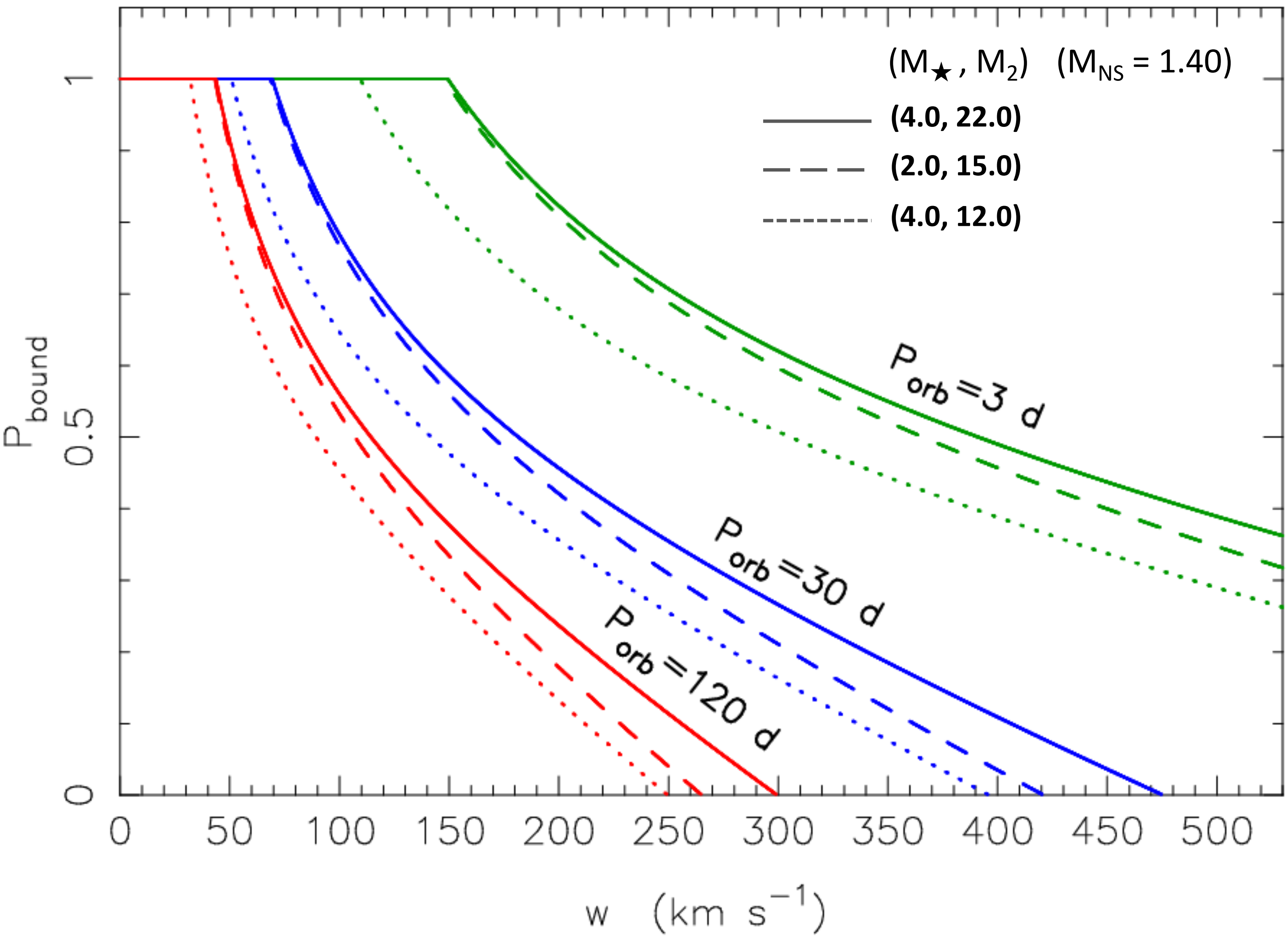

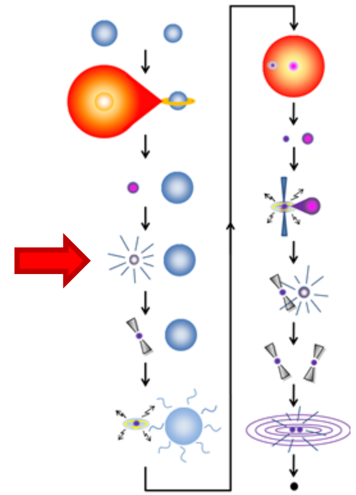

$$\frac{X_+}{A} = -\cos\beta\left[\xi\sin\gamma + (\xi-1)\sqrt{\frac{\xi}{\xi-2}}\right] \quad (38)$$

$$\frac{Y_+}{A} = \xi\cos^2\gamma - 1 - \sin\gamma\sqrt{\frac{\xi}{\xi-2}} \quad (39)$$

$$\frac{Z_+}{A} = -\sin\beta\sin\lambda\left[\xi\sin\gamma + (\xi-1)\sqrt{\frac{\xi}{\xi-2}}\right] \quad (40)$$

where we have used $u_\infty = A\,e^2$ and $u_0 = u_\infty\sqrt{\xi/(\xi-2)}$.

We now proceed to express β, γ and λ in the true input angles ϑ and φ. We cannot reach $\sin\lambda$ directly, but that doesn't matter, from Fig. 1 (bottom) we have: $u_0\sin\beta\sin\lambda = w\sin\vartheta\sin\varphi$. Intermediate results are:

$$X_+ = \frac{v + w\cos\vartheta}{1 - \xi + \sqrt{\xi(\xi-2)}\sin\gamma} \quad (41)$$

$$Y_+ = \frac{\sqrt{\xi(\xi-2)}}{1+\xi(\xi-2)\cos^2\gamma} \times \left[u_0\left(1-\frac{1}{\xi}\right) - \frac{1}{u_0}(w\sin\vartheta\cos\varphi - v_{\rm im})^2\right] - \frac{(w\sin\vartheta\cos\varphi - v_{\rm im})}{1+\xi(\xi-2)\cos^2\gamma} \quad (42)$$

$$P \equiv 1 - 2\tilde{m} + \frac{w^2}{v^2} + \frac{v_{\rm im}^2}{v^2} + 2\frac{w}{v^2}(v\cos\vartheta - v_{\rm im}\sin\vartheta\cos\varphi) \quad (44)$$

$$Q \equiv 1 + \frac{P}{\tilde{m}} - \frac{(w\sin\vartheta\cos\varphi - v_{\rm im})^2}{\tilde{m}v^2} \quad (45)$$

$$R \equiv \left(\frac{\sqrt{P}}{\tilde{m}v}(w\sin\vartheta\cos\varphi - v_{\rm im}) - \frac{P}{\tilde{m}} - 1\right)\frac{1+m_{\rm 2f}}{m_{\rm 2f}} \quad (46)$$

Inserting Eqs. (48)–(50) into Eqs. (12) and (13) gives the final velocities of the stellar components in the original reference frame.

We find for the neutron star:

$$v_{\rm NS,x} = w\cos\vartheta\left(\frac{1}{R}+1\right) + \left(\frac{1}{R} + \frac{m_2}{1+m_{\rm shell}+m_2}\right)v \quad (51)$$

$$v_{\rm NS,y} = w\sin\vartheta\cos\varphi\left(1-\frac{1}{S}\right) + \frac{1}{S}v_{\rm im} + \frac{Q\sqrt{P}}{S}v \quad (52)$$

$$v_{\rm NS,z} = w\sin\vartheta\sin\varphi\left(\frac{1}{R}+1\right) \quad (53)$$

and for the companion star:

$$v_{2x} = \frac{-w\cos\vartheta}{m_{\rm 2f}R} - \left(\frac{1}{m_{\rm 2f}R} + \frac{1+m_{\rm shell}}{1+m_{\rm shell}+m_2}\right)v \quad (54)$$

$$v_{2y} = \frac{w\sin\vartheta\cos\varphi}{m_{\rm 2f}S} + \left(1-\frac{1}{m_{\rm 2f}S}\right)v_{\rm im} - \frac{Q\sqrt{P}}{m_{\rm 2f}S}v \quad (55)$$

$$v_{2z} = \frac{-w\sin\vartheta\sin\varphi}{m_{\rm 2f}R} \quad (56)$$

Tauris & Takens (1998), A&A

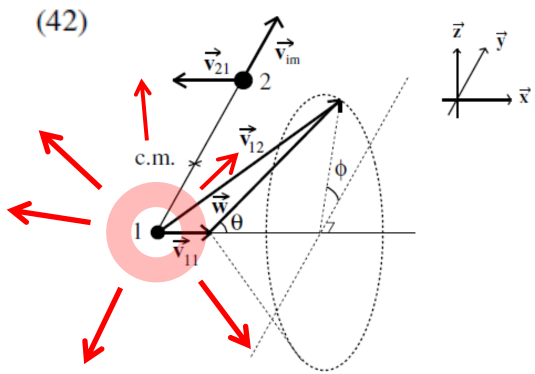

Liu, Tauris, Röpke et al. (2015), A&A

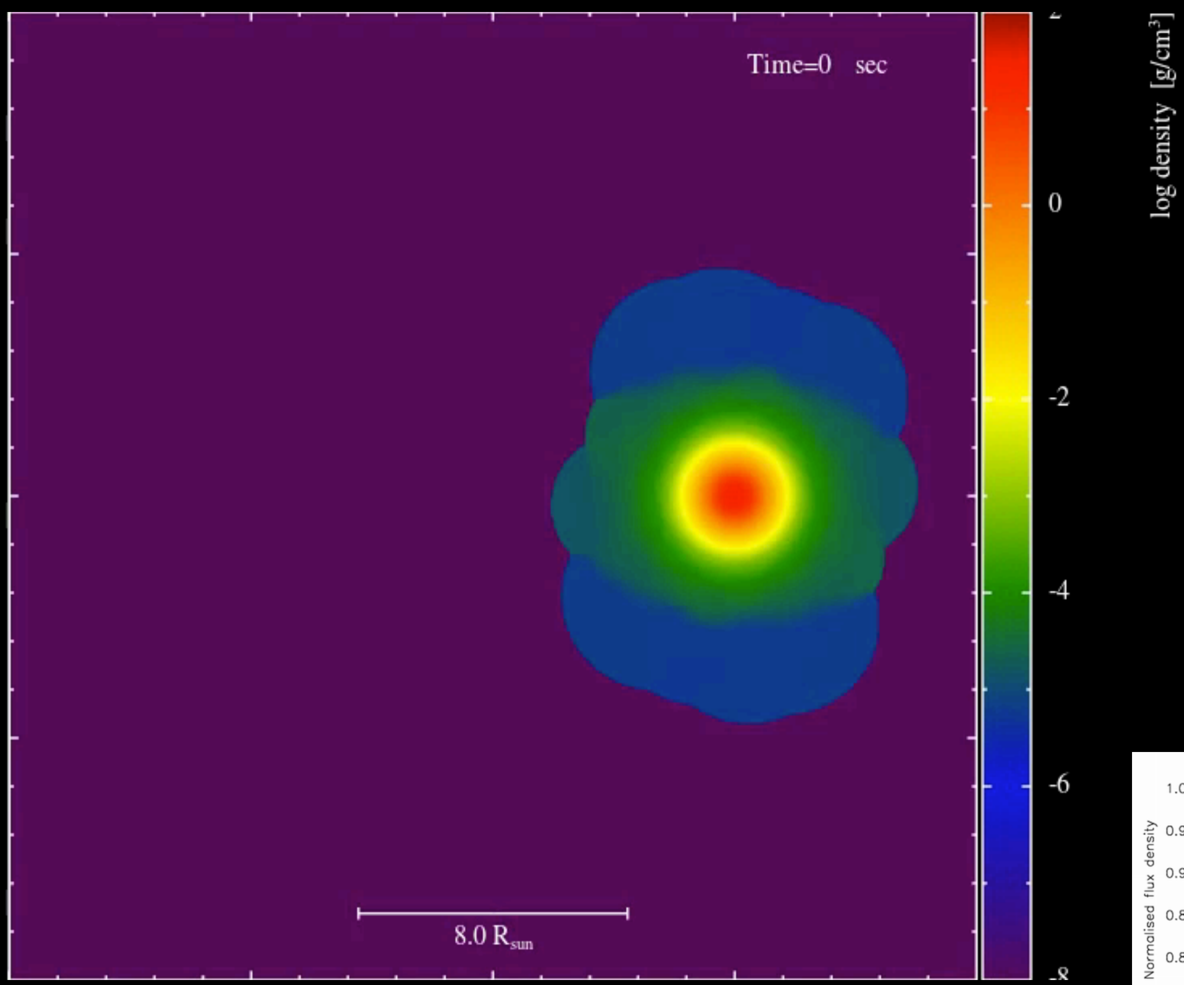

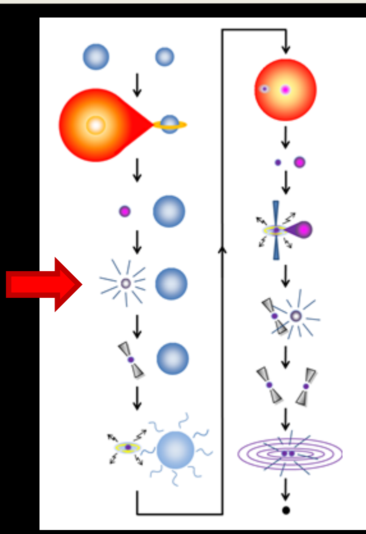

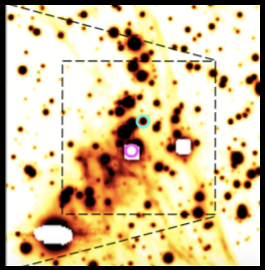

RCW 86

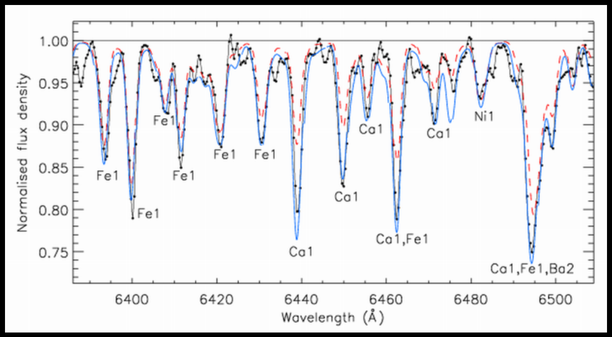

See also
Gvaramadze et al. (2017), Nature Astronomy

- 3D smoothed particle hydrodynamics (SPH) simulations using the Stellar GADGET code.

- To introduce a SN explosion, we adopt a simple analytical explosion ejecta model which is constructed based on numerical simulations of SN explosions by Matzner & McKee (1999). We assume that the SN ejecta is already in homologous expansion.

- The density profile of the expanding SN ejecta, $\rho_{ej}(v_{ej}, t)$, is described by a broken power law, $\rho_{ej} \propto r^{-n}$.

- Various momentum profiles and explosion energies.

- 1.3×10^5 to 1.5×10^7 SPH particles.
  The mass of a single particle ≈ $10^{-6} - 10^{-7}\ M_{\odot}$.

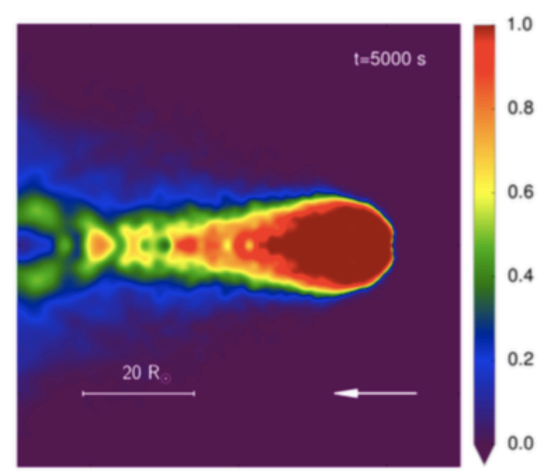

RCW 86 – GALACTIC SUPERNOVA REMNANT

Radio | DSS R-band

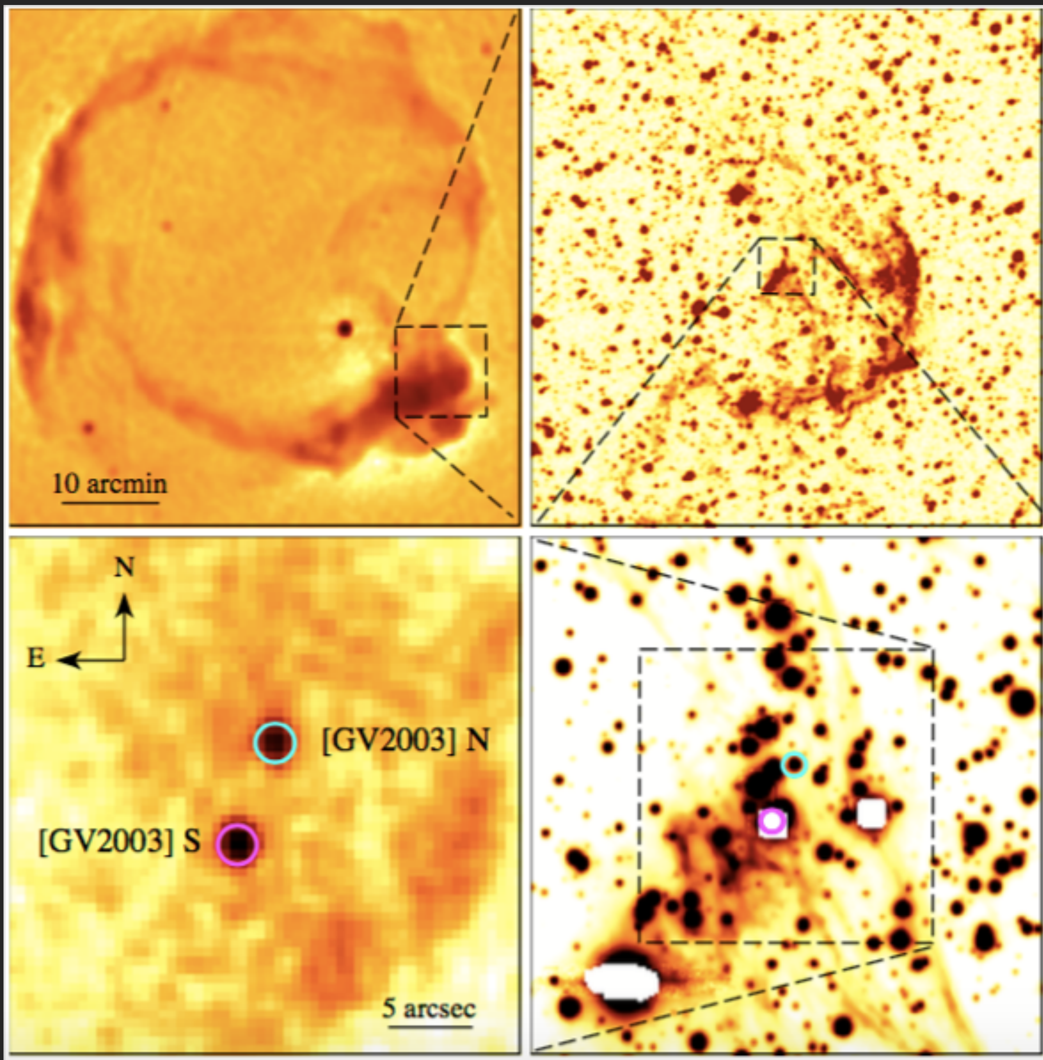

Chandra | VLT

Gvaramazde et al. (2017)
Nature Astronomy 1, 116

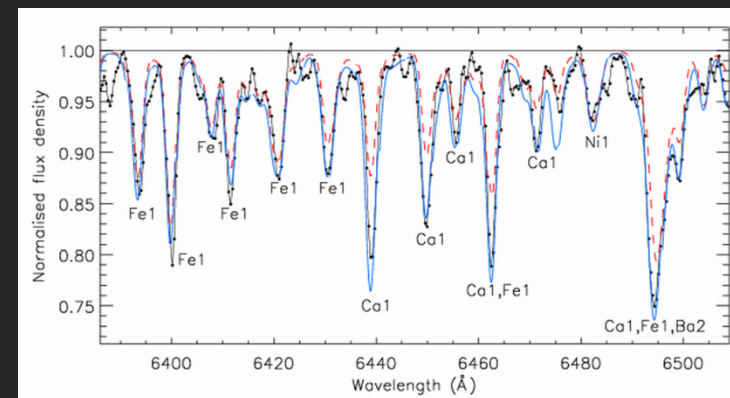

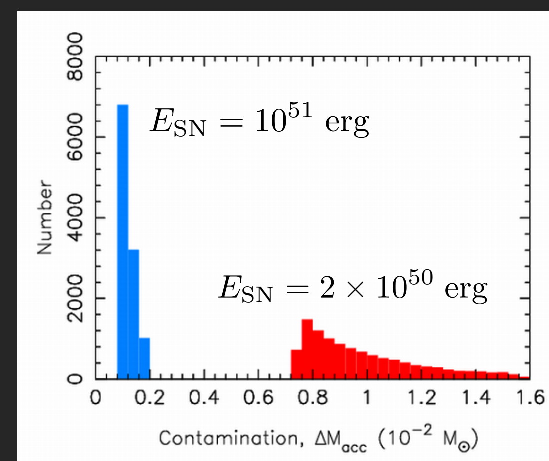

The pyriform appearance of RCW 86 (Fig. 1; see also fig. 6 in ref.17) can be explained as the result of a SN explosion near the edge of a bubble blown by the wind of a moving massive star, (Supplementary Information section 1). This interpretation implies that the SN exploded near the centre of the hemispherical optical nebula in the south-west of RCW 86 (see Fig. 1) and that the stellar remnant should still be there. Motivated by these arguments, we looked for a possible compact X-ray source using archival ***Chandra*** data and discovered **two sources** in the expected position of the SN progenitor (Fig. 1). One of them, **[GV2003] S**, has a clear optical counterpart with V =14.4 mag and its X-ray spectrum implies that this source is a **foreground late-type active star**. For the second source, **[GV2003] N**, we did not find any optical counterpart in the Digital Sky Survey II to a limiting red band magnitude of ≈21, while its **X-ray spectrum** suggests that this source could be a **young pulsar**. Our deep follow-up observation with the Parkes radio telescope in 2002, however, failed to detect any radio emission from [GV2003] N, giving an upper limit on the flux of 35 μJy at 1420 MHz (Methods). This non-detection may be a consequence of beaming or it could indicate that [GV2003] N may not be an active radio pulsar.

If [**GV2003] N** was a NS its emission in the visual was expected to be fainter than V ≈28 mag. We therefore obtained a V -band image of the field around this source with the FORS2 instrument on the ESO Very Large Telescope (**VLT)** in 2010. The FORS2 image, however, revealed a stellar- like object with V =20.69±0.02 mag just at the position of [GV2003] N (Fig. 1; Methods). To further constrain the nature of [GV2003]N, we obtained its g′r′i′z′JHKs photometry with the 7-channel optical/near-infrared imager GROND in 2013 (Extended Data Table 1). With that, we fitted the spectral energy distribution (SED) of [GV2003] N and derived a temperature of ≈5200 K and a colour excess of E (B − V)≈0.9 mag (Methods; Extended Data Fig. 1). These results exclude the possibility that [GV2003] N is an AGN and strongly suggest the optical emission to originate from a G-type star at a distance comparable to that of RCW 86 of 2.3±0.2 kpc. Since the X-ray luminosity of [GV2003]N of ~1032 ergs−1 (ref.18,20) is far too high for a G star, we arrived at the possibility that we are dealing with **a G star orbiting the NS**.

Consequently, we searched for **radial velocity (RV) variability** and **traces of the SN ejecta**

From the FORS2 spectra we derived the abundances of Si, Ca, Ti, V, Cr, Mn, Fe, Co, Ni, and Ba (Methods). Fig. 3 shows that many elements are enhanced by a factor of about 3 with respect to the solar abundances, with the silicon and iron being less than doubled. **Calcium is particularly overabundant, by a factor of ≈6**, which, to our knowledge, makes [GV2002] N the most Ca-rich star known to date.

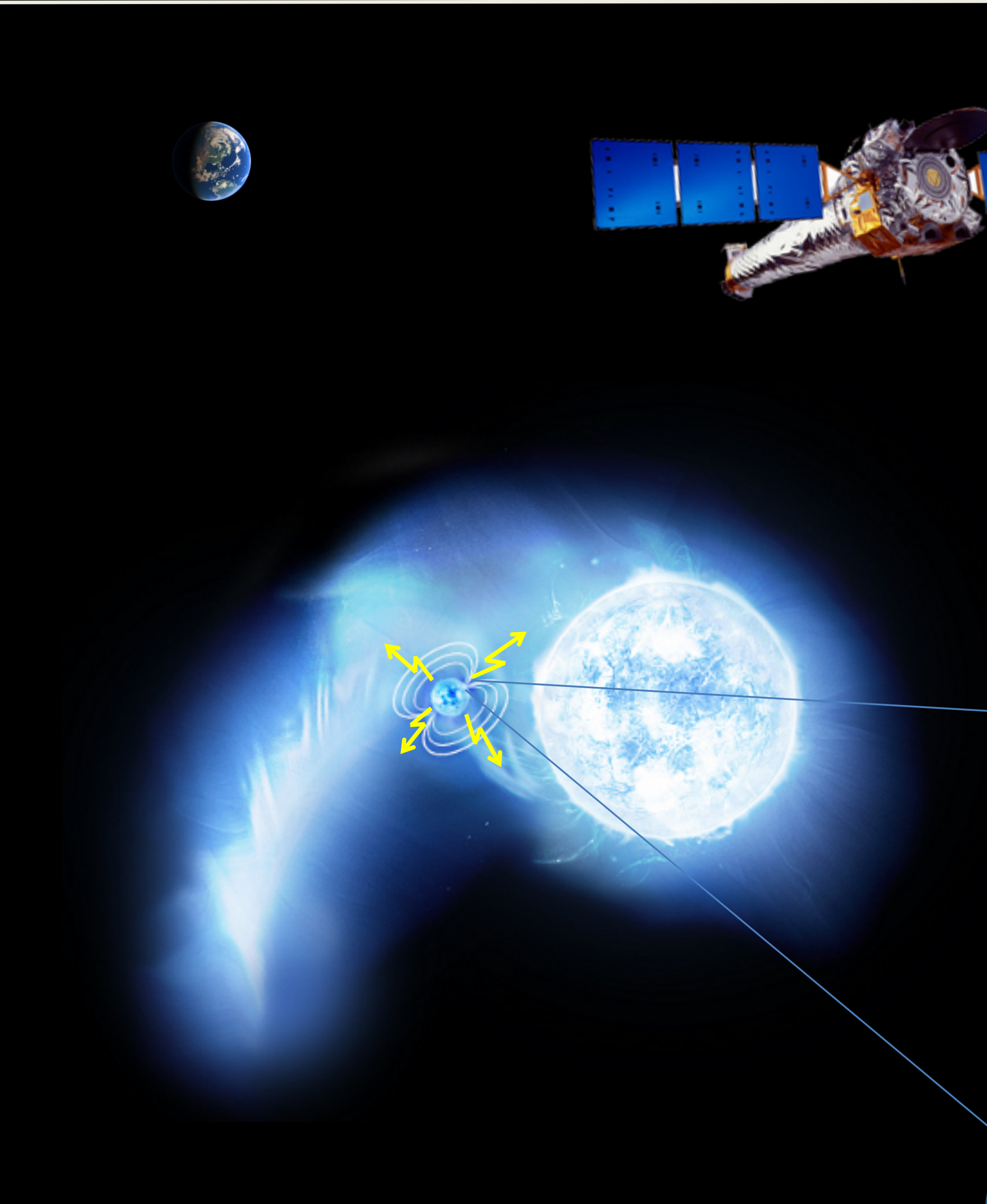

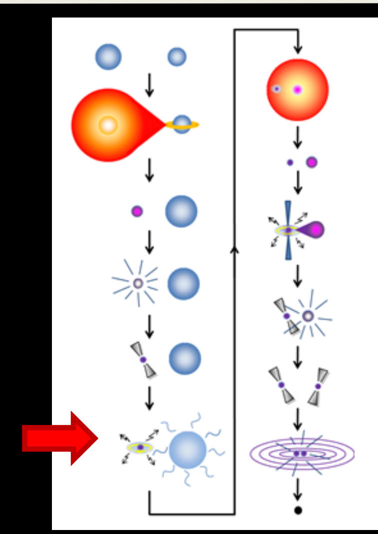

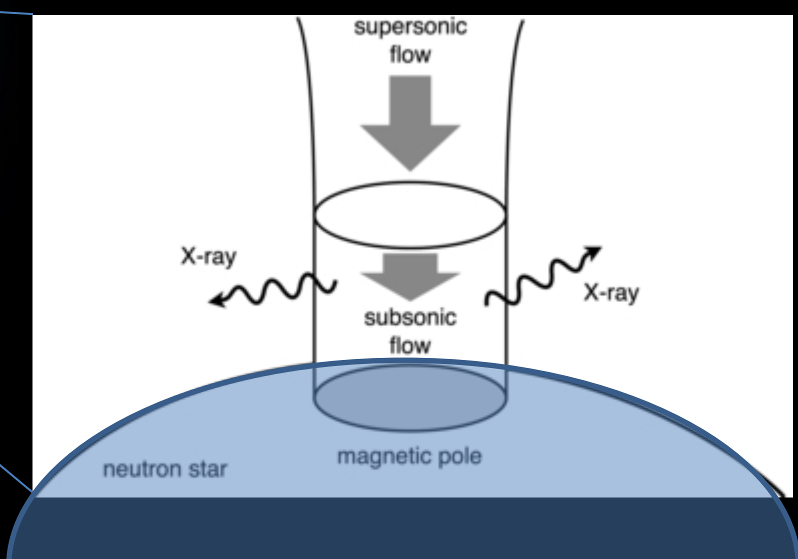
supersonic
flow
X-ray
X-ray
subsonic
flow
neutron star
magnetic pole

$$\left(\frac{dE_{orb}}{dt}\right) = -\frac{GM_{donor}M_X}{2a^2}\frac{da}{dt} = \xi(\mu)\pi R_{acc}^2 \rho_{donor} v^3$$

Dissipation of E_{orb} by drag force (Bondi & Hoyle 1944)

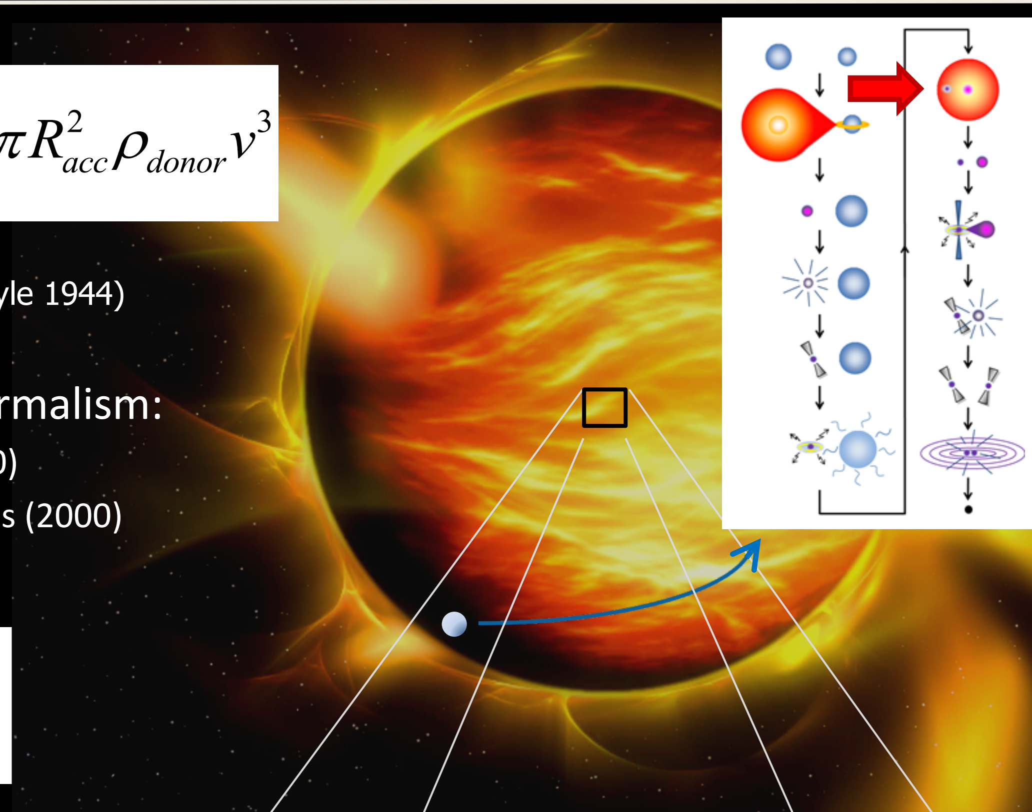

Energy budget (α, λ)-formalism:

Webbink (1984), de Kool (1990)

Han et al. (1994), Dewi & Tauris (2000)

$$E_{env} \equiv \alpha \, \Delta E_{orb}$$

Review by Ivanova et al. (2013)

$$E_{env} = \int_{M_{core}}^{M_{donor}} \left(-\frac{GM(r)}{r} + \eta_{th} U\right) dm$$

gravitational binding energy

internal thermodynamic energy

- thermal energy
- energy of radiation
- recombination energy

NSs in CEs:

MacLeod & Ramirez-Ruiz (2015)

Kruckow, Tauris et al. (2016)

Fragos et al. (2019)

Where does the envelope ejection terminate?

Kruckow, Tauris et al. (2016), A&A

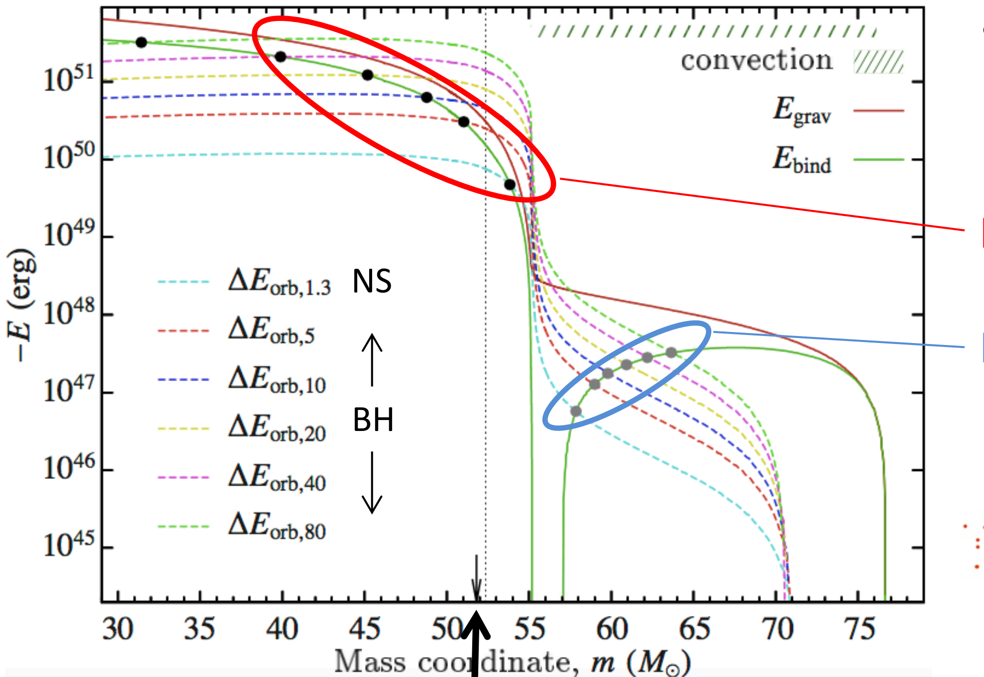

Core boundary: X_H=0.10
(close to local max. sonic velocity)

$88\ M_\odot$ star @ $Z = Z_\odot/50$

$R = 3530\ R_\odot$

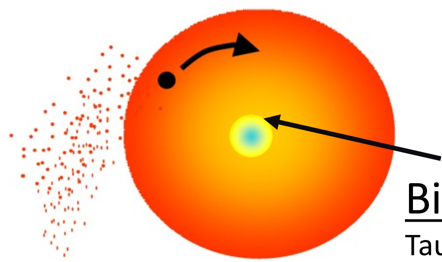

Bifurcation point?
Tauris & Dewi (2001)
Ivanova (2011)

Response of star to mass loss?

- Convective or radiative layer (Hjelming & Webbink 1987)
- Remaining amount of hydrogen?

Kruckow, Tauris et al. (2016), A&A

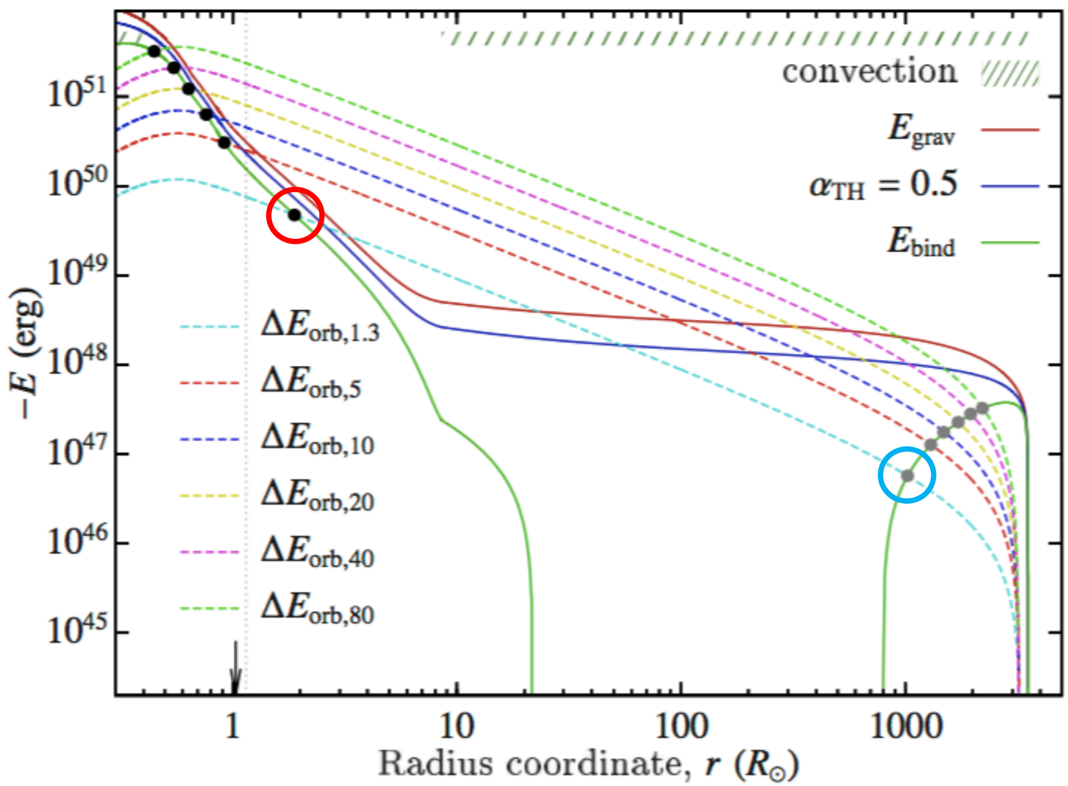

Difference in mass coordinate of about 4 $M_\odot$ corresponds to a **radius difference** by a **factor 500!** Extremely important for the final orbital separation.

Can an in-spiralling BH or NS eject the envelope of a massive star?

Minimum mass of in-spiralling star to successfully eject the envelope?

Kruckow, Tauris, Langer, Szecsi, Marchant & Podsiadlowski (2016), A&A
Common-envelope ejection in massive binary stars
– Implications for the progenitors of GW150914 and GW151226

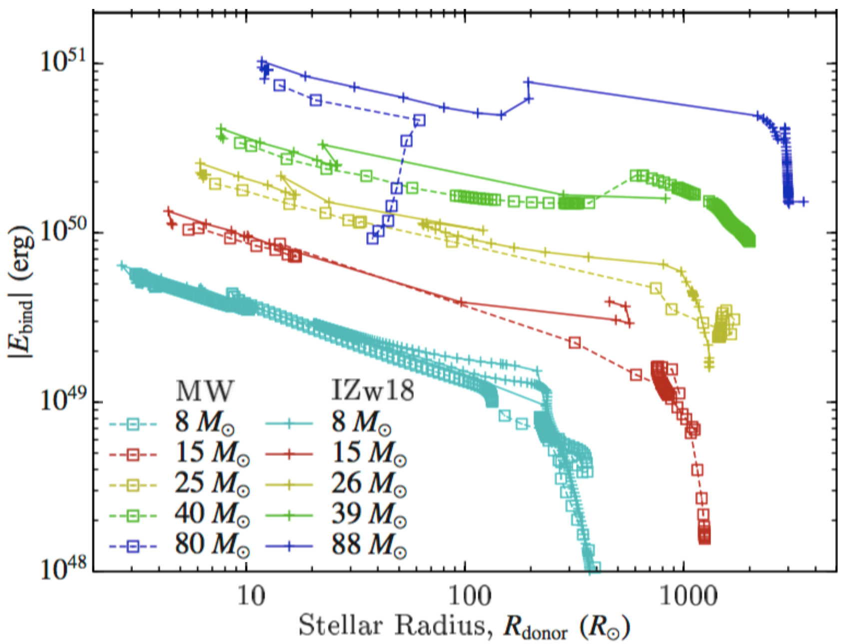

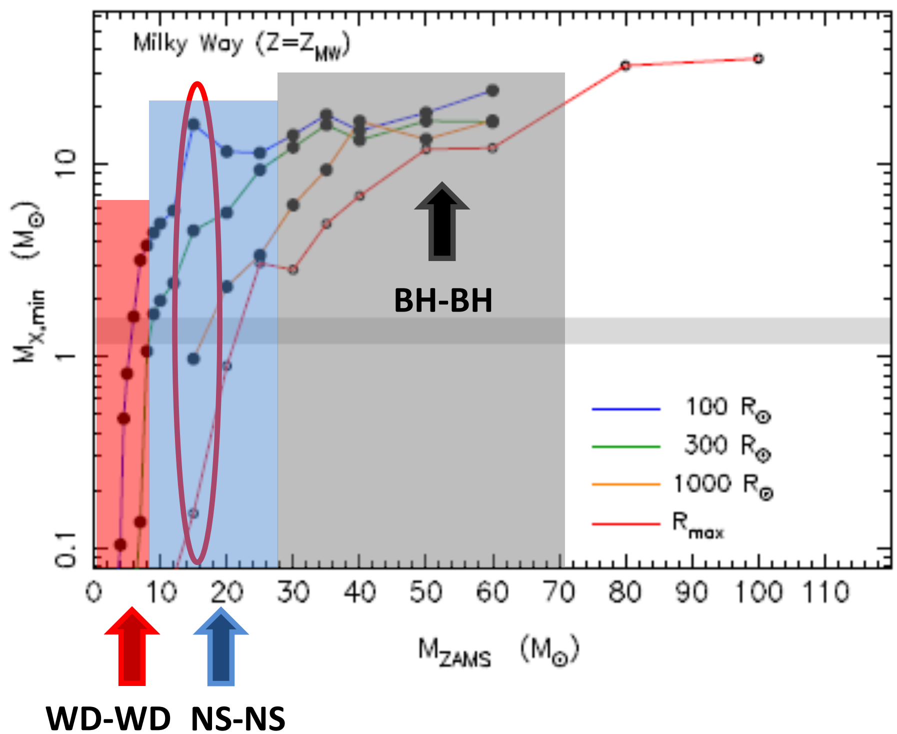

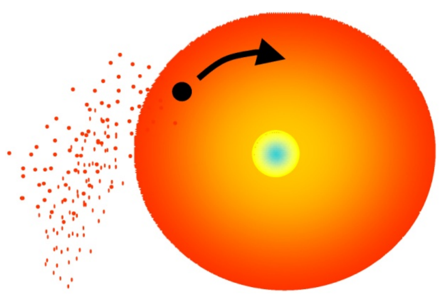

Example:

$M = 15\ M_\odot$: $R < 500\ R_\odot$ no CE ejection → coalescence

$M = 15\ M_\odot$: $R > 500\ R_\odot$ succesful CE ejection

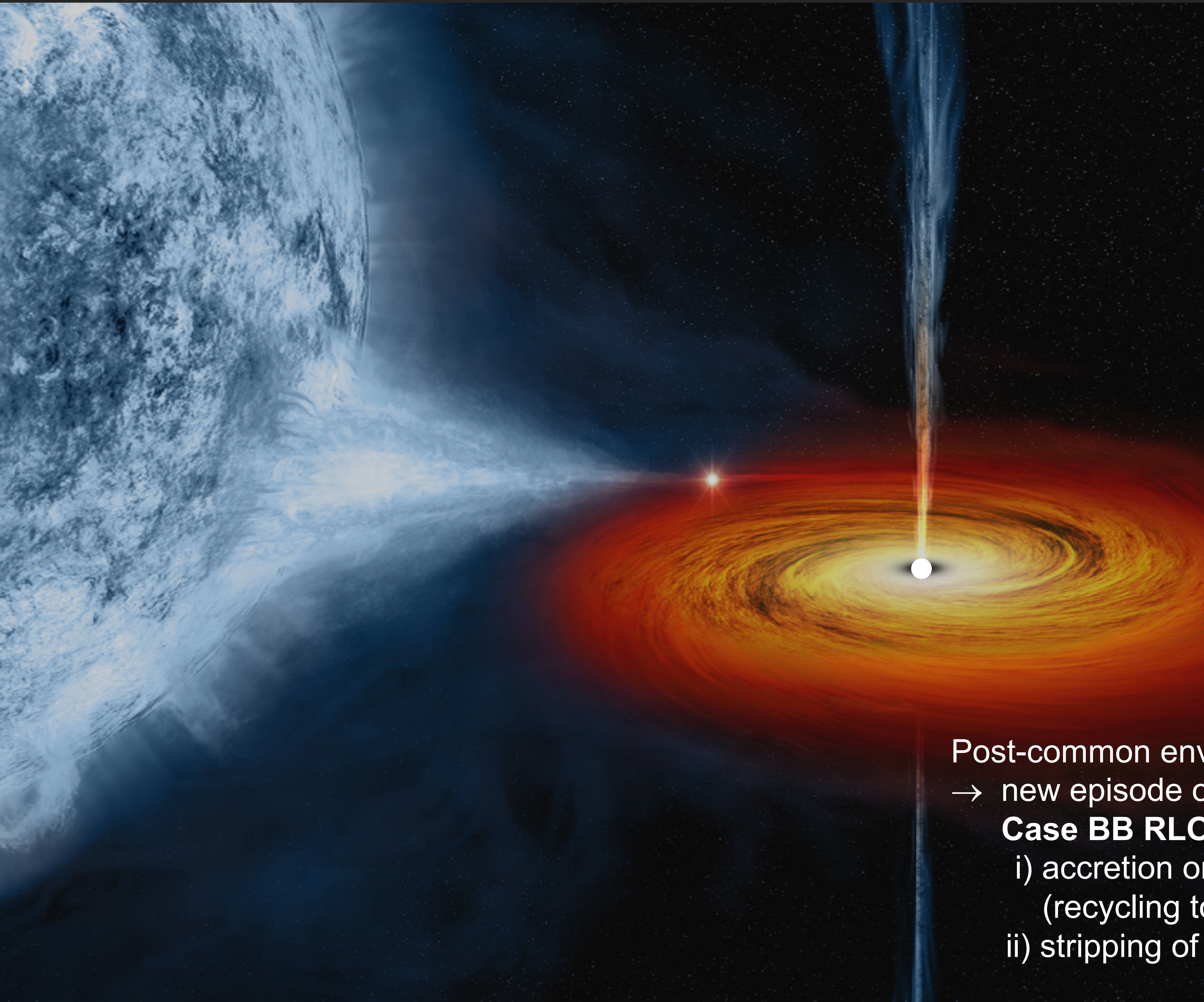

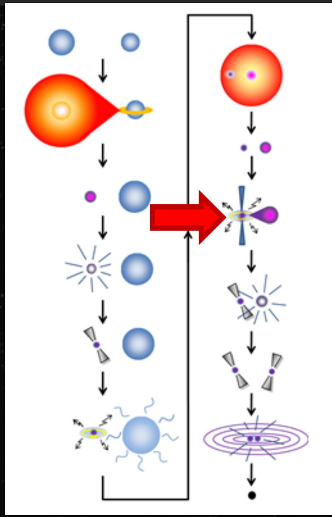

Post-common envelope binary

→ new episode of mass transfer

Case BB RLO

i) accretion onto neutron star (recycling to high spin freq.)

ii) stripping of donor star

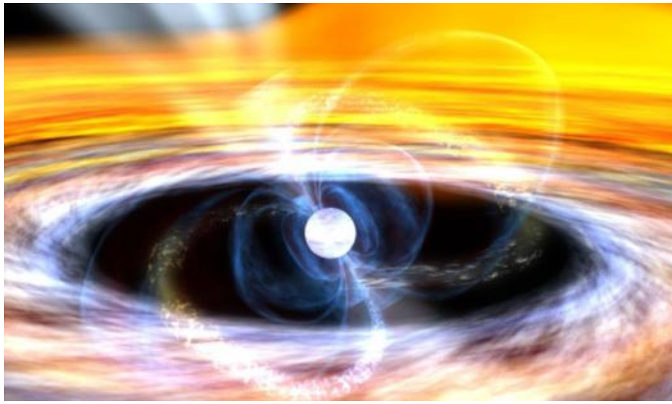

$$P_{eq} = 2\pi \sqrt{\frac{r_{mag}^3}{GM}} \frac{1}{\omega_c} \quad \wedge \quad r_{mag}(\dot{M}, B) \quad \wedge \quad B(P, \dot{P})$$

$$\dot{P} = \frac{2^{1/6}\, G^{5/3}}{\pi^{1/3} c^3} \frac{\dot{M} M^{5/3} P_{eq}^{4/3}}{I} \cdot (1 + \sin^2\alpha) \cdot \varphi^{-7/2} \cdot \omega_c^{7/3}$$ spin-up line in $P\dot{P}$ – diagram

Tauris, Langer & Kramer (2012)

Important!

disk –magnetosphere parameters:

$$R_{mag} = \varphi R_{Alfven}$$

$$\Omega_{NS} = \omega_c \, \Omega_{mag}^{Kep.}$$

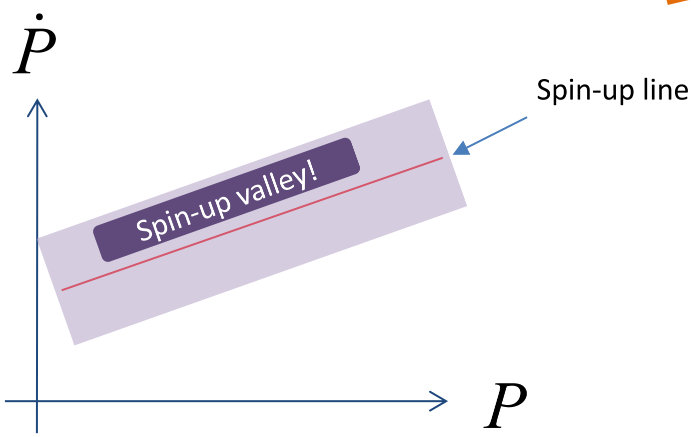

Classical spin-up line

e.g. Bhattacharya & van den Heuvel (1991)

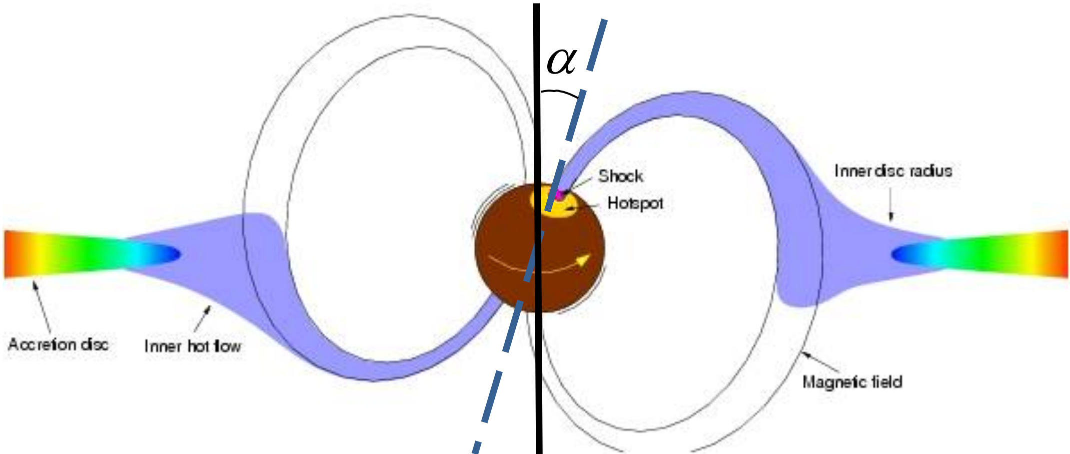

stellar evolution code

$$\Delta J_\star = \int n(\omega, t)\, \dot{M}(t)\, \sqrt{G M(t) r_{\rm mag}(t)}\, \xi(t)\, dt$$

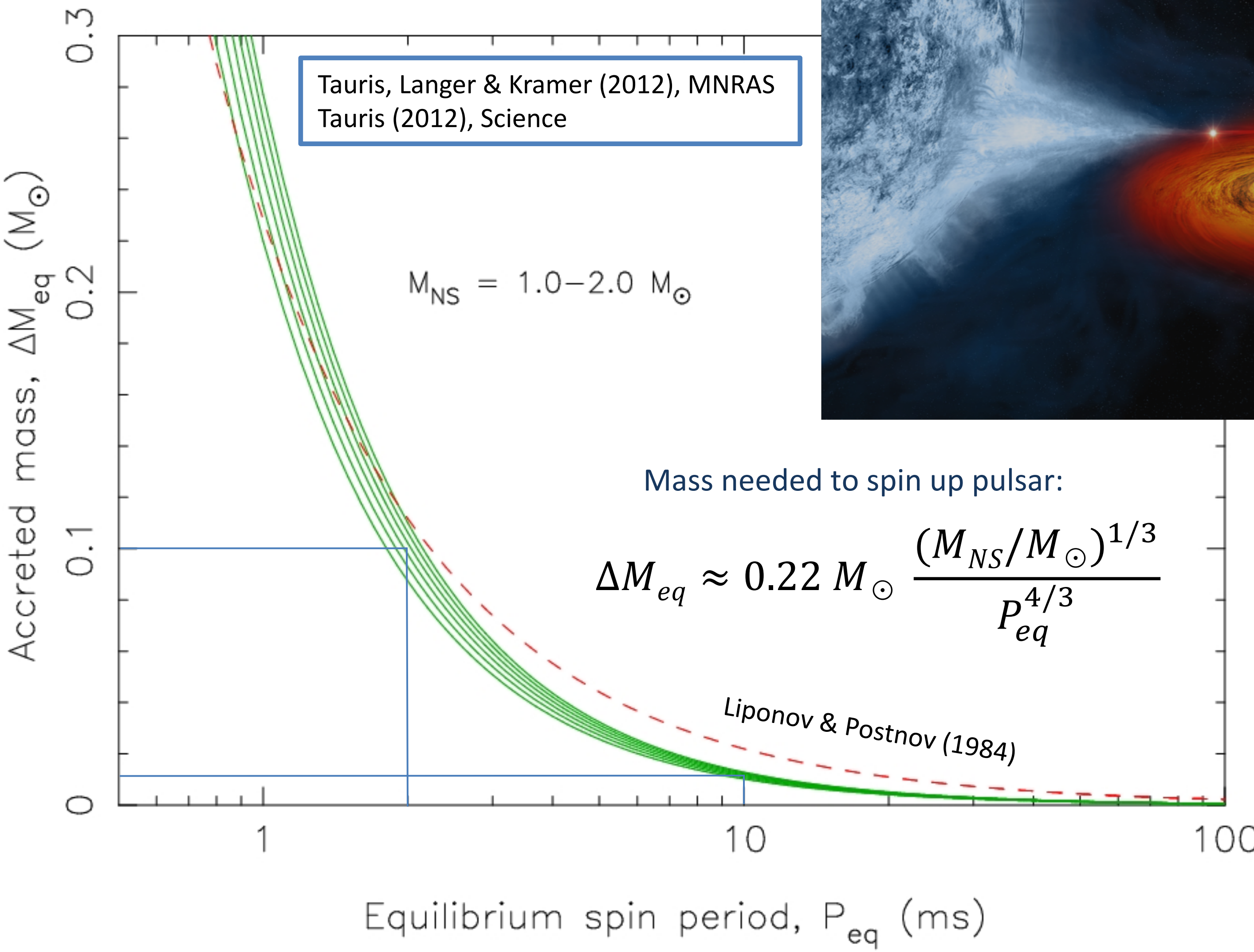

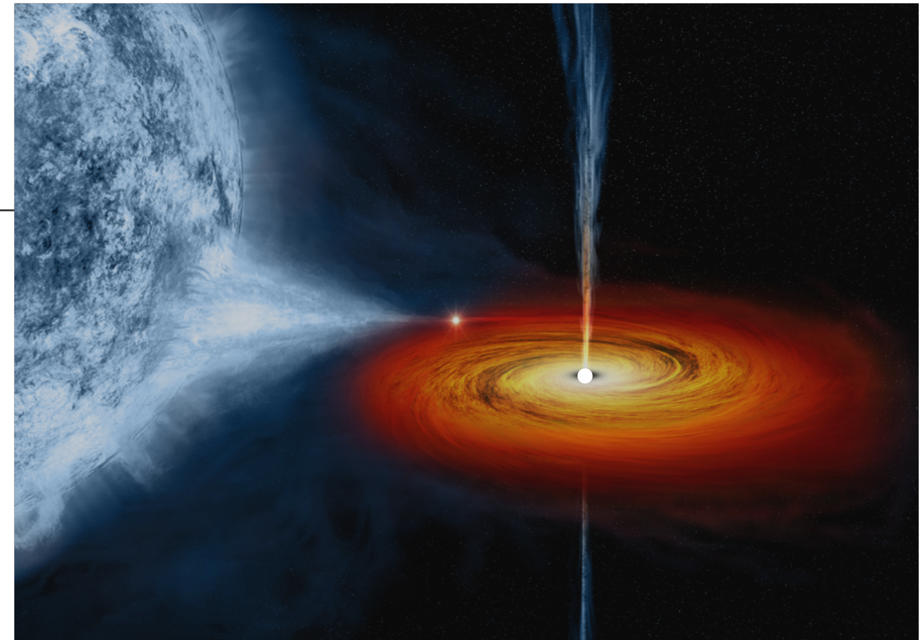

Mass needed to spin up pulsar:

$$\Delta M_{eq} \approx 0.22\, M_\odot \frac{(M_{NS}/M_\odot)^{1/3}}{P_{eq}^{4/3}}$$

P (ms) final spin	M ($M_\odot$) accreted
0.7	0.40
2	0.10
5	0.03
10	0.01
50	0.001

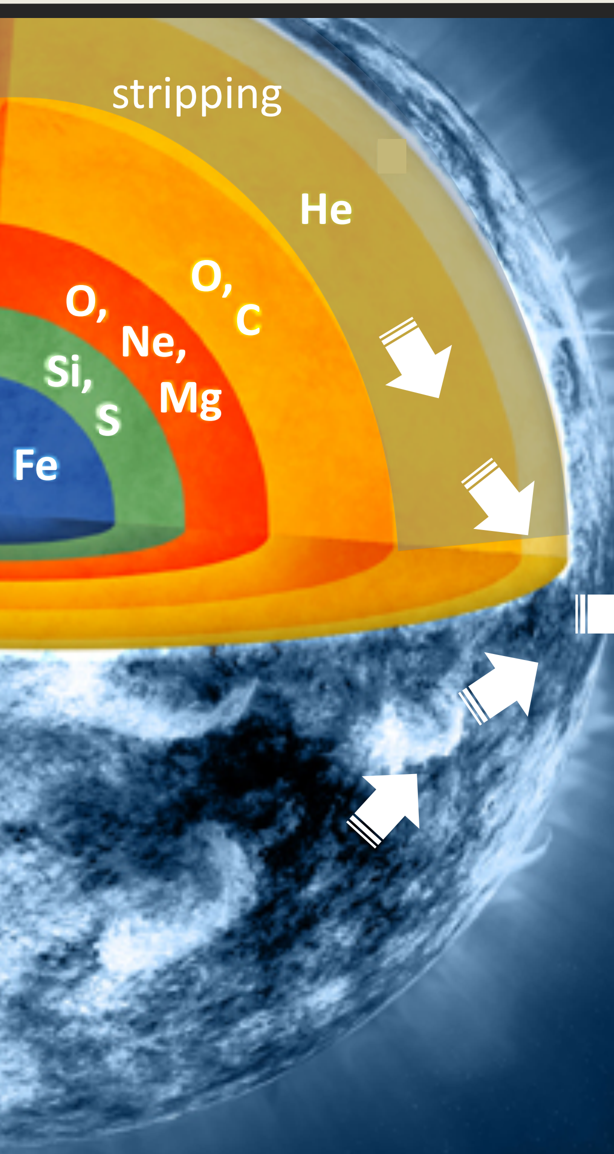

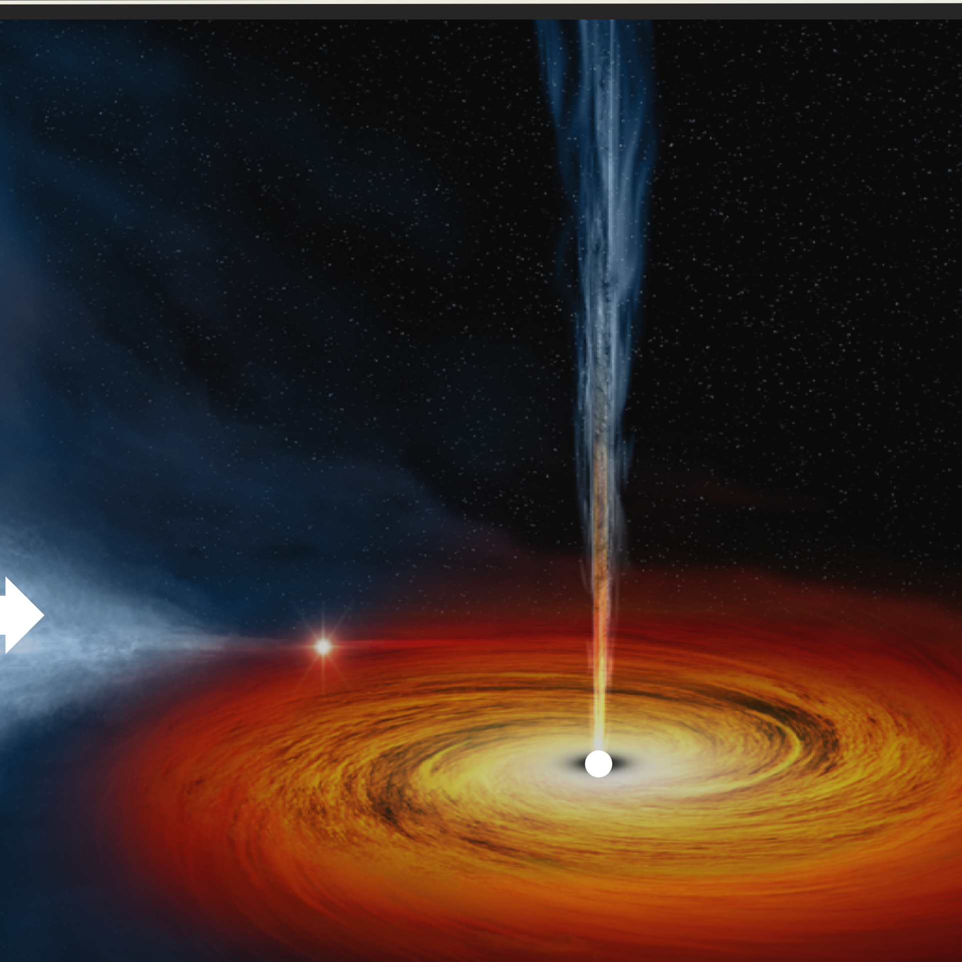

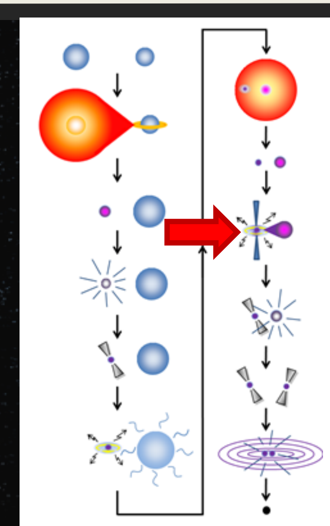

Ultra-stripped supernova explosion

Post-common envelope binary
→ new episode of mass transfer
Case BB RLO
i) accretion onto neutron star (recycling to high spin freq.)
ii) stripping of donor star

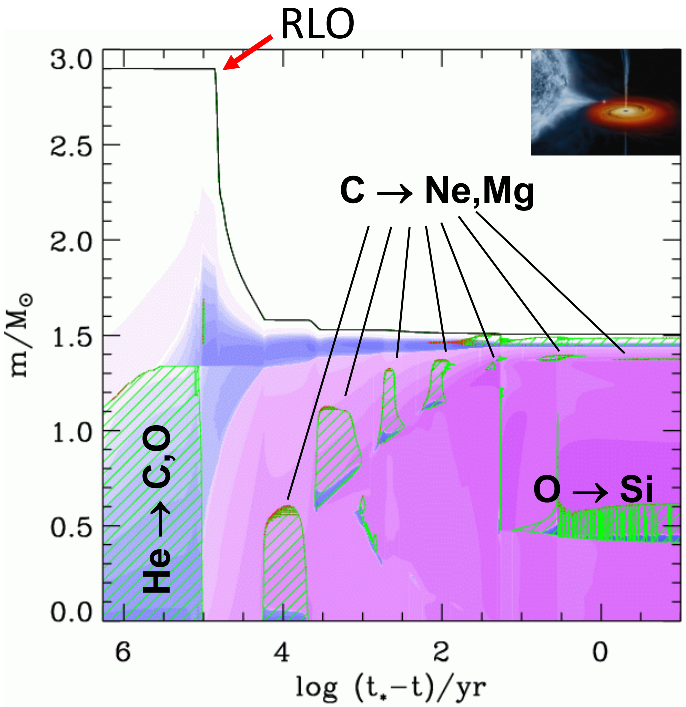

Models calculated for the first time.
We predict a new subclass of SNe
ultra-stripped SNe
with ejecta masses of ~ 0.1 M_{sun}

Tauris et al. (2013), ApJL
Tauris, Langer & Podsiadlowski (2015), MNRAS

Suwa et al. (2015), MNRAS
Moriya et al. (2017), MNRAS — LCs + spectra
Newton, Steiner & Yagi (2018), ApJ
Müller et al. (2018, 2019), MNRAS — 3D explosion modelling

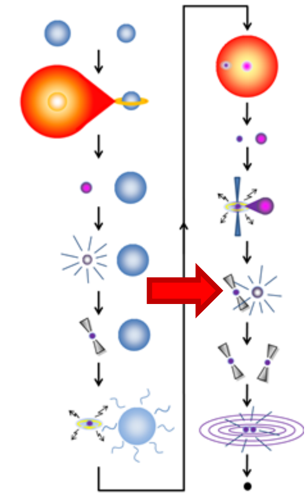

Observational evidence for ultra-stripped SNe…

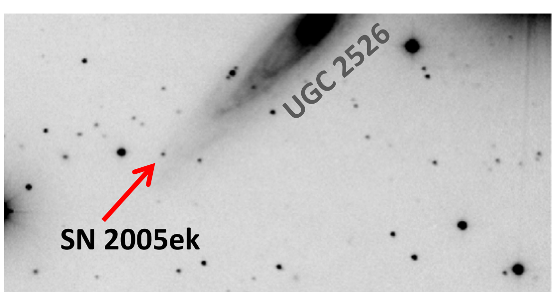

Drout et al. (2013), ApJ
De et al. (2018), Science

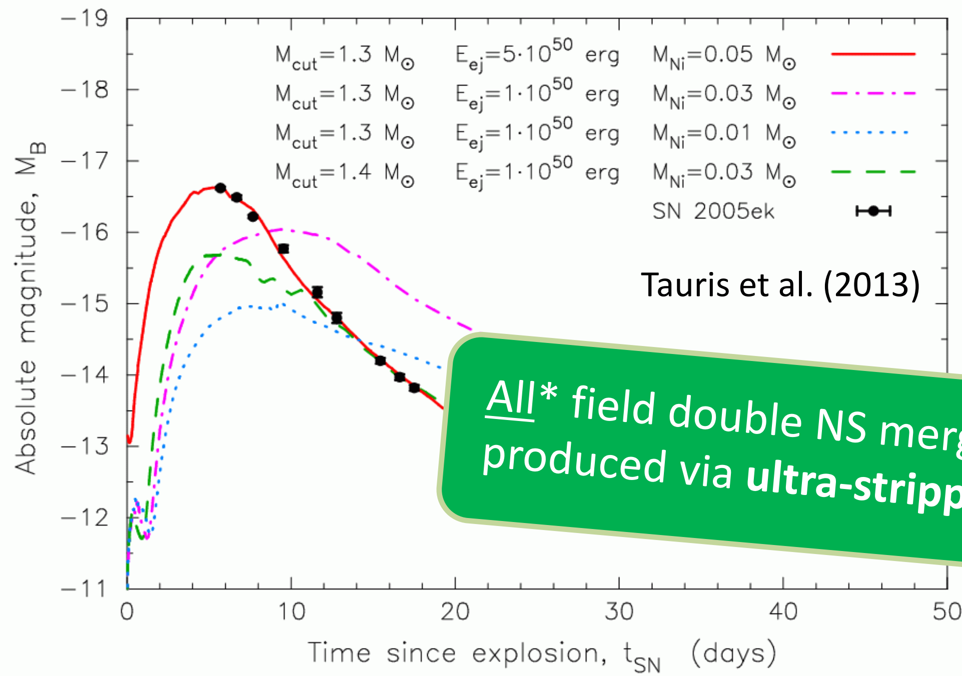

All* field double NS mergers are produced via **ultra-stripped SNe**

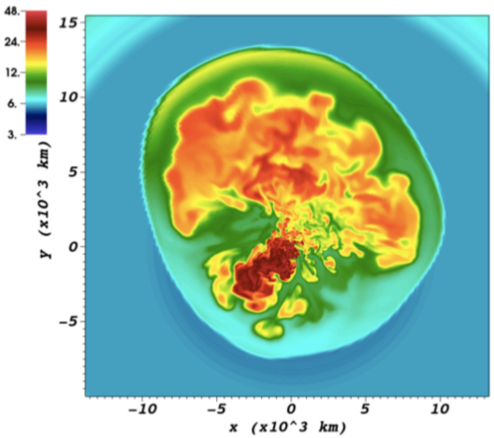

Three-Dimensional Simulations of Neutrino-Driven Core-Collapse Supernovae from Low-Mass Single and Binary Star Progenitors

Bernhard Müller[1⋆], Thomas M. Tauris[2], Alexander Heger[1,3], Projjwal Banerjee[4], Yong-Zhong Qian[5,3], Jade Powell[6], Conrad Chan[1], Daniel W. Gay[7,1], Norbert Langer[8,9]

Müller et al. (2019), MNRAS

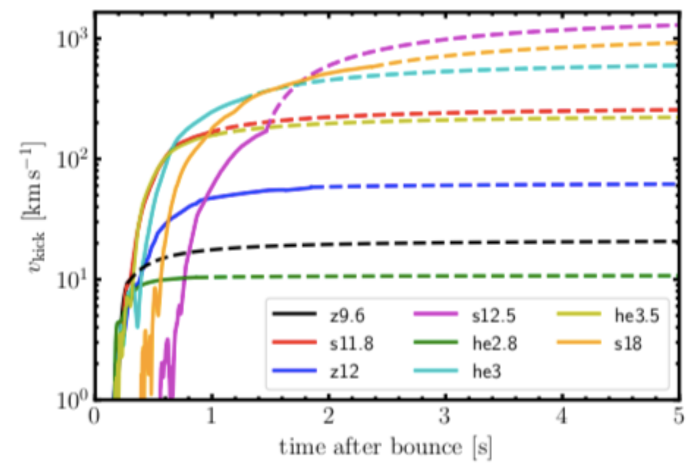

Example of **<u>ultra-stripped SN</u>**
2.80 M_{sun} He-star stripped down to 1.49 M_{sun} prior to explosion (DNS progenitor)

Table 2. Explosion and neutron star properties.

Model	$t_{\rm fin}$ (ms)	$E_{\rm expl}$ (10^{50} erg)	$M_{\rm IG}$ ($M_\odot$)	$M_{\rm by}$ ($M_\odot$)	$M_{\rm grav}$ ($M_\odot$)	$v_{\rm PNS}$ (km s^{-1})	$v_{\rm PNS,\,ex}$ (km s^{-1})	$P_{\rm PNS}$ (ms)	α
z9.6	273	1.32	0.014	1.35	1.22	9.2	21	1060	48°
s11.8	963	1.99	0.024	1.35	1.23	164	278	152	64°
z12	1847	4.10	0.039	1.35	1.22	58	64	205	62°
s12.5	1461	1.56	0.013	1.61	1.44	170	>170	20	55°
he2.8	860	1.12	0.010	1.42	1.28	10.4	11	2749	55°
he3.0	1242	3.66	0.035	1.48	1.33	308	695	93	76°
he3.5	1023	2.78	0.031	1.57	1.41	159	238	98	80°

Notes: $t_{\rm fin}$ is the final post-bounce time reached by each simulation, $E_{\rm expl}$ is the final diagnostic explosion energy at the end of the simulations, $M_{\rm IG}$ is the mass of iron-group ejecta, $M_{\rm grav}$ is the gravitational neutron star mass, $v_{\rm PNS}$ is the kick velocity at the end of the run, $v_{\rm PNS,\,ex}$ is the extrapolated kick obtained from equation (6), $P_{\rm PNS}$ is the estimated neutron star spin period, and α is the angle between the spin and kick vector at the end of the simulations.

Tauris, Langer & Podsiadlowski (2015), MNRAS

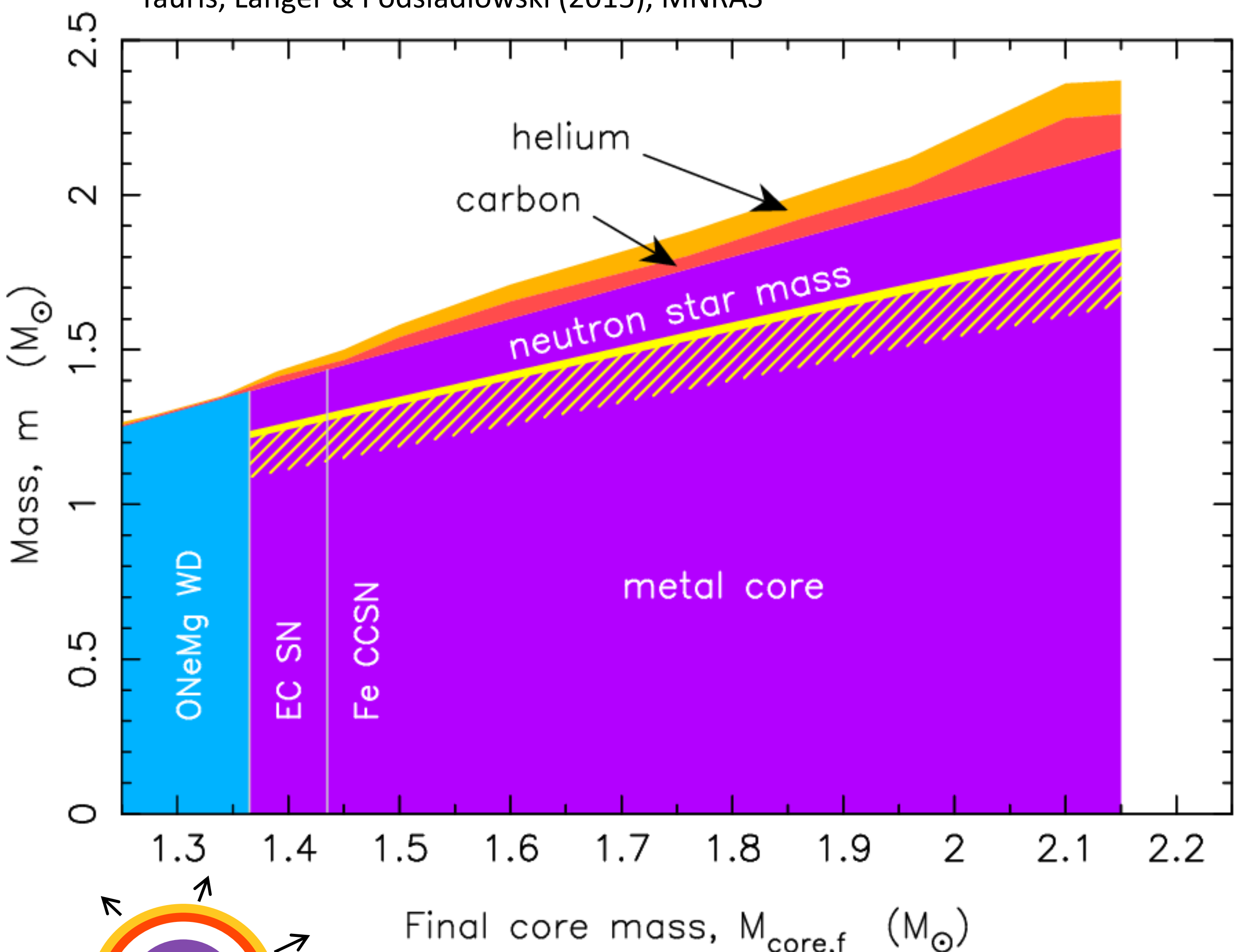

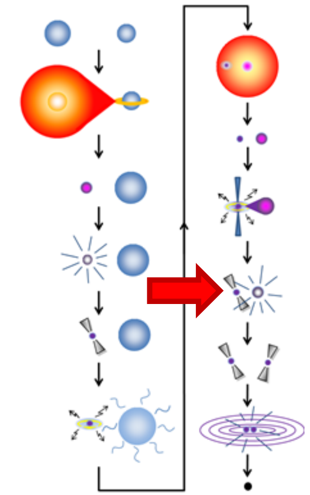

3-D simulations

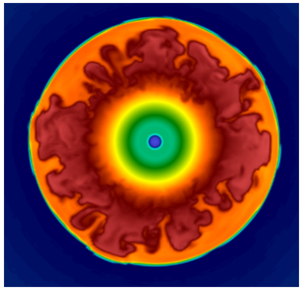

Müller et al. (2018)
Müller et al. (2019)

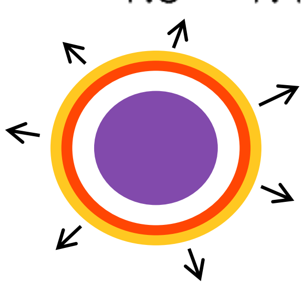

Tiny envelopes (loosely bound, little mass) often yield small SN kicks!

Tauris, Langer & Podsiadlowski (2015), MNRAS

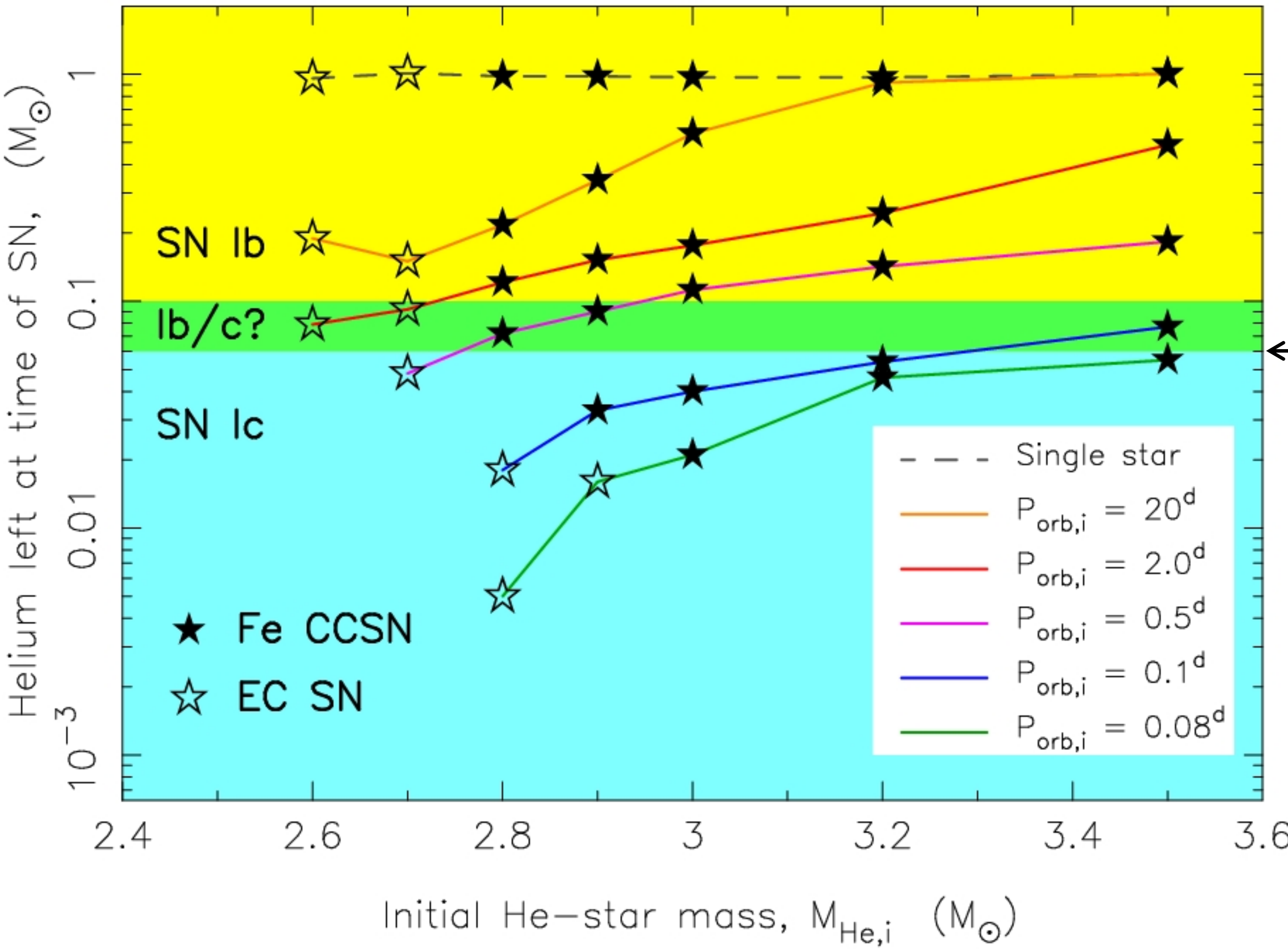

He limit: 0.06 M_{sun}
(Hachinger et al. 2012)

Tauris, Langer & Podsiadlowski (2015), MNRAS

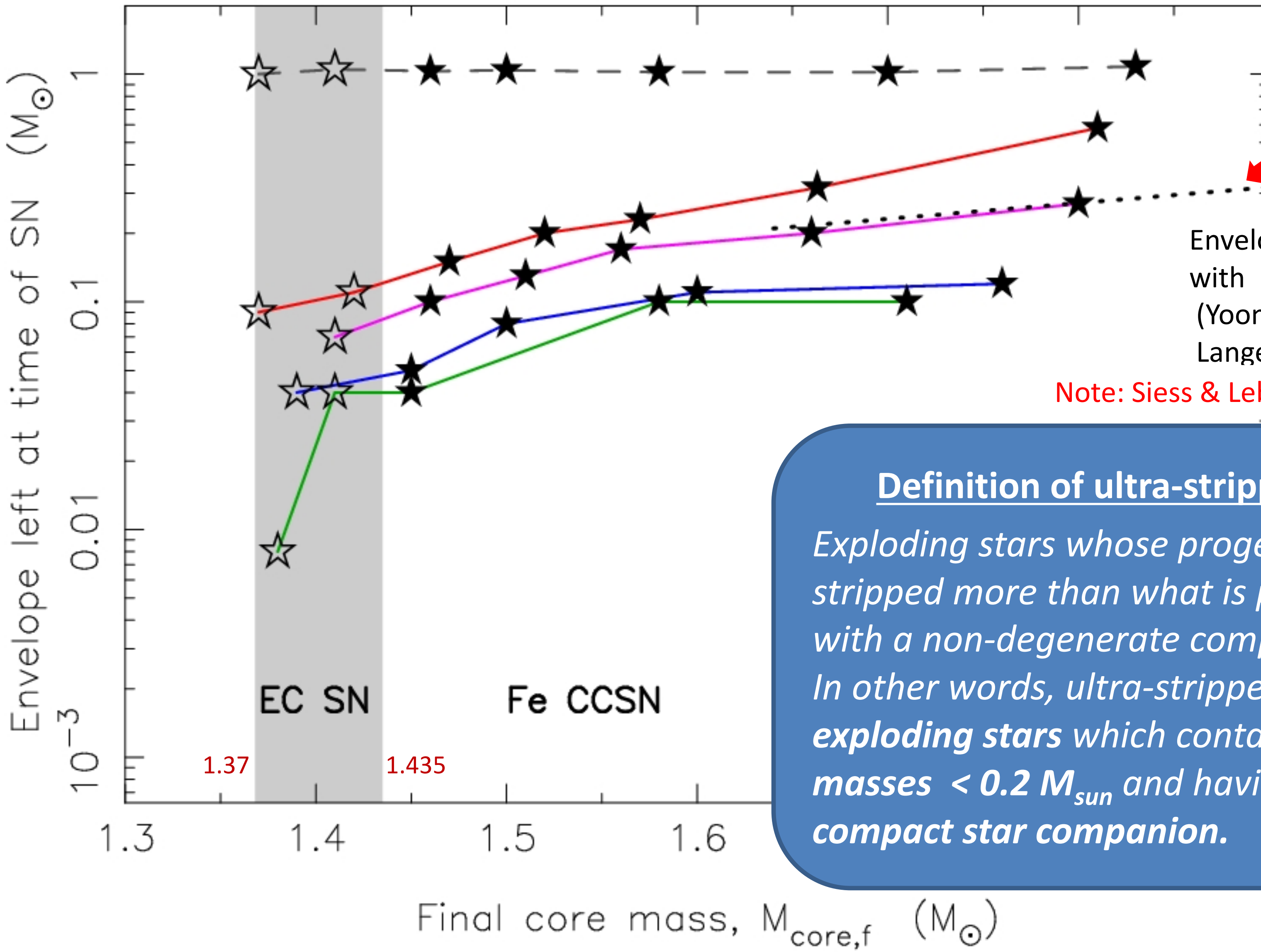

Envelope limit for SNe with MS companions (Yoon, Woosley & Langer 2010)

Note: Siess & Lebreuilly (2018) !!!

Definition of ultra-stripped SNe

Exploding stars whose progenitors are stripped more than what is possible with a non-degenerate companion.
In other words, ultra-stripped SNe are ***exploding stars*** *which contain envelope* ***masses < 0.2 M_{sun}*** *and having a* ***compact star companion.***

Table 2. Expected properties of the light curves resulting from ultra-stripped SNe. The assumed explosion energy ($E_{\rm SN}$) is given in the left column. For each of the different SN ejecta masses ($M_{\rm ej}$) in the following four columns, estimated values of the rise time ($\tau_{\rm r}$) and the decay time ($\tau_{\rm d}$) of the SN light curve are stated.

$E_{\rm SN}$ (erg)	$M_{\rm ej} = 0.2\ M_\odot$	$0.1\ M_\odot$	$0.03\ M_\odot$	$0.01\ M_\odot$
10^{50}	$\tau_{\rm r}$ = 8.4 days	5.0 days	2.0 days	0.9 days
	$\tau_{\rm d}$ = 50 days	25 days	7.5 days	2.5 days
3×10^{50}	$\tau_{\rm r}$ = 6.4 days	3.8 days	1.5 days	0.7 days
	$\tau_{\rm d}$ = 29 days	14 days	4.3 days	1.4 days
10^{51}	$\tau_{\rm r}$ = 4.7 days	2.8 days	1.1 days	0.5 days
	$\tau_{\rm d}$ = 16 days	7.9 days	2.4 days	0.8 days

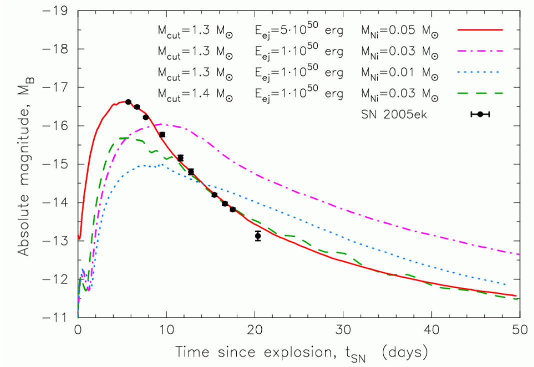

light diffusion time through the SN:

$$\tau_{\rm r} = 5.0 \text{ days } \ M_{0.1}^{3/4}\, \kappa_{0.1}^{1/2}\, E_{50}^{-1/4}$$

time when the electron scattering optical depth of SN light curve = 1:

$$\tau_{\rm d} = 25 \text{ days } \ M_{0.1}\, \kappa_{0.1}^{1/2}\, E_{50}^{-1/2}$$

Peak brightness (Arnett's rule 1979;1982)

M_{Ni} /M_{sun}	M (abs mag)
0.001	-11.8
0.005	-13.4
0.01	-15.0
0.05	-16.6

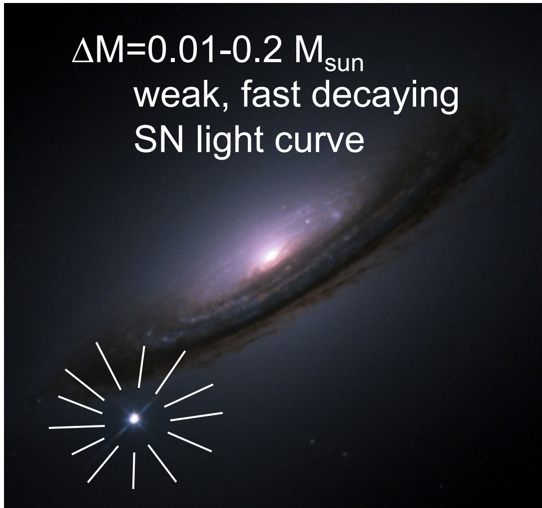

Tauris, Langer & Podsiadlowski (2015)

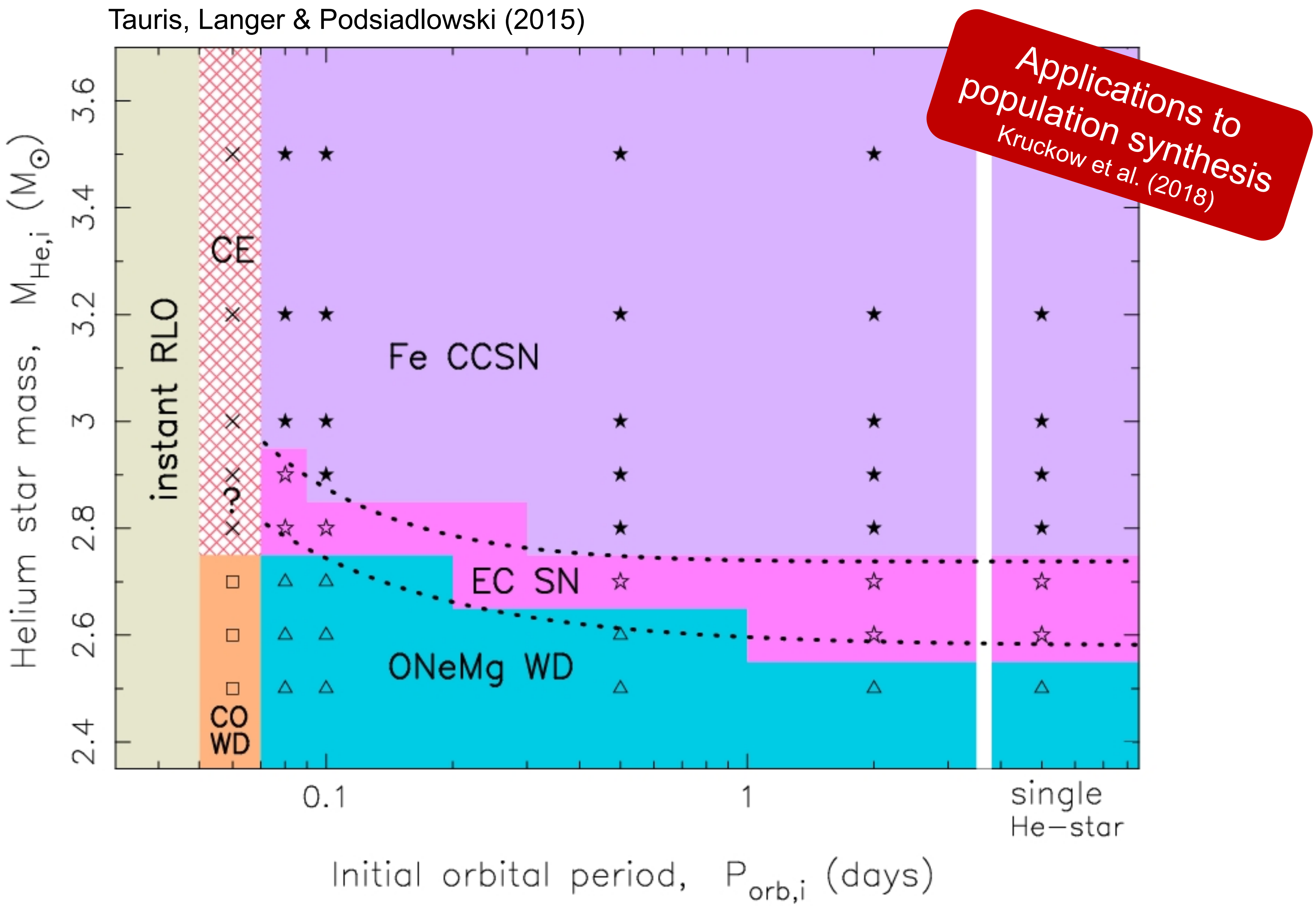

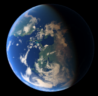

Burgay et al. (2003), Lyne et al. (2004), Kramer et al. (2006)

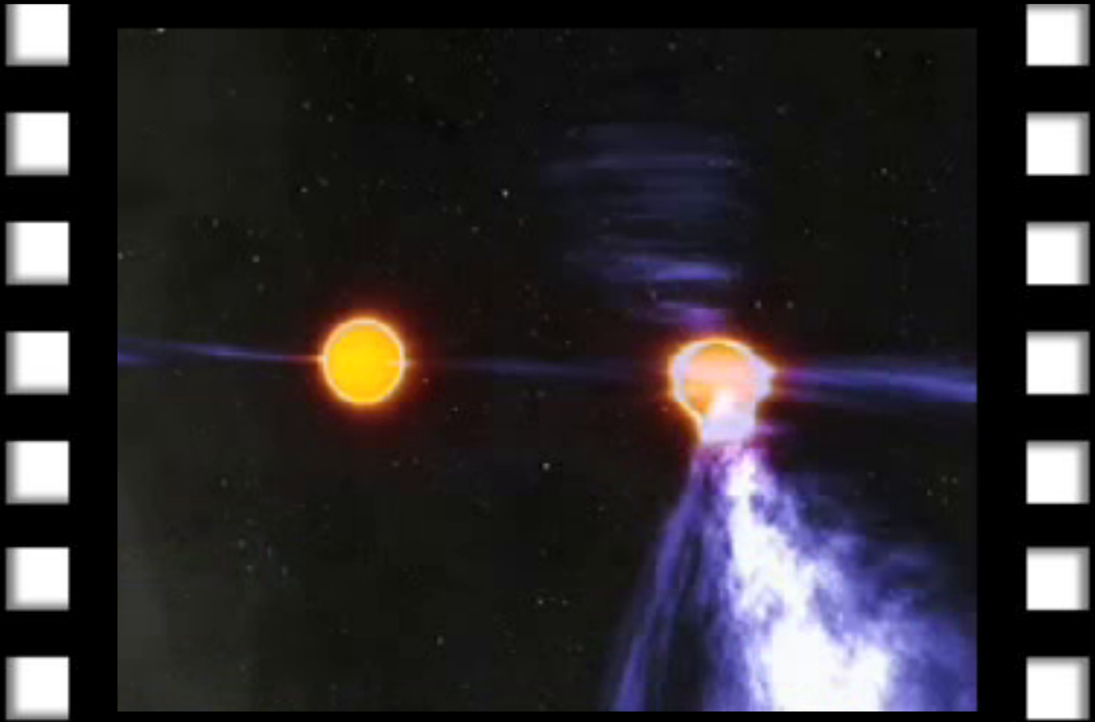

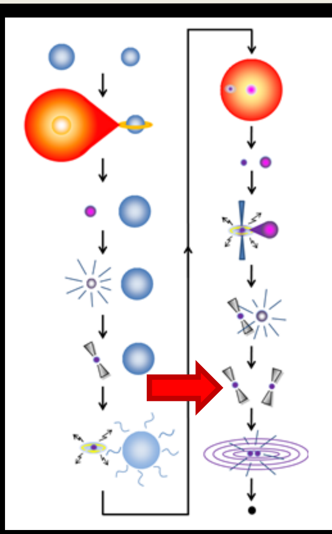

Pulsar J0737-3039A: P=22.7 ms
Pulsar J0737-3039B: P=2.77 sec

PSR B1913+16 (Hulse-Taylor pulsar, P_{orb}=7.75 hr, ecc=0.61)

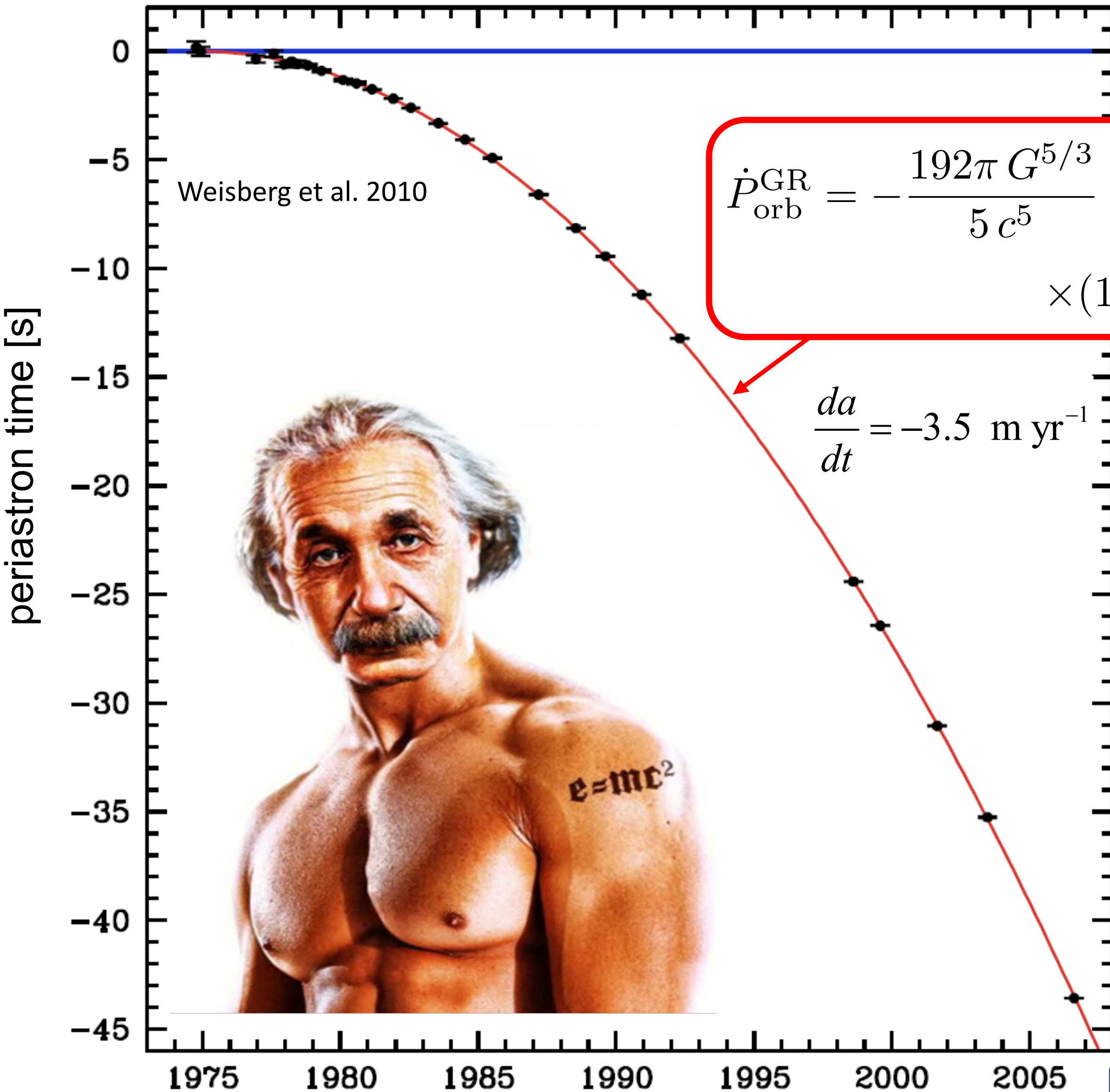

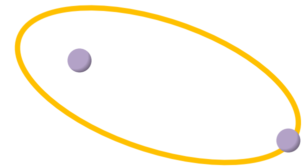

Peters (1964)

$$\dot{P}_{\rm orb}^{\rm GR} = -\frac{192\pi\, G^{5/3}}{5\, c^5} \left(\frac{P_{\rm orb}}{2\pi}\right)^{-5/3} \left(1 + \frac{73}{24}e^2 + \frac{37}{96}e^4\right) \times (1-e^2)^{-7/2}\, M_1 M_2\, (M_1+M_2)^{-1/3}$$

Merge in
τ = 301 Myr

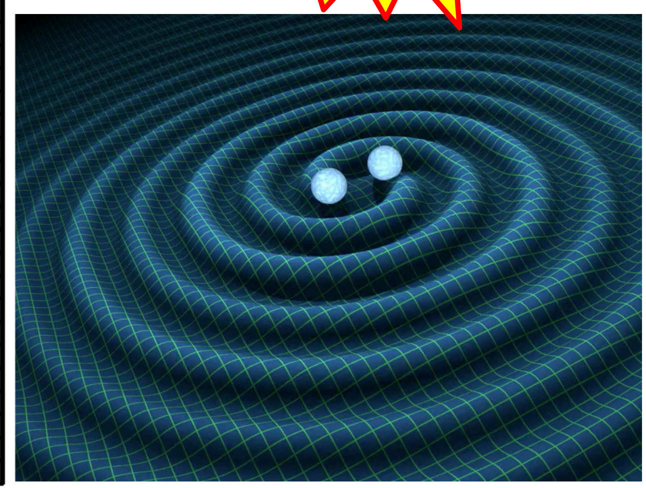

$L_{\rm GW} = 7\times 10^{24}$ W $\qquad (L_{\rm GW,\odot} = 5000$ W$)$

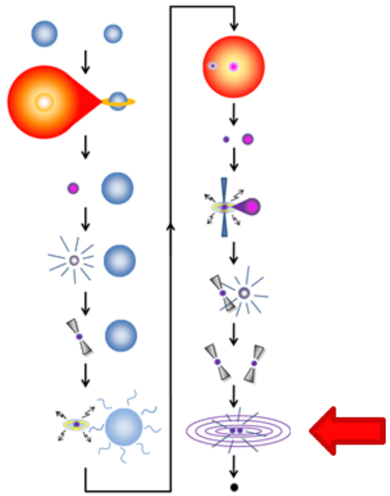

Double neutron star mergers: **GW170817**

→ gravitational wave burst

→ short γ-ray burst

→ ejection of a few $0.01\ M_{\odot}$ heavy r-process elements

→ macro/kilonovae (EM follow-up)

Abbott et al. (2017), Coulter et al. (2017), Soares-Santos et al. (2017), Smartt et al. (2017), Drout et al. (2017)

Review: Giacomazzo et al. (2019)

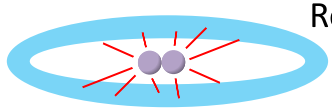

NS+BH

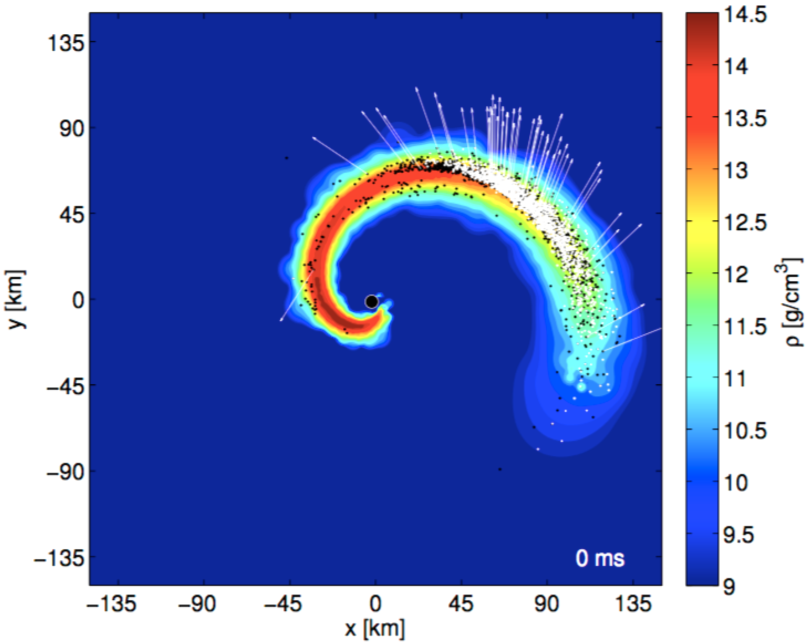

Just et al. (2015)

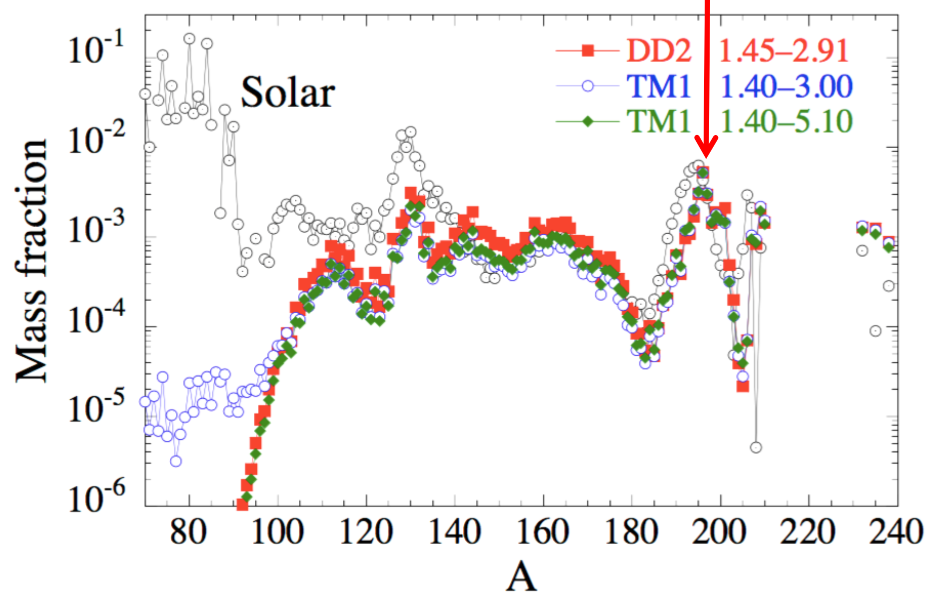

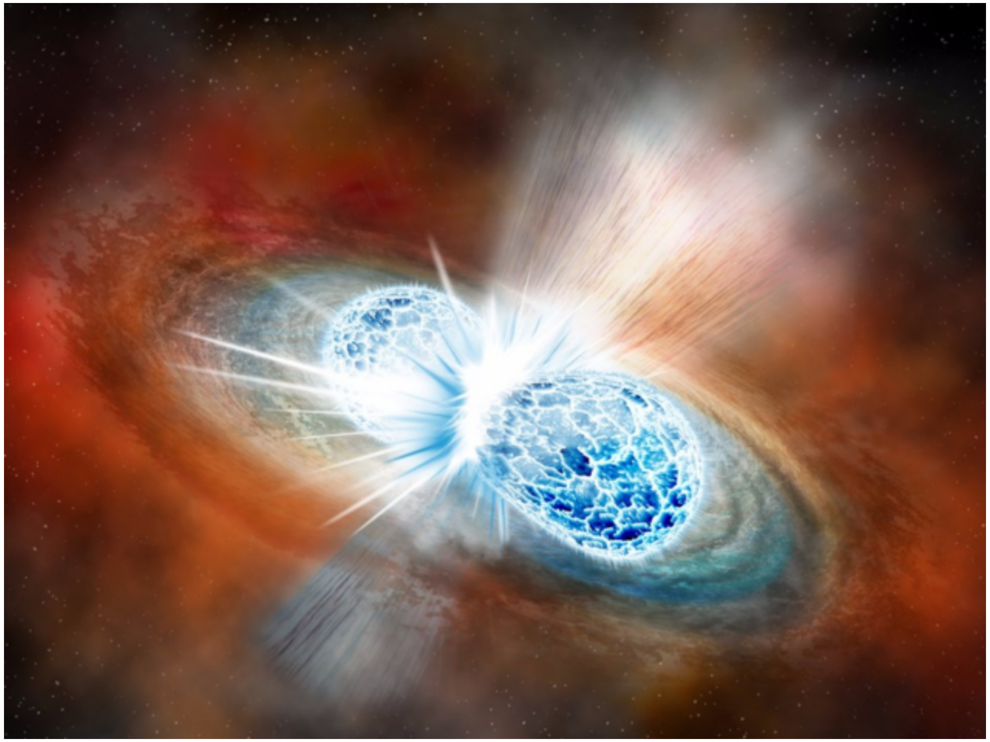

- Masses
- Spins
- B-fields

- Orbital period
- Eccentricity

- Age at merger time
- Kicks
- Location relative to host galaxy

- Merger rates

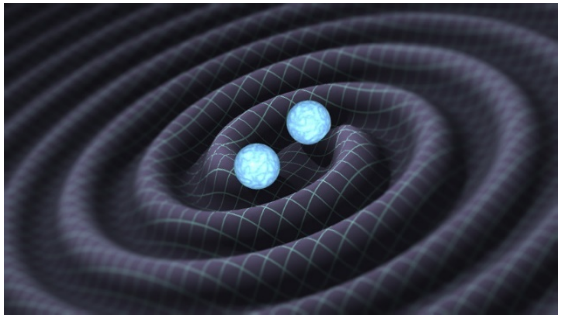

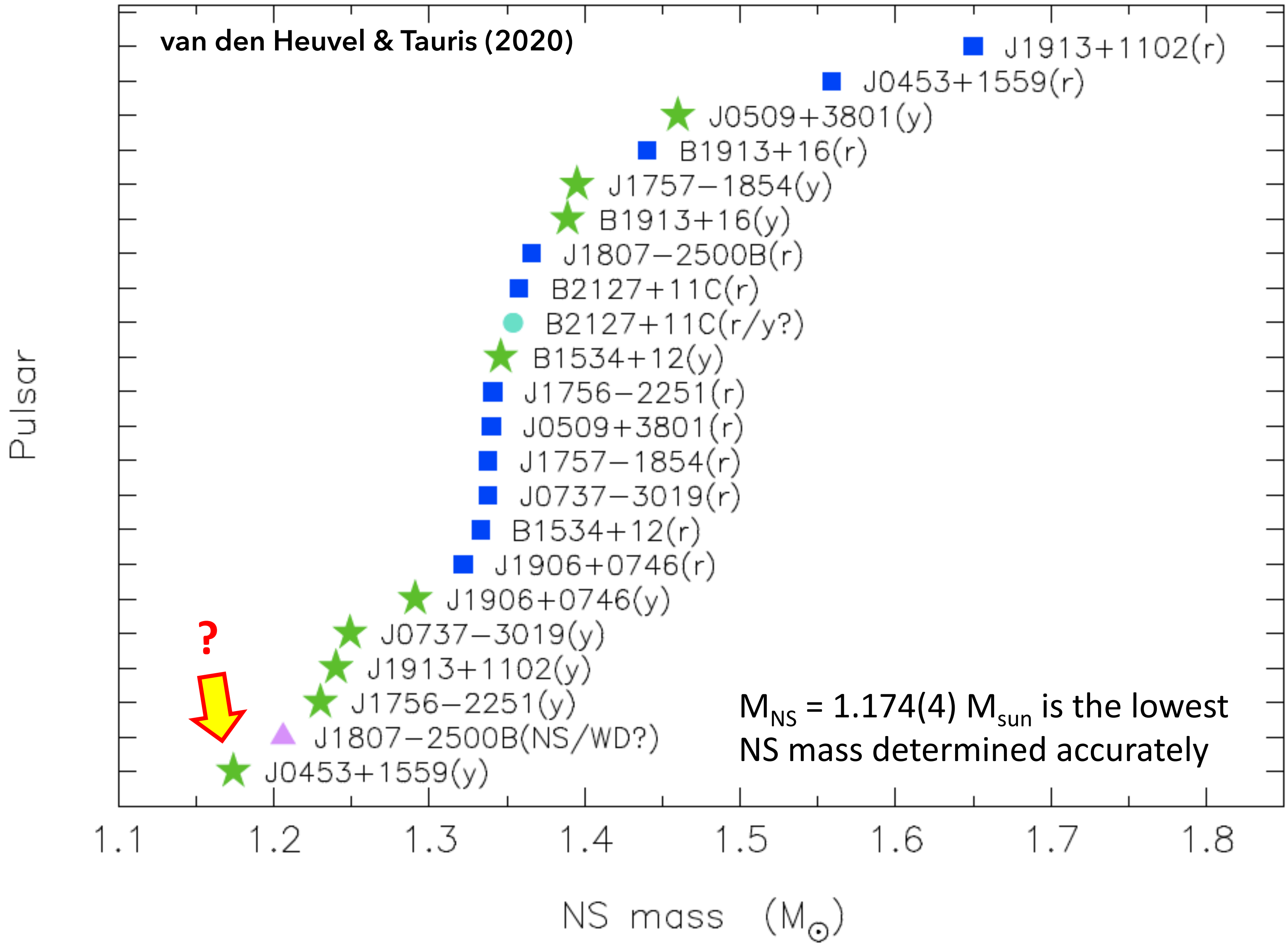

M_{NS} = 1.174(4) M_{sun} is the lowest NS mass determined accurately

PSR J0453+1559: discovered by Martinez et al. (2015).
Evidence for a DNS system: eccentricity
+ binary properties (kinematic + recycling, Tauris et al. 2017)

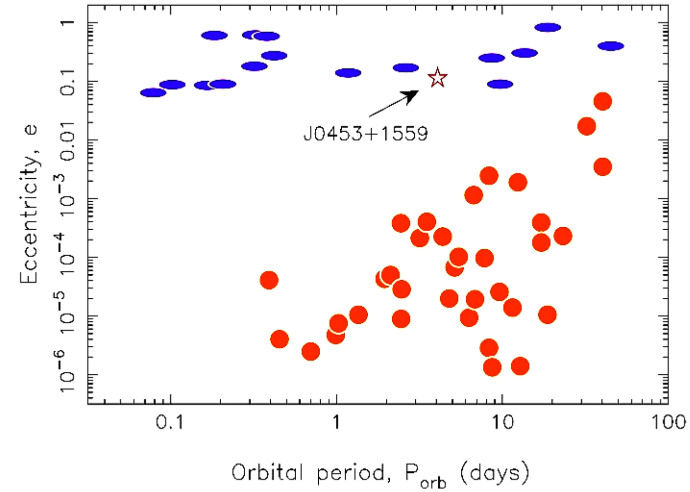

Tauris & Janka (2019), submitted
arXiv: 1909.12318

Is this instead a NS+WD system?
i.e. is the companion star e.g. an **ONeFe WD** formed in a ***thermonuclear electron-capture SN* (tECSN) event?**
(Jones et al. 2016; 2019; Kirsebom et al. 2019
- see also discussions in Nomoto & Kondo 1991)

Tauris & Janka (2019), submitted

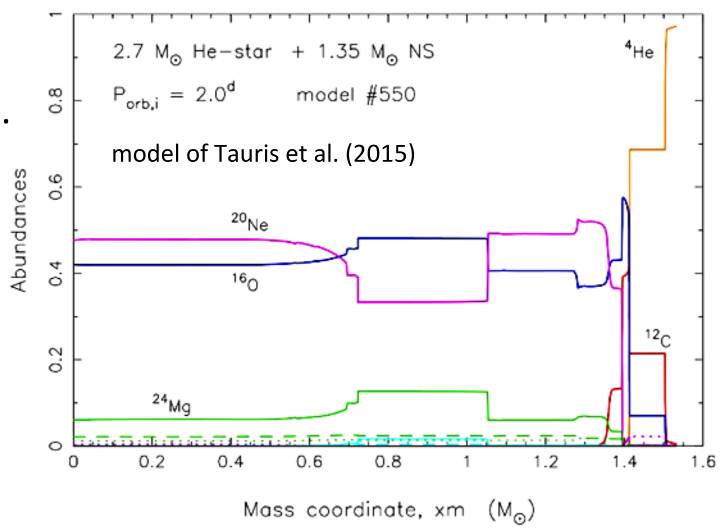

Explaining a 1.17 M_{sun} NS from stellar CC SNe is difficult.
1) Stellar evolution modeling for $M_{ZAMS} < 11\ M_{sun}$ is challenging.
ONeMg cores of super-AGB stars have M_{core} ~1.36 M_{sun} and collapse to NS gravitational masses between 1.22–1.24 M_{sun}
(Woosley & Heger 2015; Zha et al. 2019)

2) State-of-the-art **SN explosion** simulations do not support NS formation with masses below ~1.20 M_{sun}.
(Sukhbold et al. 2016; Burrows at el. 2019; Ertl et al. 2019)

Tauris & Janka (2019), submitted

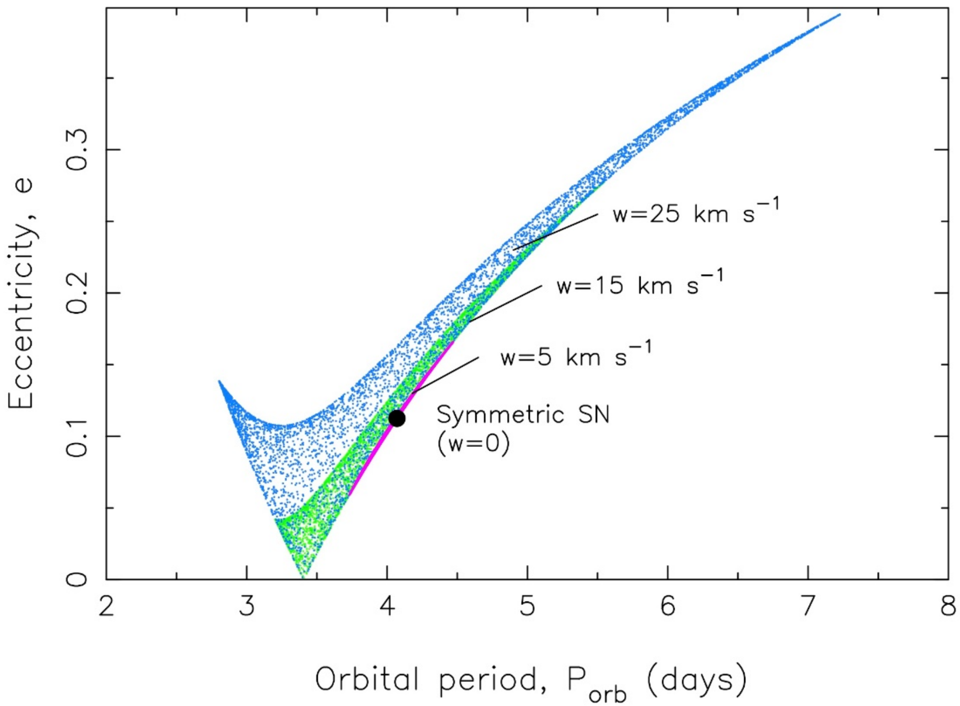

PSR J0453+1559: A NS+WD binary formed in a tECSN?

Tauris & Janka (2019), submitted

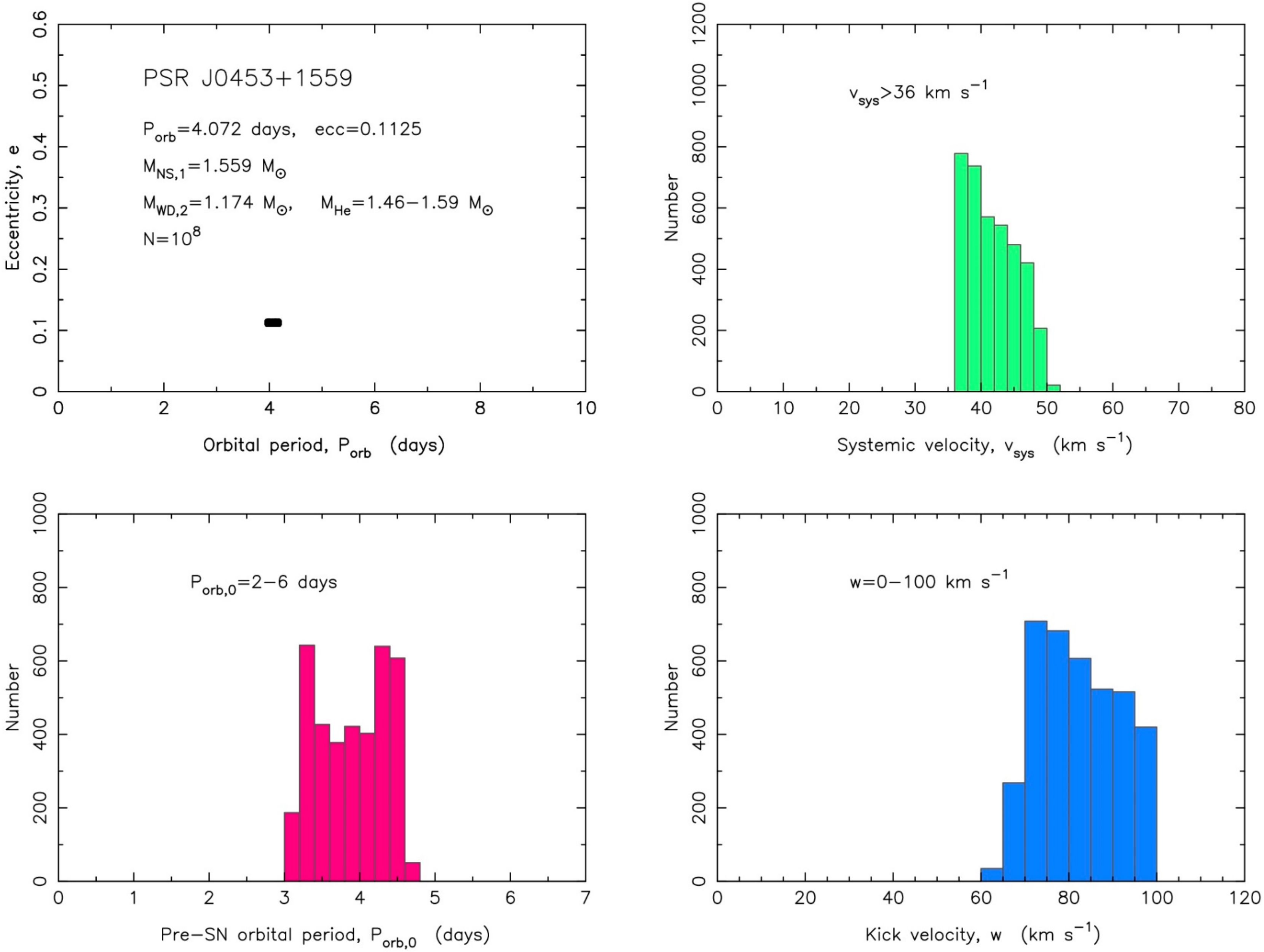

Moving atomic clocks in space!

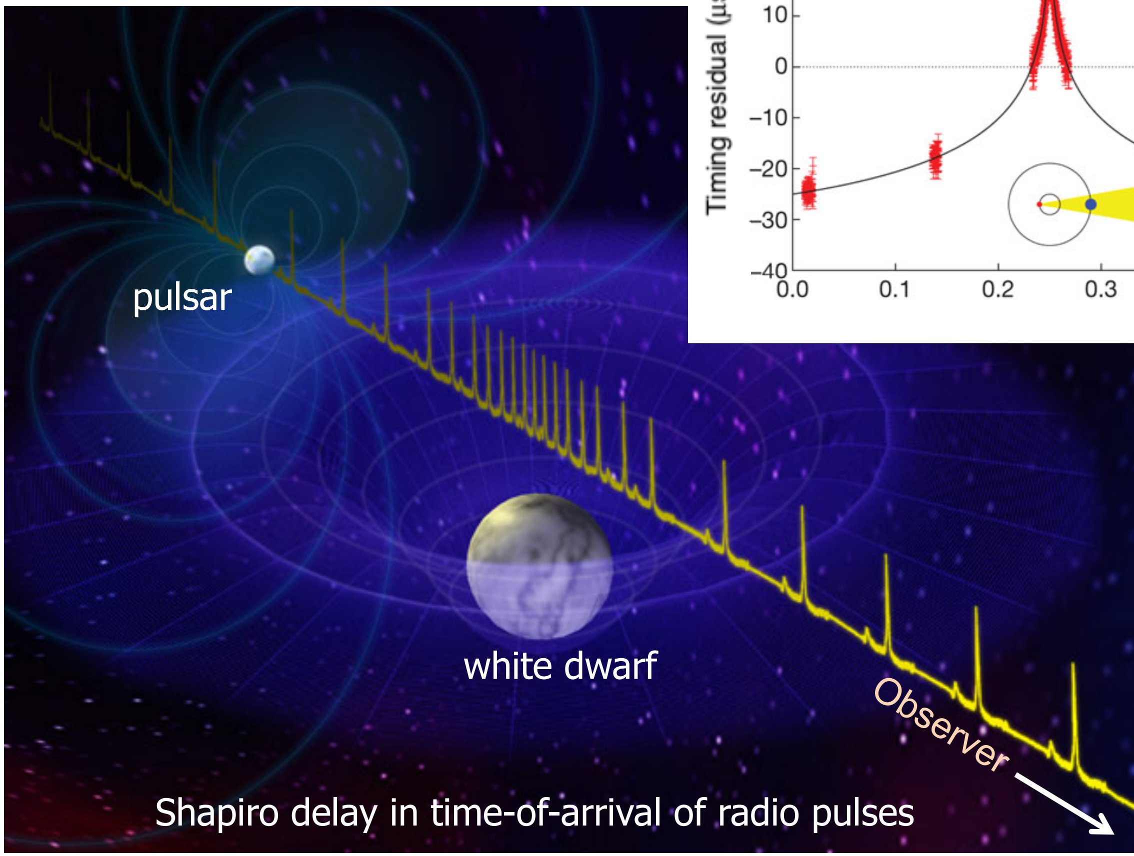

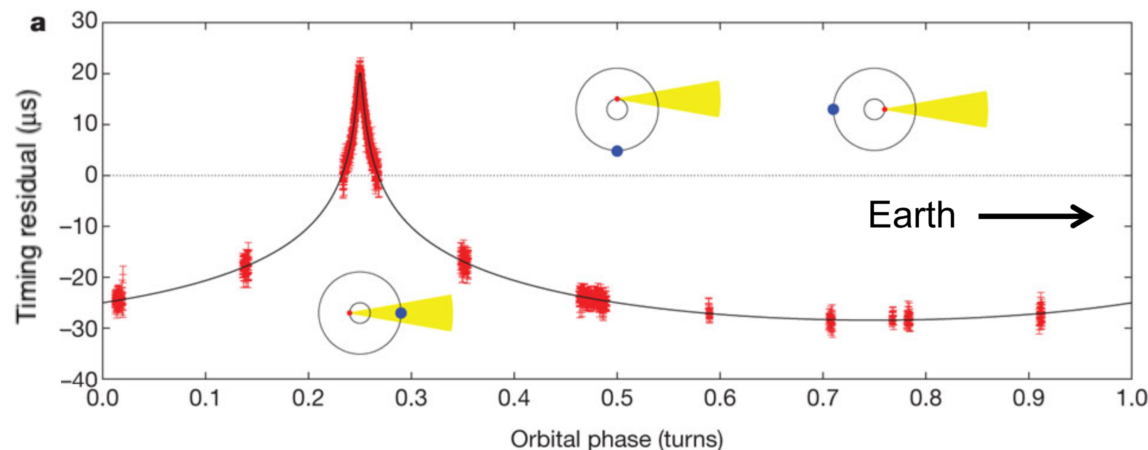

Example

<u>Demorest et al. (2010)</u>

Pulsar mass:	$1.97 \pm 0.04\ M_{sun}$
White dwarf mass:	$0.500 \pm 0.006\ M_{sun}$
Orbital period:	8.69 days
Pulsar spin period:	3.15 ms

FIRST EVER IN A BINARY STAR SYSTEM

DETECTION OF LENSE-THIRRING PRECESSION (FRAME DRAGGING)

Venkatraman Krishnan et al. (re-submitted a few weeks ago)

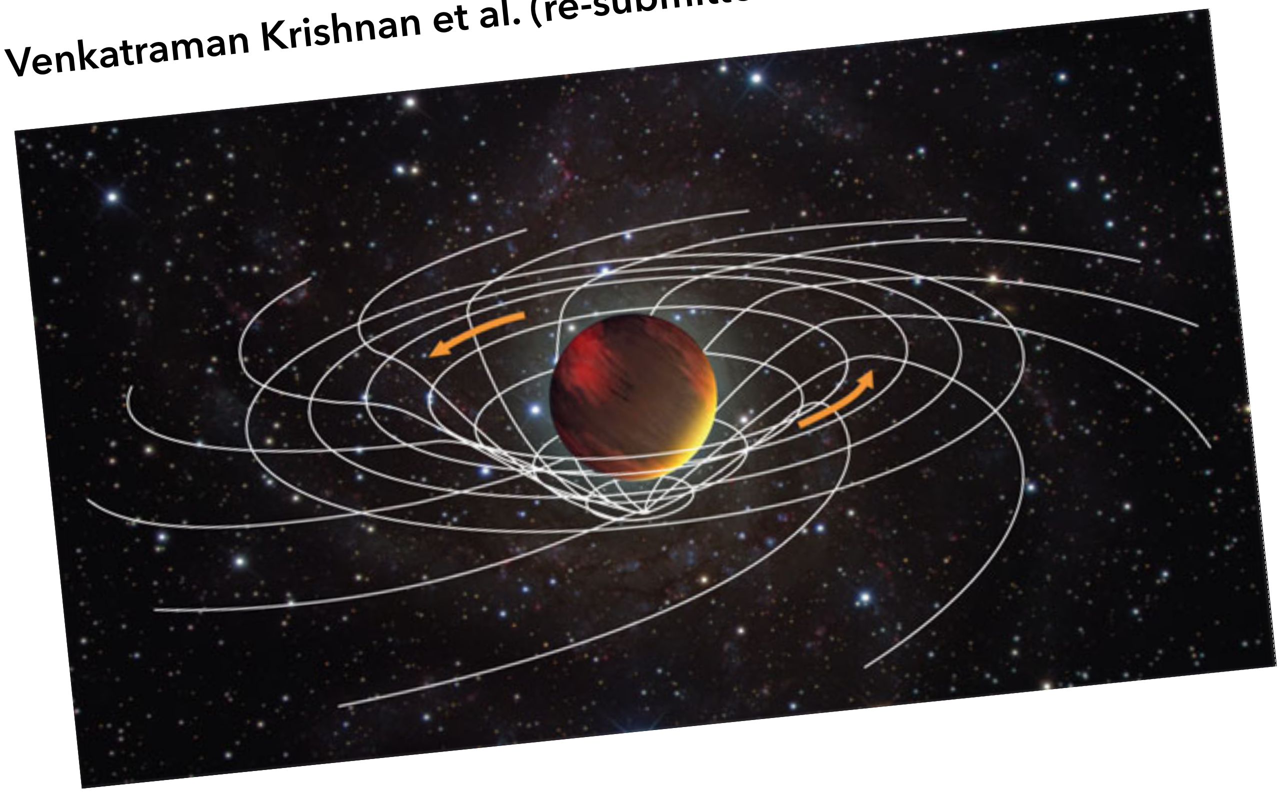

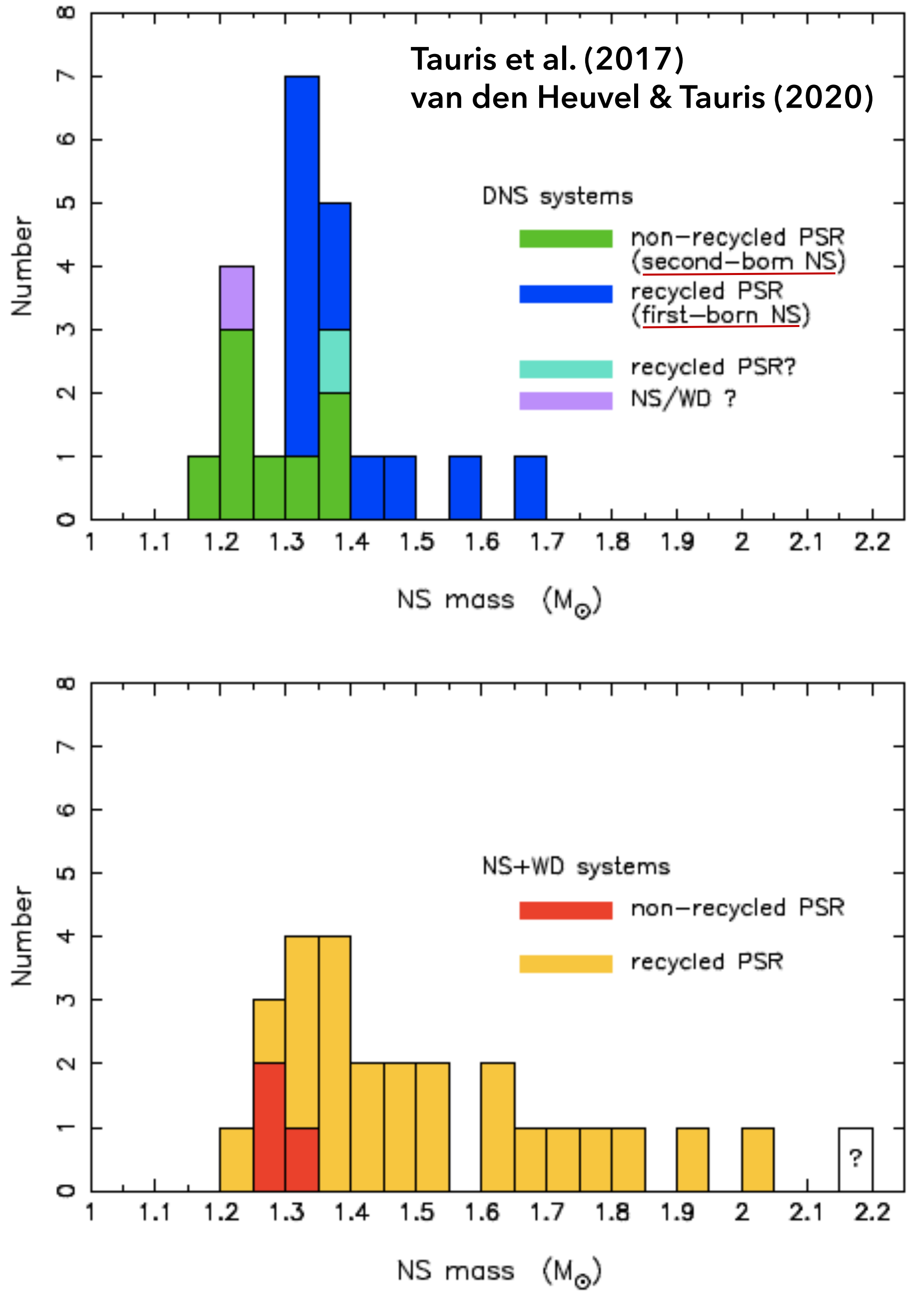

In DNS systems, the first-born NS accretes max. 0.02 M_{sun}

⇓

Measured masses of recycled NSs are close to their birth masses!

There is a difference in birth masses of 1st and 2nd born NSs.

In NS+WD sytems produced via LMXBs, the accretion phase is much longer (up to several Gyr)

However, some fully recycled NSs only have masses of ~1.3 M_{sun}.

⇓

Accretion is very *inefficient* even at sub-Eddington accretion levels.

Observed mass distribution reflects spread in NS birth masses.

Accretion of first-born NS

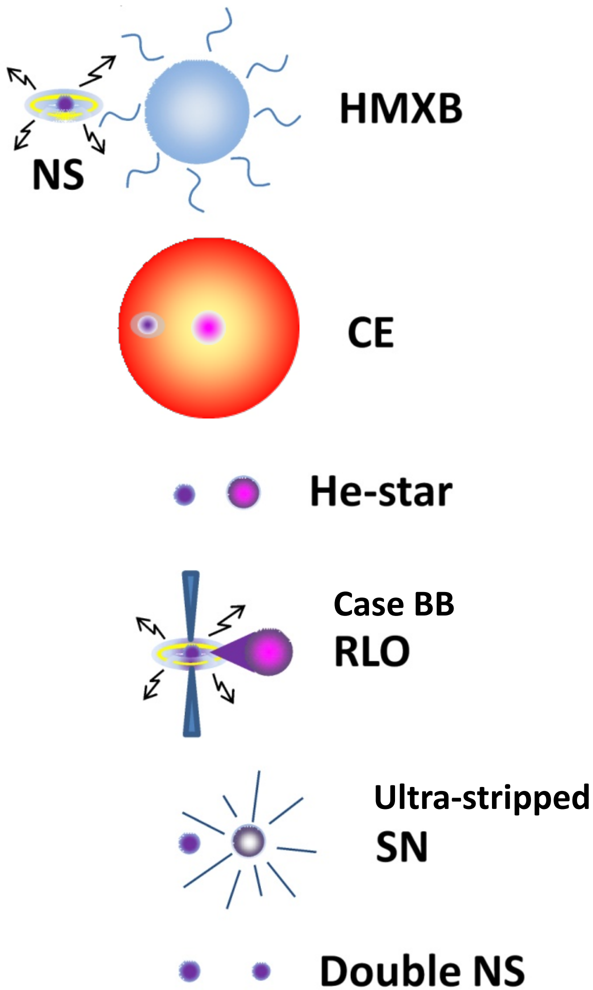

Accretion I — $\Delta M_{acc} \approx 3\times10^{-3}\ M_{\odot}$ Tauris et al. (2017)

+

Accretion II — $\Delta M_{acc} \ll 0.1\ M_{\odot}$ $(\sim 0.01\ M_{\odot})$ MacLeod & Ramirez-Ruiz (2015a,b)

+

Accretion III — $\Delta M_{acc} \approx 4\times10^{-4}\ M_{\odot}$ Tauris et al. (2017)

+

Accretion IV — $\Delta M_{acc} \approx 5\times10^{-5} - 3\times10^{-3}\ M_{\odot}$ Tauris, Langer & Podsiadlowski (2015)

+

Accretion V — $\Delta M_{acc} \ll 10^{-3}\ M_{\odot}$ Fryer et al. (2014)

In total $\boxed{\Delta M_{acc} \leq 0.02\ M_{\odot}}$

Wind accretion from (WR) He-stars

$$\dot{M}_{NS} \approx \pi R_{acc}^2 \rho v_{rel}$$

$$R_{acc} = \frac{2GM_{NS}}{v_{rel}^2 + c_s^2} \quad \wedge \quad v_{rel}^2 = v_{orb}^2 + v_{vind}^2$$

$$v_{wind} \approx v_{esc} = \sqrt{2GM_{He} / R_{He}} > 10^3 \ km\, s^{-1} \quad (v_{wind} \gg v_{orb})$$

$$v_{wind} > c_s \quad c_s = \sqrt{\gamma \frac{P}{\rho}} \approx 10 \left(\frac{T}{10^4 \ K} \right)^{1/2} km\, s^{-1}$$

$$\dot{M}_{He} \approx 4\pi a^2 \rho v_{rel}$$

$$\Rightarrow \quad \dot{M}_{NS} = \frac{(GM_{NS})^2}{a^2 v_{wind}^4} \dot{M}_{He}$$

$$\dot{M}_{NS} \approx 10^{-5} - 10^{-4} \dot{M}_{He}$$

$$M_{He} = 3.5 \ M_\odot \quad M_{NS} = 1.35 \ M_\odot$$

$$P_{orb} = 2.0 \ d \quad (a = 11.3 \ R_\odot)$$

$$v_{wind} = 500 - 1600 \ km\, s^{-1} \quad (10^3 \ km\, s^{-1})$$

$$\Rightarrow \quad \dot{M}_{He} \approx 5 \times 10^{-7} \ M_\odot \ yr^{-1}$$

$$\Rightarrow \quad \dot{M}_{NS} \approx 3 \times 10^{-10} \ M_\odot \ yr^{-1}$$

$$\Rightarrow \quad \Delta M_{NS} \approx 4 \times 10^{-4} \ M_\odot$$

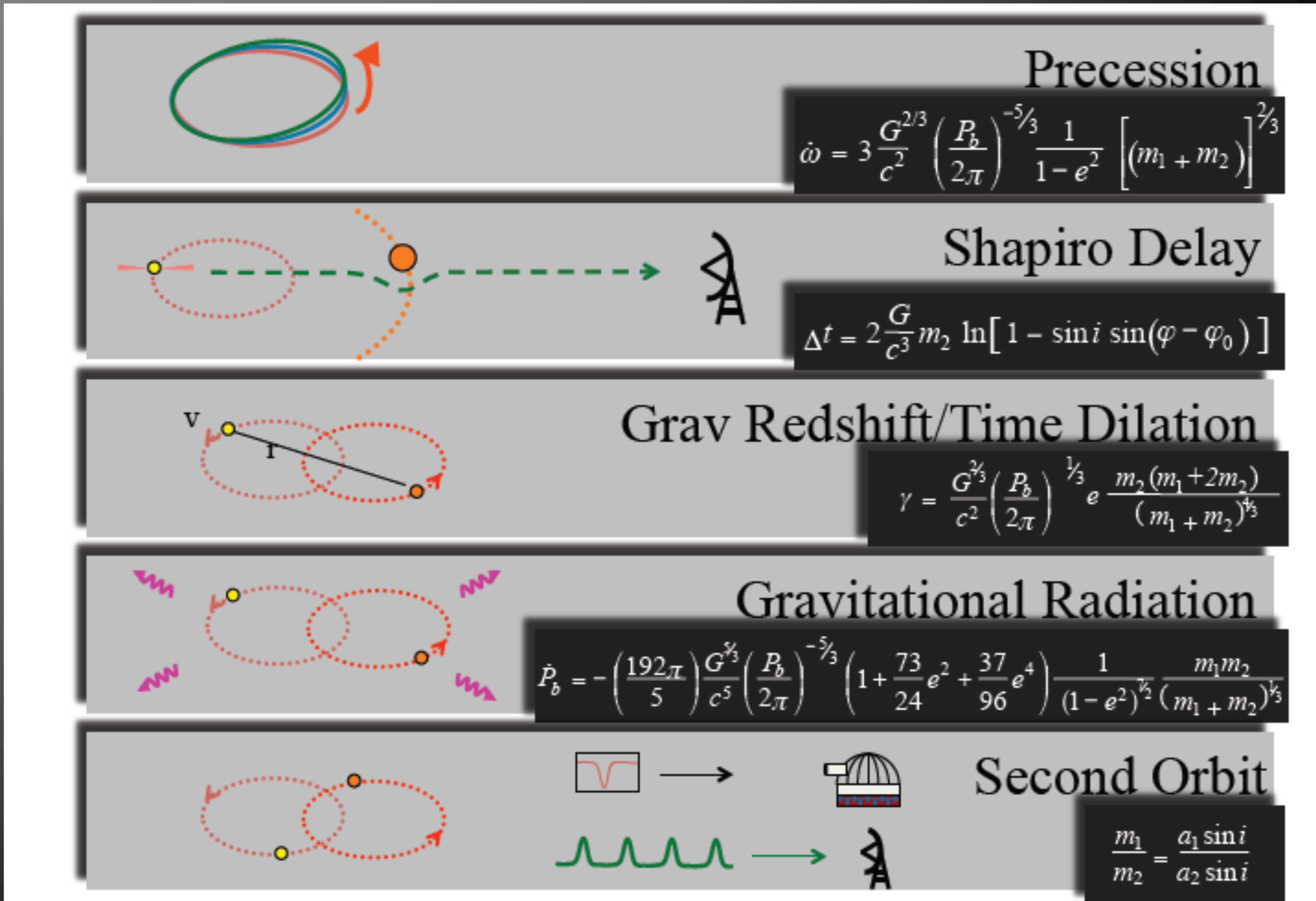

Any PK measurement yields a line in the (m_1,m_2)-plane.
Hence, two PK parametres determines m_1 and m_2 uniquely.

Kruckow et al. (2018)

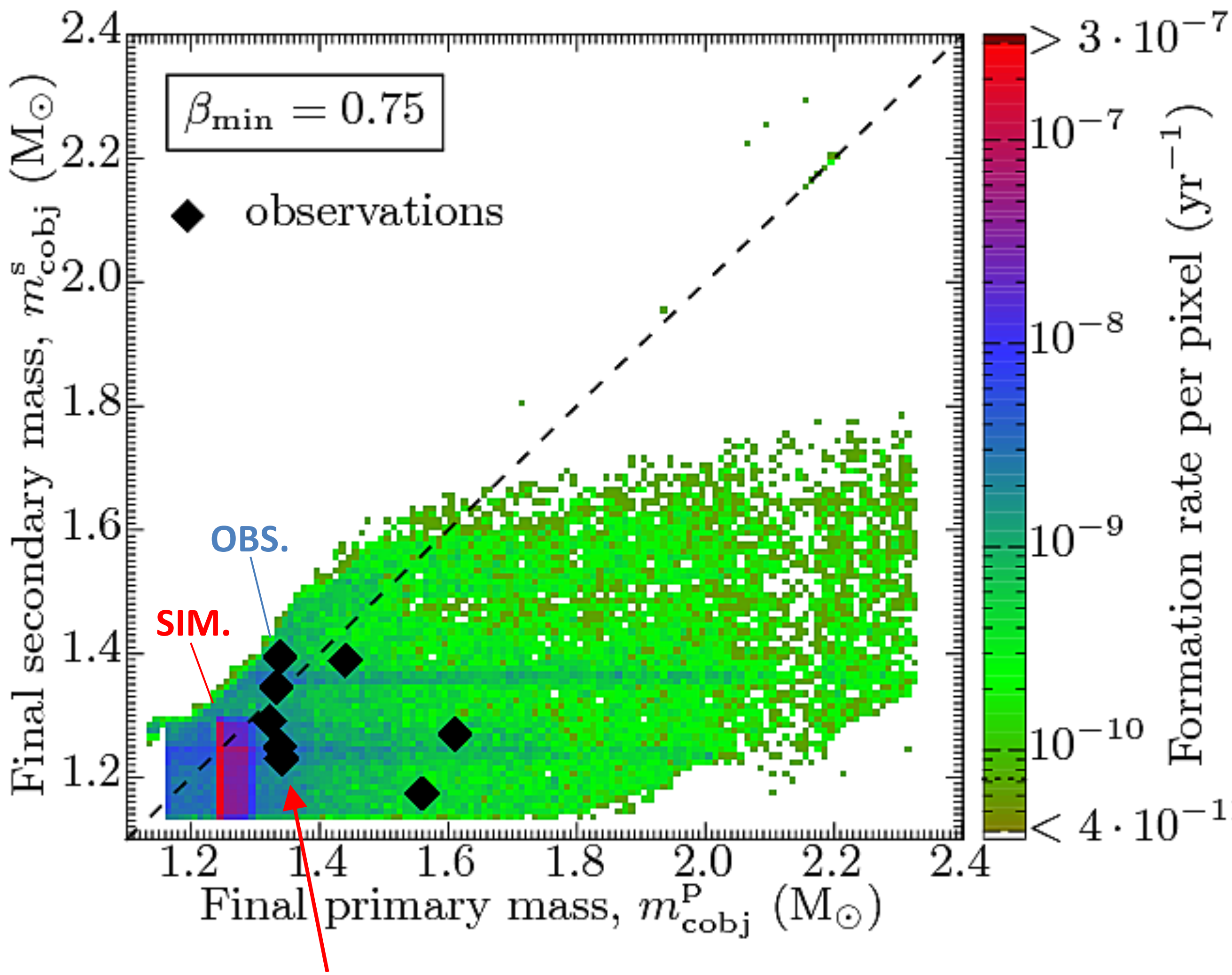

Binary effects!

1st SN: wide binary to survive later CE (small kick is often from ECNSe)

2nd SN: tight binary to produce merger (larger kicks are ok)

Do ECSNe produce NSs which are more massive by ~ 0.06 M_{sun} ? (after correction for accretion)

PROPERTIES OF DOUBLE NS MERGERS: SPINS and ORBITAL PERIODS

Tauris et al. (2017), ApJ + updated data

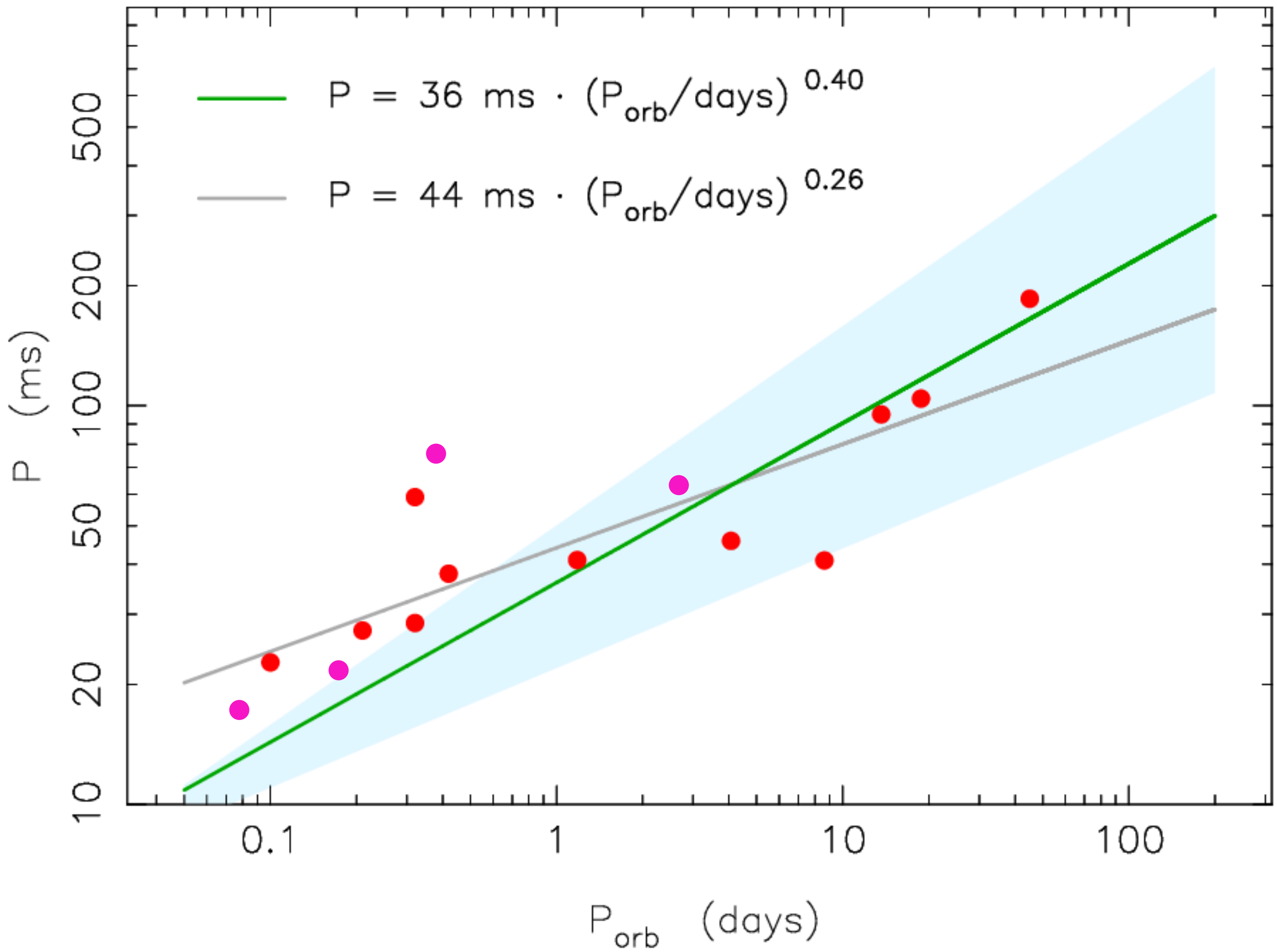

Tauris et al. (2017), ApJ 846, 170

The Astrophysical Journal, 846:170 (58pp), 2017 September 10 https://doi.org/10.3847/1538-4357/aa7e89

Formation of Double Neutron Star Systems

T. M. Tauris[1,2], M. Kramer[1], P. C. C. Freire[1], N. Wex[1], H.-T. Janka[3], N. Langer[2], Ph. Podsiadlowski[2,4], E. Bozzo[5], S. Chaty[6,7], M. U. Kruckow[2], E. P. J. van den Heuvel[8], J. Antoniadis[1,9], R. P. Breton[10], and D. J. Champion[1]

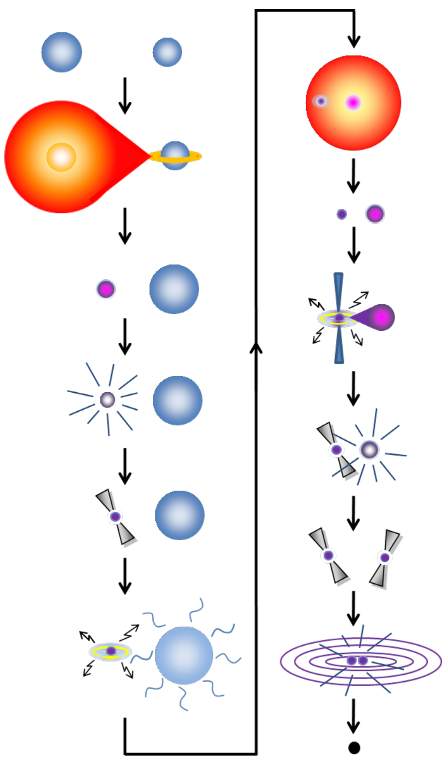

Tauris et al. (2017), ApJ

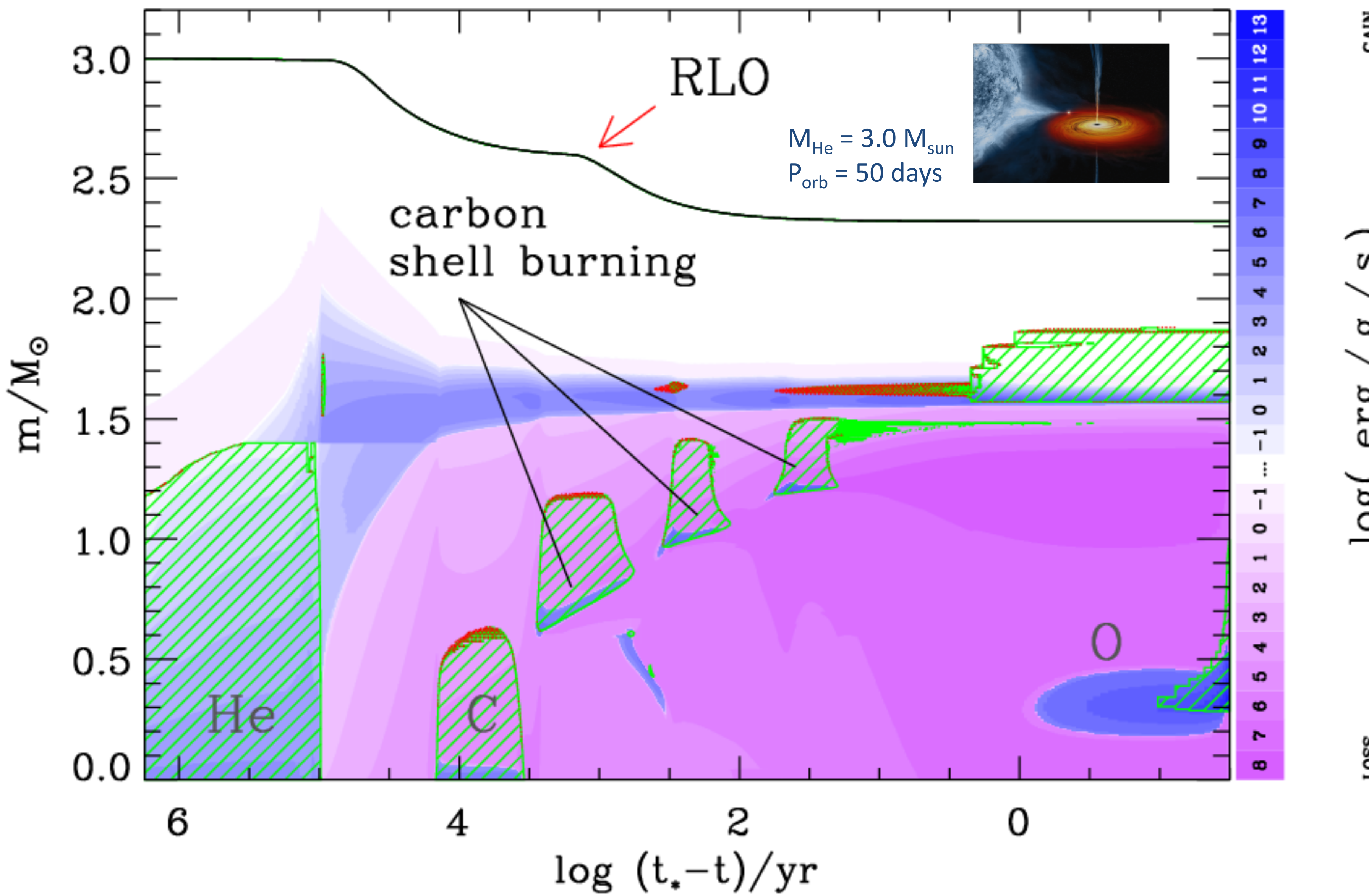

PROPERTIES OF DOUBLE NS MERGERS: SPINS and ORBITAL PERIODS

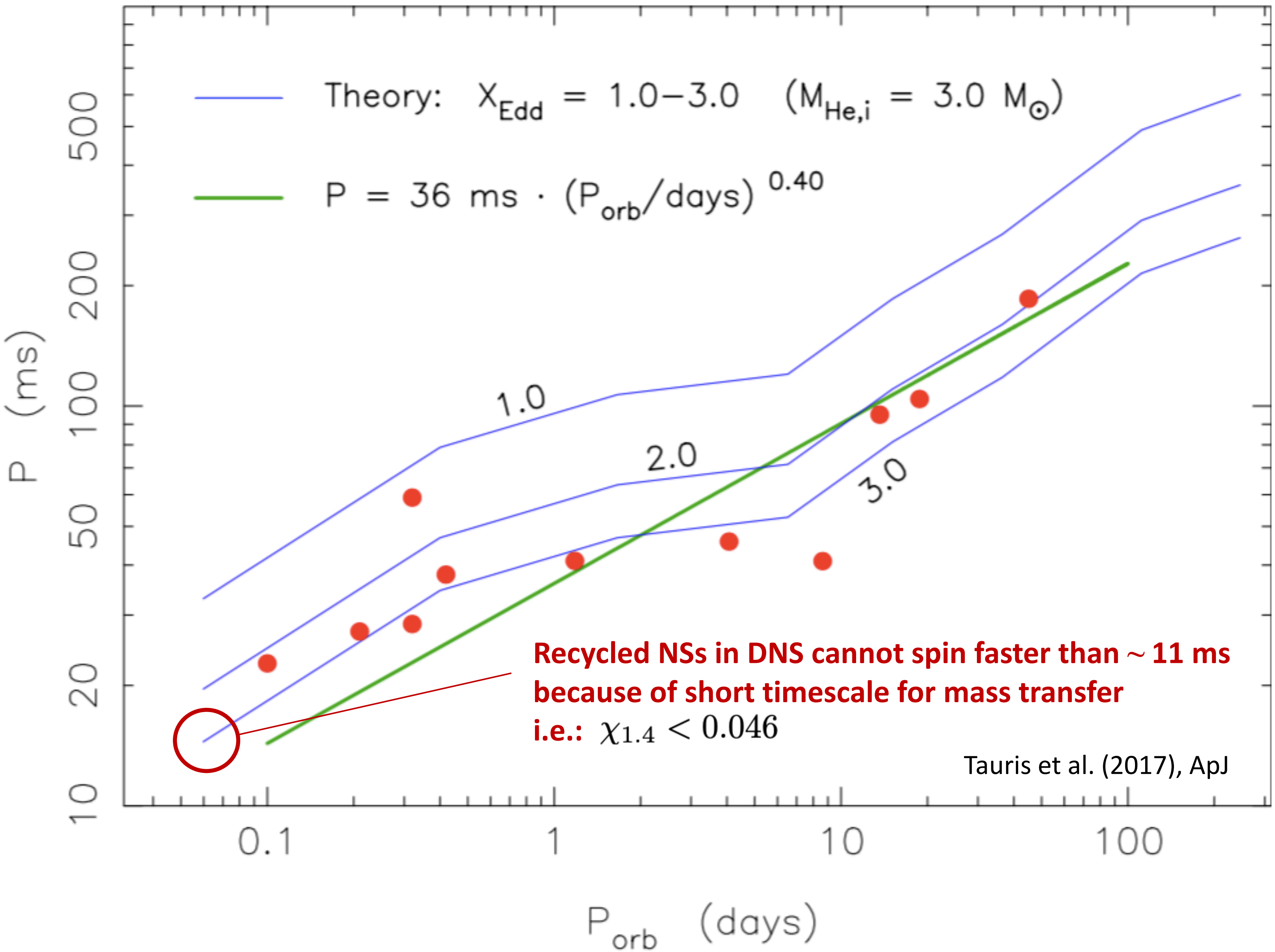

Recycled NSs in DNS cannot spin faster than ~ 11 ms because of short timescale for mass transfer i.e.: $\chi_{1.4} < 0.046$

Tauris et al. (2017), ApJ

Assuming symmetric SNe and different initial helium star donors

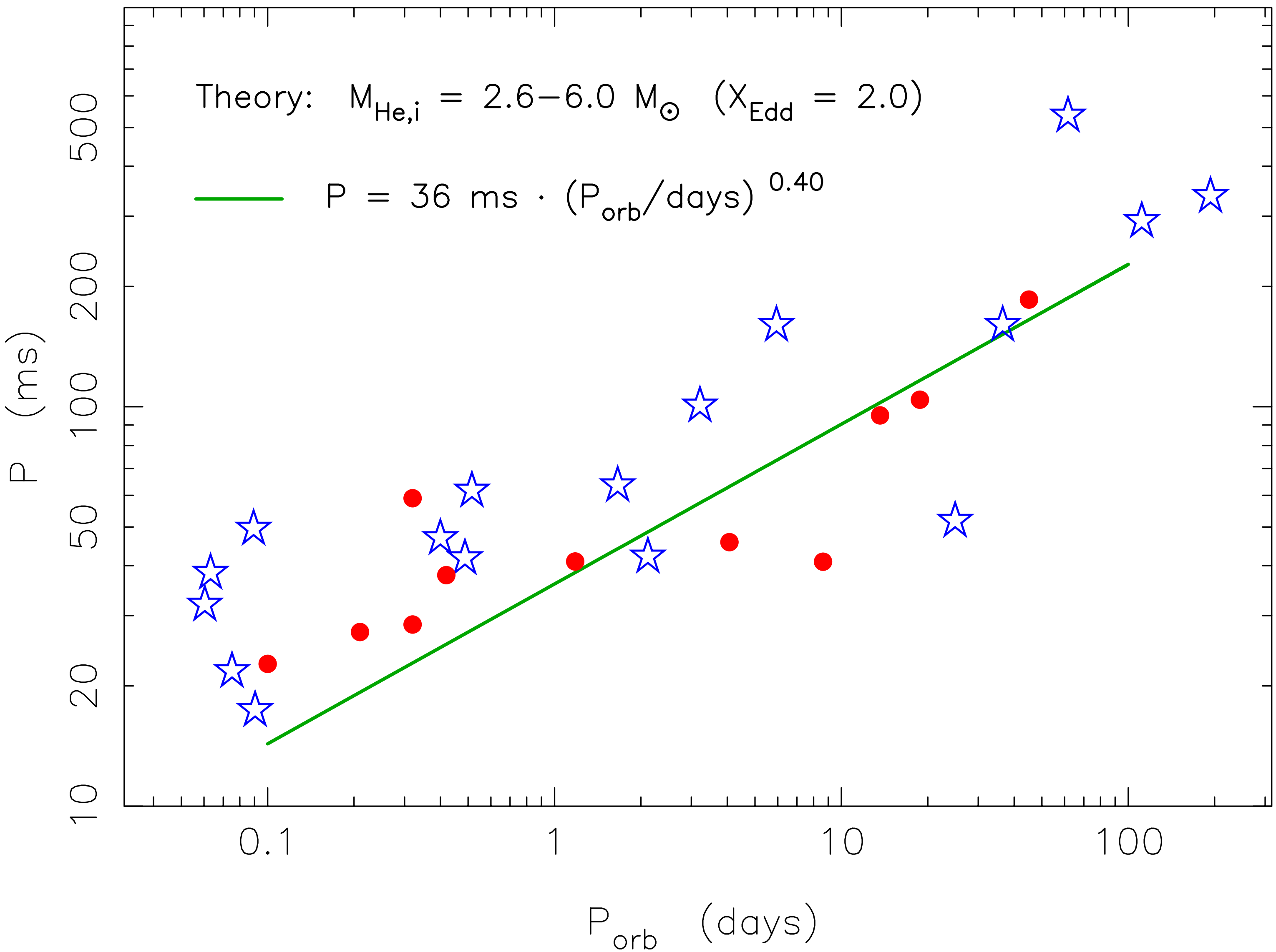

Assuming asymmetric SNe with isotropic kicks of 50 km s^{-1} and same initial helium star donor

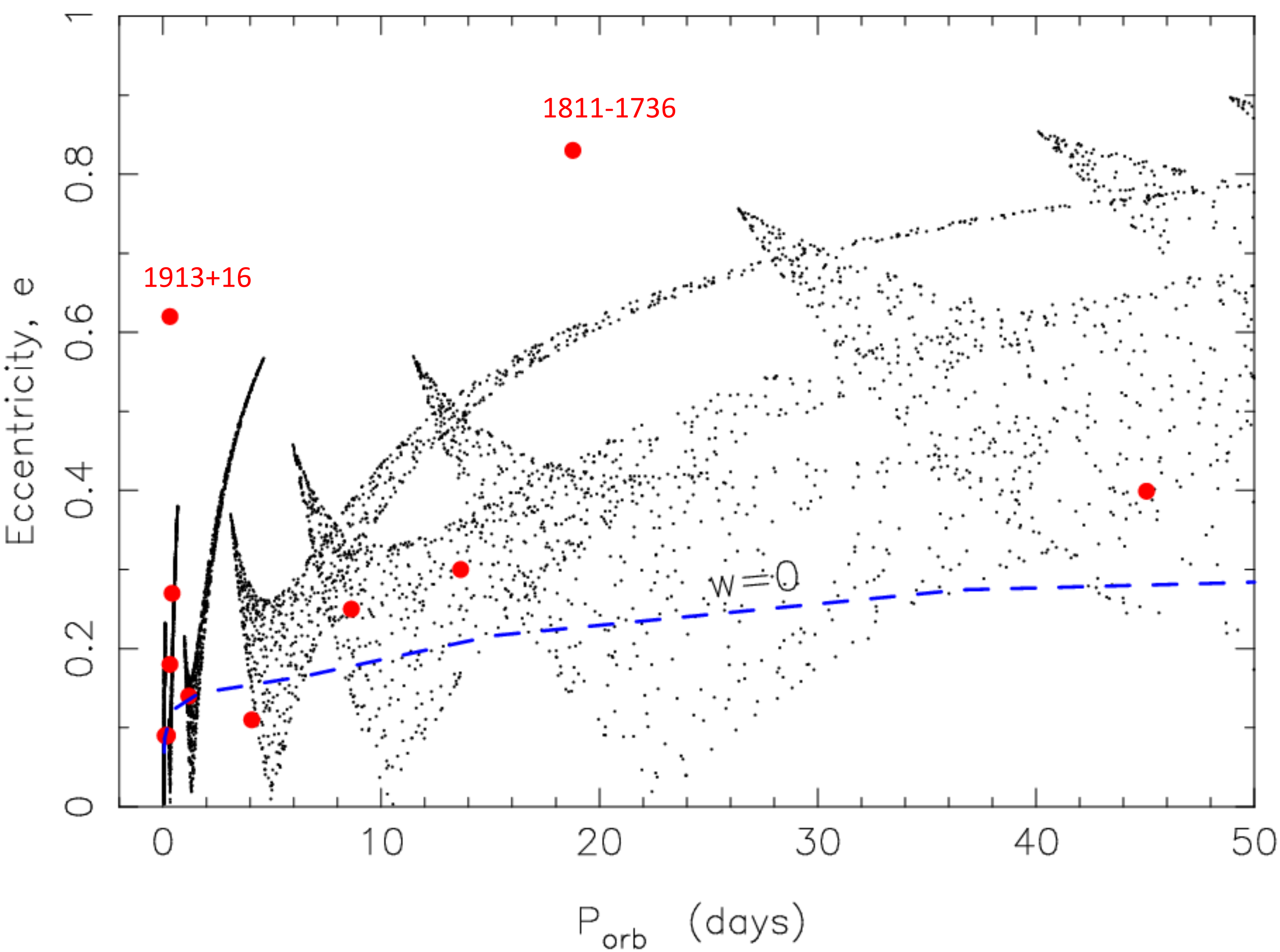

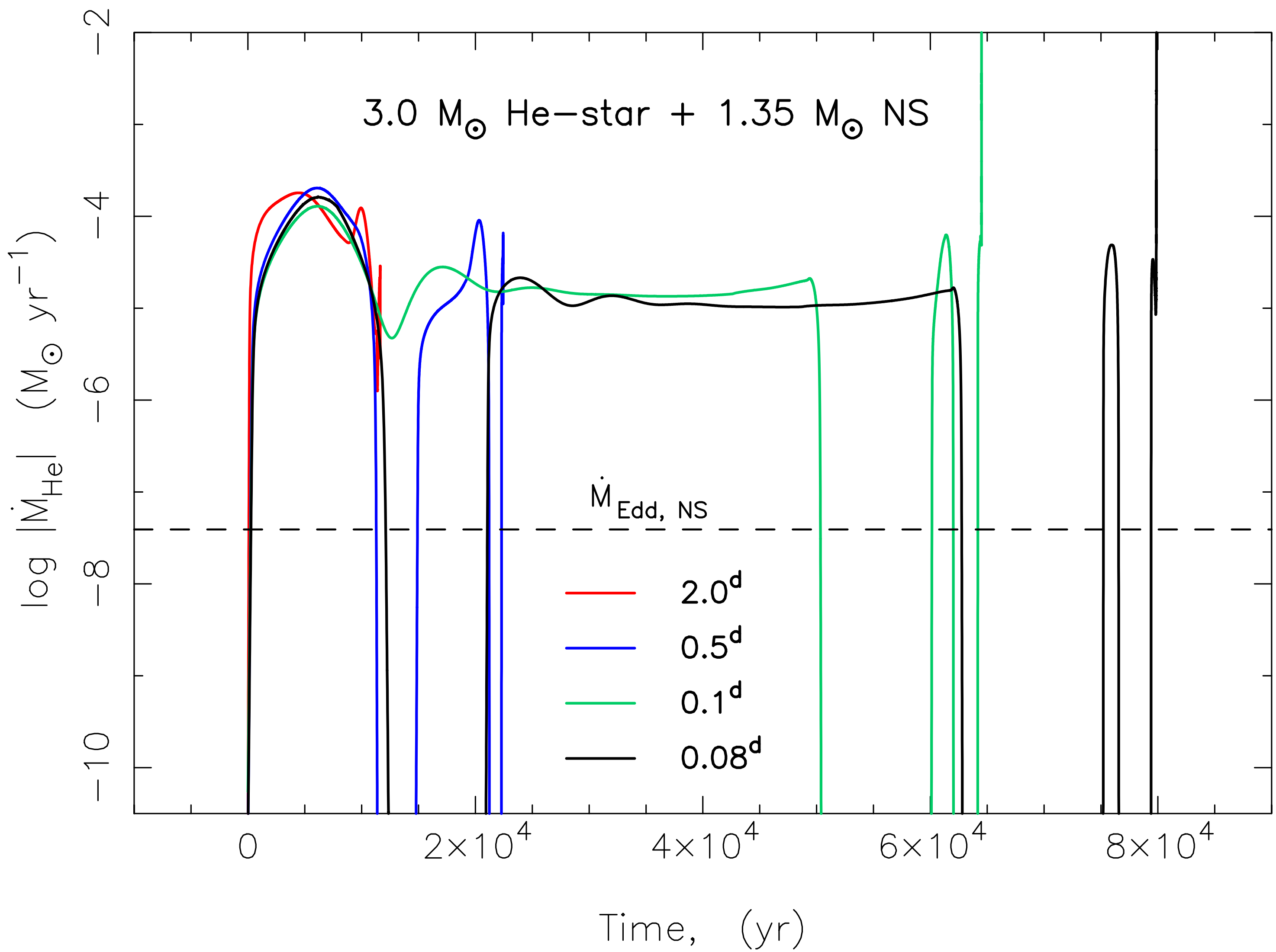

3.0 M⊙ He–star + 1.35 M⊙ NS
log |Ṁ_He| (M⊙ yr⁻¹)
−2
−4
−6
−8
−10
Ṁ Edd, NS
2.0^d
0.5^d
0.1^d
0.08^d
0
2×10^4
4×10^4
6×10^4
8×10^4
Time, (yr)

van den Heuvel & Tauris (2020)

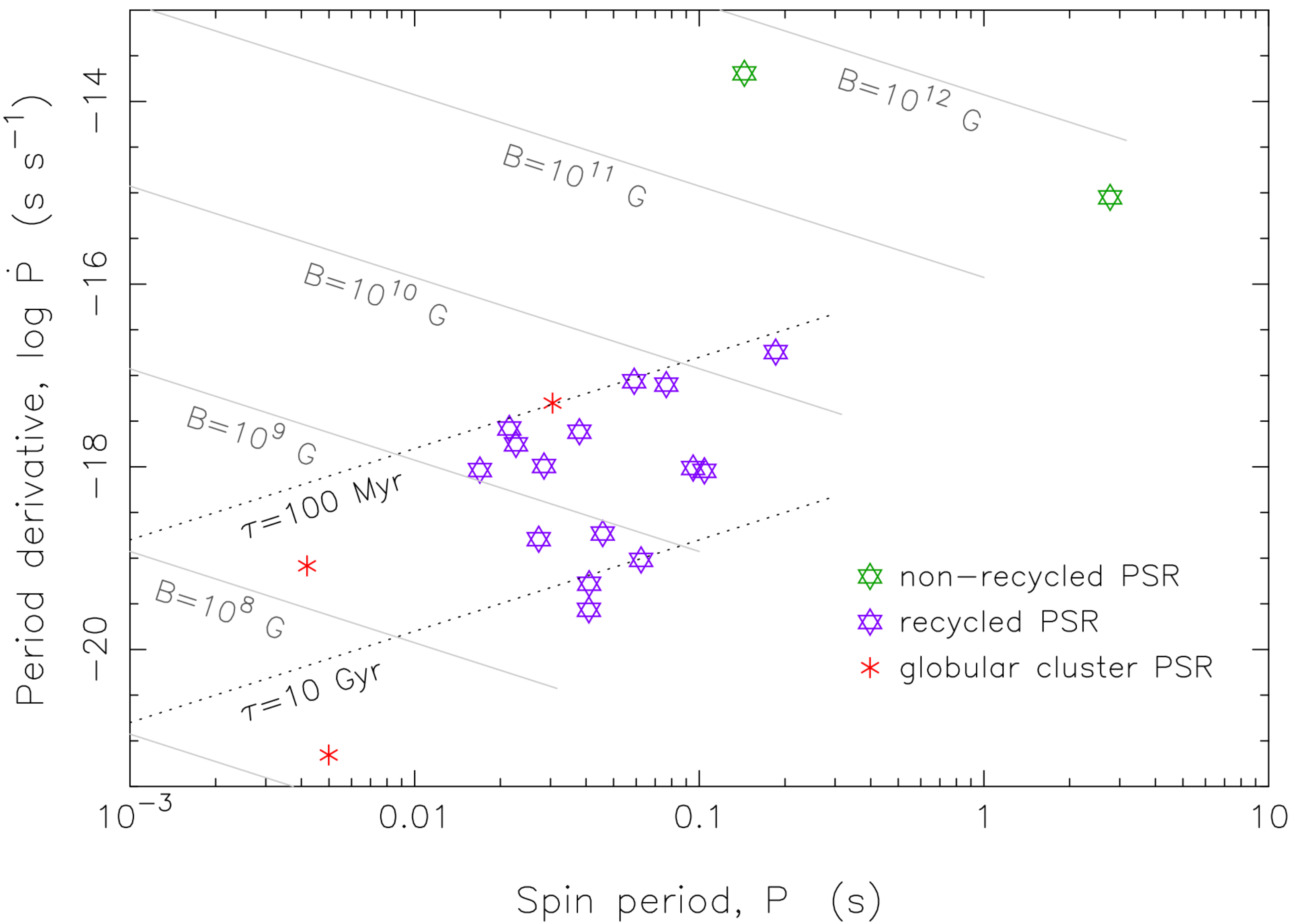

van den Heuvel & Tauris (2020)

Table 1.4: Properties of 20 DNS systems with published data (including a few unconfirmed candidates).

Radio Pulsar	Type	P (ms)	$\dot{P}$ (10^{-18})	B (10^9 G)	$P_{\rm orb}$ (days)	e	$M_{\rm psr}$ ($M_\odot$)	$M_{\rm comp}$ ($M_\odot$)	$M_{\rm total}$ ($M_\odot$)	δ (deg)	Dist. (kpc)	$v^{\rm LSR}$ ** (km s^{-1})	$\tau_{\rm gwr}$ (Myr)
J0453+1559[a]	recycled	45.8	0.186	1.1	4.072	0.113	1.559	1.174	2.734	–	1.07	82	∞
J0509+3801[b]	recycled	76.5	7.93	7.2	0.380	0.586	~ 1.34	~ 1.46	2.805	–	1.56	–	579
J0737−3039A[c]	recycled	22.7	1.76	1.8	0.102	0.088	1.338	1.249	2.587	< 3.2	1.15	32	86
J0737−3039B[c]	young	2773.5	892	410	−‖−	−‖−	1.249	1.338	−‖−	130 ± 1	−‖−	−‖−	−‖−
J1411+2551[d]	recycled	62.5	0.0956	0.66	2.616	0.170	< 1.62	> 0.92	2.538	–	1.13	–	∞
J1518+4904[e]	recycled	40.9	0.0272	0.33	8.634	0.249	***	***	2.718	–	0.63	30	∞
B1534+12[f]	recycled	37.9	2.42	2.8	0.421	0.274	1.333	1.346	2.678	27 ± 3	1.05	143	2730
J1753−2240[g]	recycled	95.1	0.970	2.5	13.638	0.304	–	–	–	–	3.46	–	∞
J1755−2550[h]*	young	315.2	–	270	9.696	0.089	–	> 0.40	–	–	10.3	–	∞
J1756−2251[i]	recycled	28.5	1.02	1.6	0.320	0.181	1.341	1.230	2.570	< 34	0.73	39****	1660
J1757−1854[j]	recycled	21.5	2.63	2.2	0.184	0.606	1.338	1.395	2.733	–	19.6	–	76
J1811−1736[k]	recycled	104.2	0.901	2.7	18.779	0.828	< 1.64	> 0.93	2.57	–	5.93	–	∞
J1829+2456[l]	recycled	41.0	0.0525	0.42	1.176	0.139	< 1.38	> 1.22	2.59	–	0.74	–	∞
J1906+0746[m]*	young	144.1	20300	470	0.166	0.085	1.291	1.322	2.613	–	7.40	–	309
J1913+1102[n]	recycled	27.3	0.161	0.83	0.206	0.090	~ 1.65	~ 1.24	2.888	–	–	–	470
B1913+16[o]	recycled	59.0	8.63	7.3	0.323	0.617	1.440	1.389	2.828	18 ± 6	9.80	241	301
J1930−1852[p]	recycled	185.5	18.0	16	45.060	0.399	< 1.32	> 1.30	2.59	–	1.5	–	∞
J1946+2052[q]	recycled	17.0	0.92	1.0	0.078	0.064	< 1.31	> 1.18	2.50	–	1.5	–	46
J0514−4002A[r]*	GC	5.0	0.00070	0.016	18.79	0.888	~ 1.25	~ 1.22	2.473	–	12.1	–	∞
J1807−2459B[s]*	GC	4.2	0.0823	0.18	9.957	0.747	1.366	1.206	2.572	–	3.0	–	∞
B2127+11C[t]	GC	30.5	4.99	3.7	0.335	0.681	1.358	1.354	2.713	–	12.9	–	217

Globular cluster sources! These NSs were most likely recycled in LMXBs (WD progenitors as donor stars) which were afterwards disrupted and the recycled NSs were paired with other NSs.

9/10 Galactic DNS mergers are from isolated binaries
(1/10 are in globular clusters)

LIGO DNS merger rate density: 1520 Gpc^{-3} yr^{-1} $\Rightarrow$ 150-450 Myr^{-1} MWEG^{-1}
i.e. at least ~7000 DNSs in the MW in the pipeline with $\tau_{\rm GW}$ < 46 Myr SCIENCE FICTION!!

POPULATION SYNTHESIS: CALIBRATION

Eccentricity, e

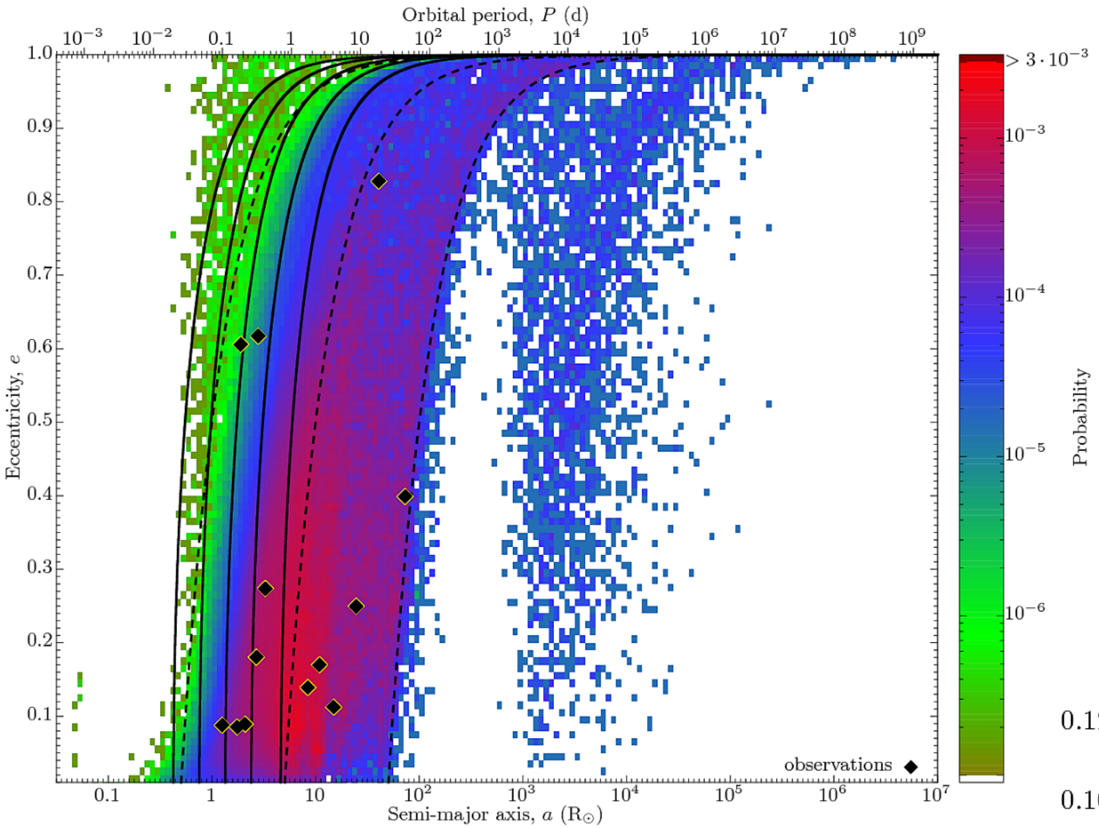

Semi-major axis, a (R_{sun})

Kruckow, Tauris, et al. (2018), MNRAS

Important calibration data!!!

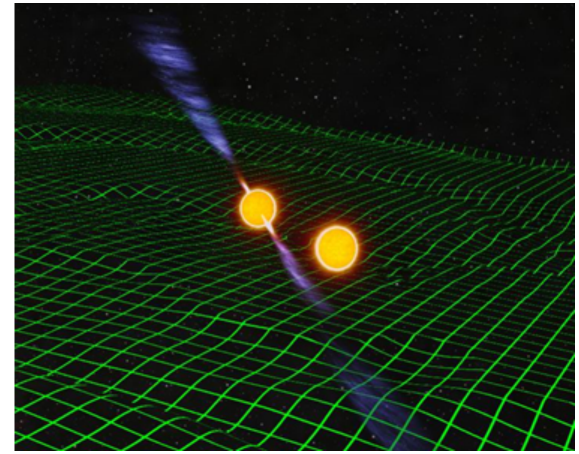

Do not trust population synthesis if it cannot reproduce observed Galactic DNS systems

NS mass ratios

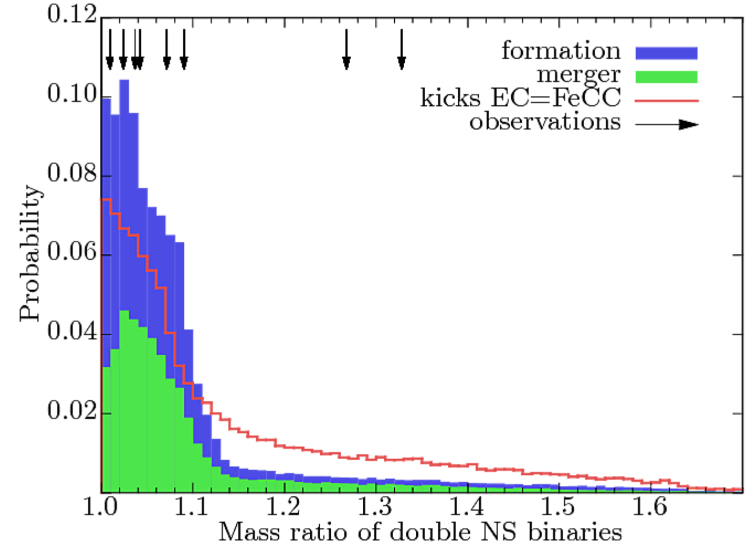

@design sensitivity: 1–5 detections per yr

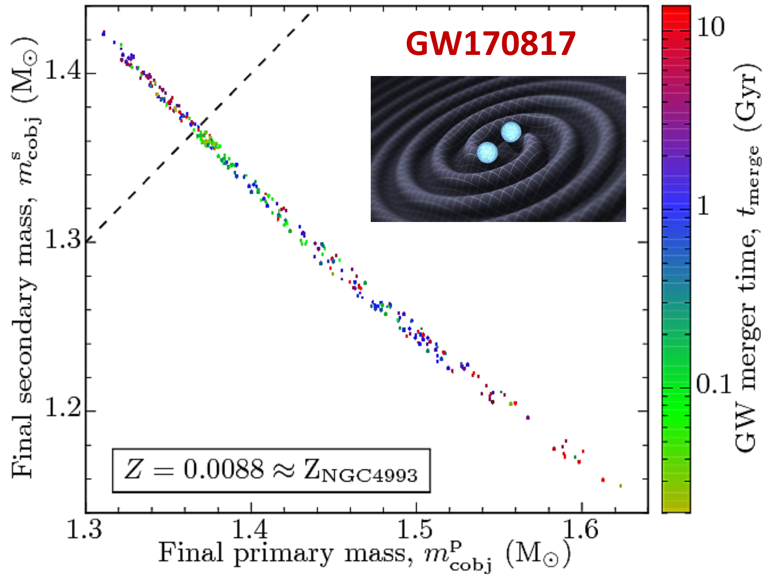

Delay time

Kruckow, Tauris, et al. (2018), MNRAS

We find age solutions from <100 Myr to >10 Gyr

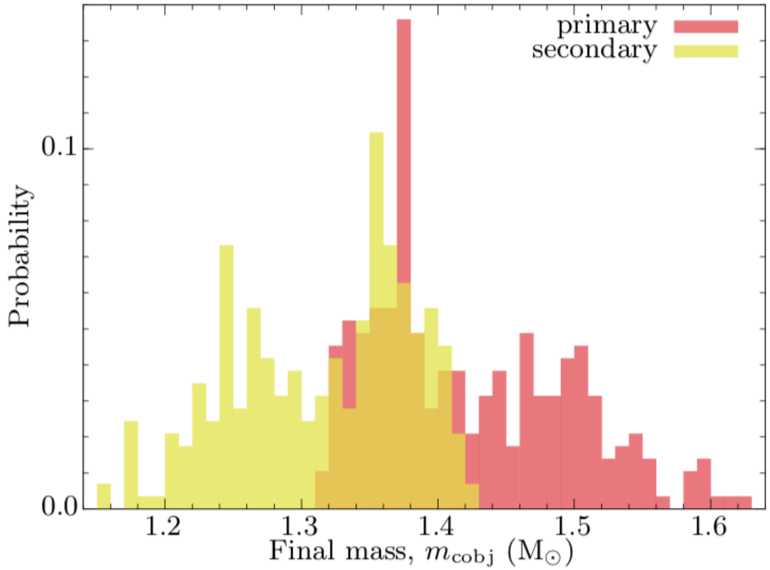

Our NS mass solutions for GW170817 are typical for Galactic DNS systems

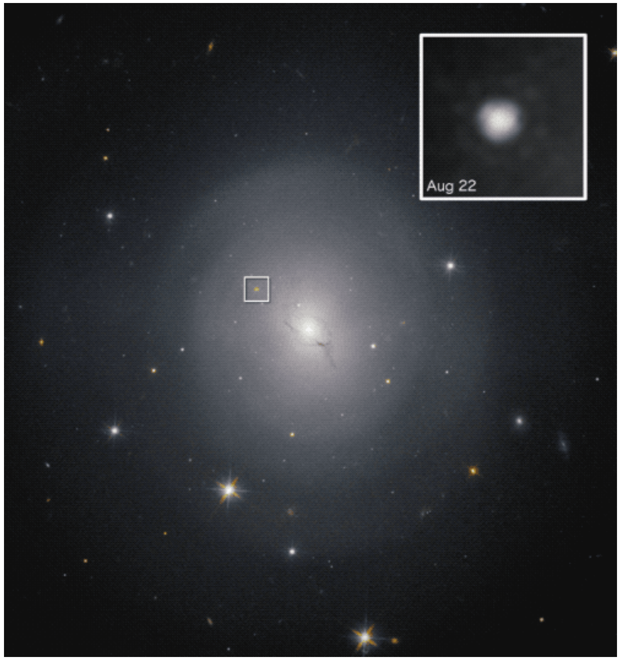

NGC 4993

Kruckow et al. (2018), MNRAS

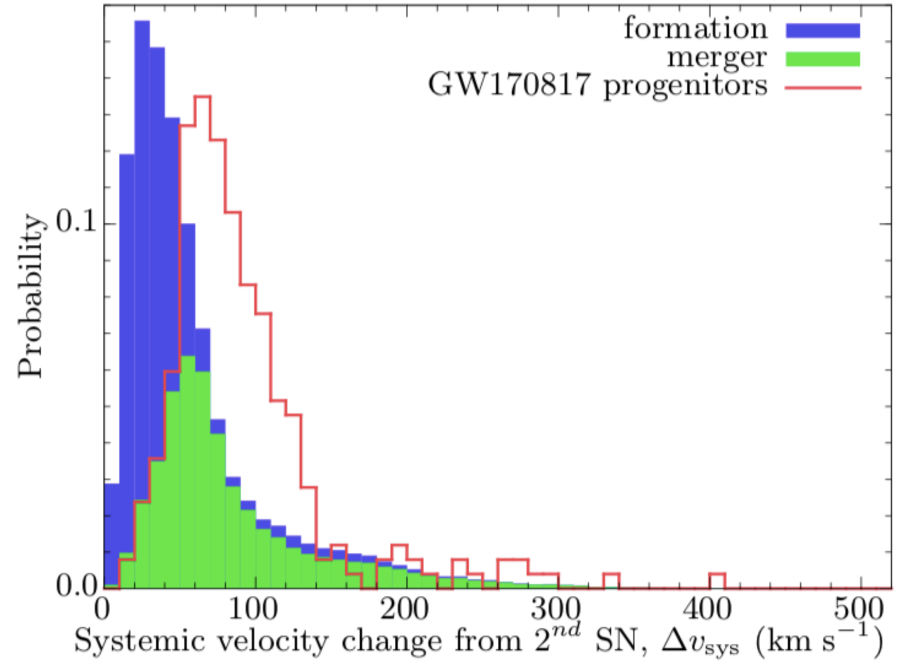

For NGC 4393, the escape velocity at the location of GW170817 is about 350 km s^{-1} (Pan et al. 2017), much larger than the typical systemic velocities we obtain in our simulations.

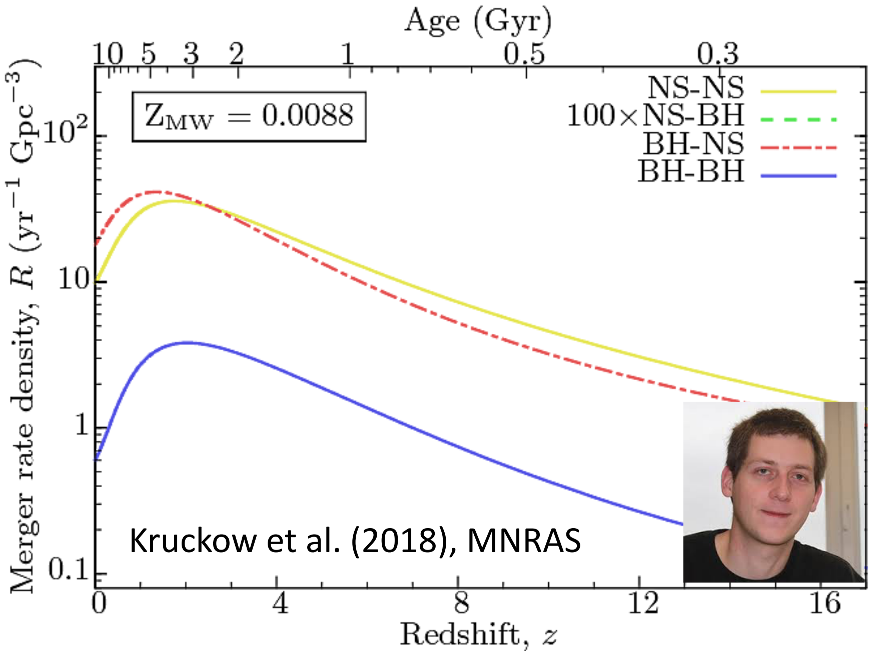

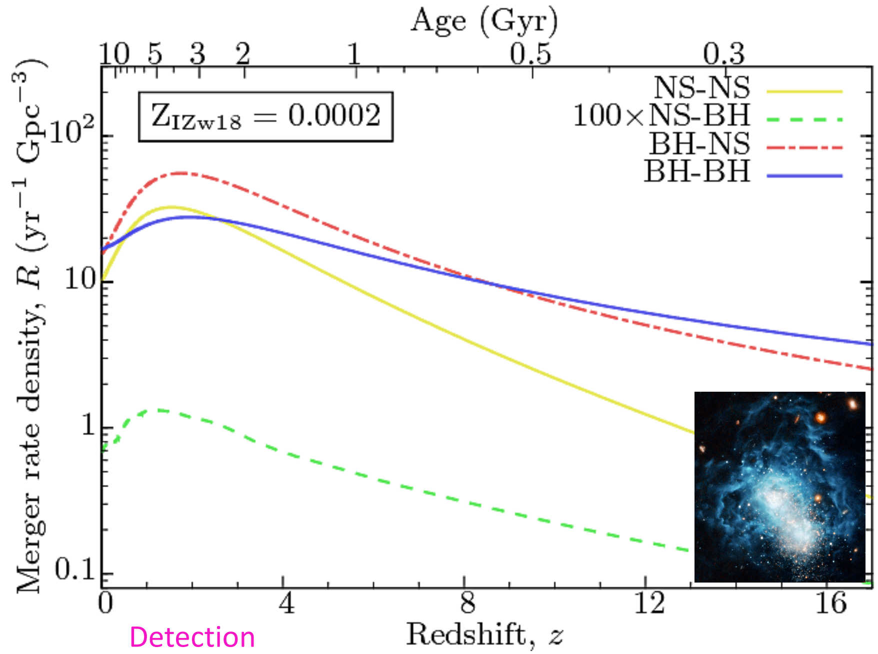

local Universe

Detection rates

Z_{MW}	$\langle M^{2.5} \rangle$	$R_{z=0}$	R_D	R_{cSFR}	$R_{D,cSFR}$
NS-NS	1.36 $M_\odot^{2.5}$	9.85×10^0 yr^{-1} Gpc^{-3}	0.28 yr^{-1}	3.47×10^1 yr^{-1} Gpc^{-3}	0.98 yr^{-1}
NS-BH	20.0 $M_\odot^{2.5}$	0.00×10^0 yr^{-1} Gpc^{-3}	0.00 yr^{-1}	0.00×10^0 yr^{-1} Gpc^{-3}	0.00 yr^{-1}
BH-NS	15.7 $M_\odot^{2.5}$	1.80×10^1 yr^{-1} Gpc^{-3}	5.88 yr^{-1}	4.72×10^1 yr^{-1} Gpc^{-3}	15.43 yr^{-1}
BH-BH	233 $M_\odot^{2.5}$	6.01×10^{-1} yr^{-1} Gpc^{-3}	2.92 yr^{-1}	3.08×10^0 yr^{-1} Gpc^{-3}	14.95 yr^{-1}
Z_{IZw18}	$\langle M^{2.5} \rangle$	$R_{z=0}$	R_D	R_{cSFR}	$R_{D,cSFR}$
NS-NS	1.27 $M_\odot^{2.5}$	1.00×10^1 yr^{-1} Gpc^{-3}	0.27 yr^{-1}	3.28×10^1 yr^{-1} Gpc^{-3}	0.87 yr^{-1}
NS-BH	32.3 $M_\odot^{2.5}$	6.61×10^{-3} yr^{-1} Gpc^{-3}	0.00 yr^{-1}	1.55×10^{-2} yr^{-1} Gpc^{-3}	0.01 yr^{-1}
BH-NS	35.5 $M_\odot^{2.5}$	1.54×10^1 yr^{-1} Gpc^{-3}	11.40 yr^{-1}	5.32×10^1 yr^{-1} Gpc^{-3}	39.34 yr^{-1}
BH-BH	1720 $M_\odot^{2.5}$	1.68×10^1 yr^{-1} Gpc^{-3}	603.02 yr^{-1}	3.45×10^1 yr^{-1} Gpc^{-3}	1235.27 yr^{-1}
optimistic	$\langle M^{2.5} \rangle$	$R_{z=0}$	R_D	R_{cSFR}	$R_{D,cSFR}$
NS-NS	1.31 $M_\odot^{2.5}$	7.09×10^1 yr^{-1} Gpc^{-3}	1.94 yr^{-1}	1.59×10^2 yr^{-1} Gpc^{-3}	4.37 yr^{-1}
NS-BH	19.4 $M_\odot^{2.5}$	0.00×10^0 yr^{-1} Gpc^{-3}	0.00 yr^{-1}	0.00×10^0 yr^{-1} Gpc^{-3}	0.00 yr^{-1}
BH-NS	21.9 $M_\odot^{2.5}$	1.34×10^1 yr^{-1} Gpc^{-3}	6.11 yr^{-1}	2.44×10^1 yr^{-1} Gpc^{-3}	11.17 yr^{-1}
BH-BH	275 $M_\odot^{2.5}$	4.34×10^1 yr^{-1} Gpc^{-3}	248.34 yr^{-1}	1.09×10^2 yr^{-1} Gpc^{-3}	623.03 yr^{-1}

@design sensitivity: 1–5 detections per yr

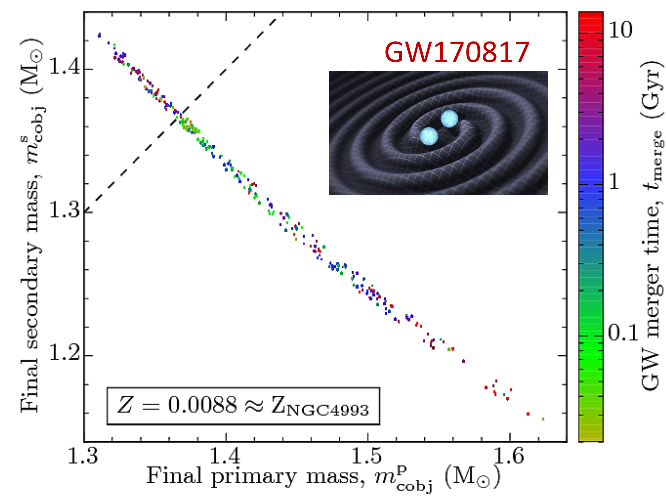

Kruckow et al. (2018), MNRAS

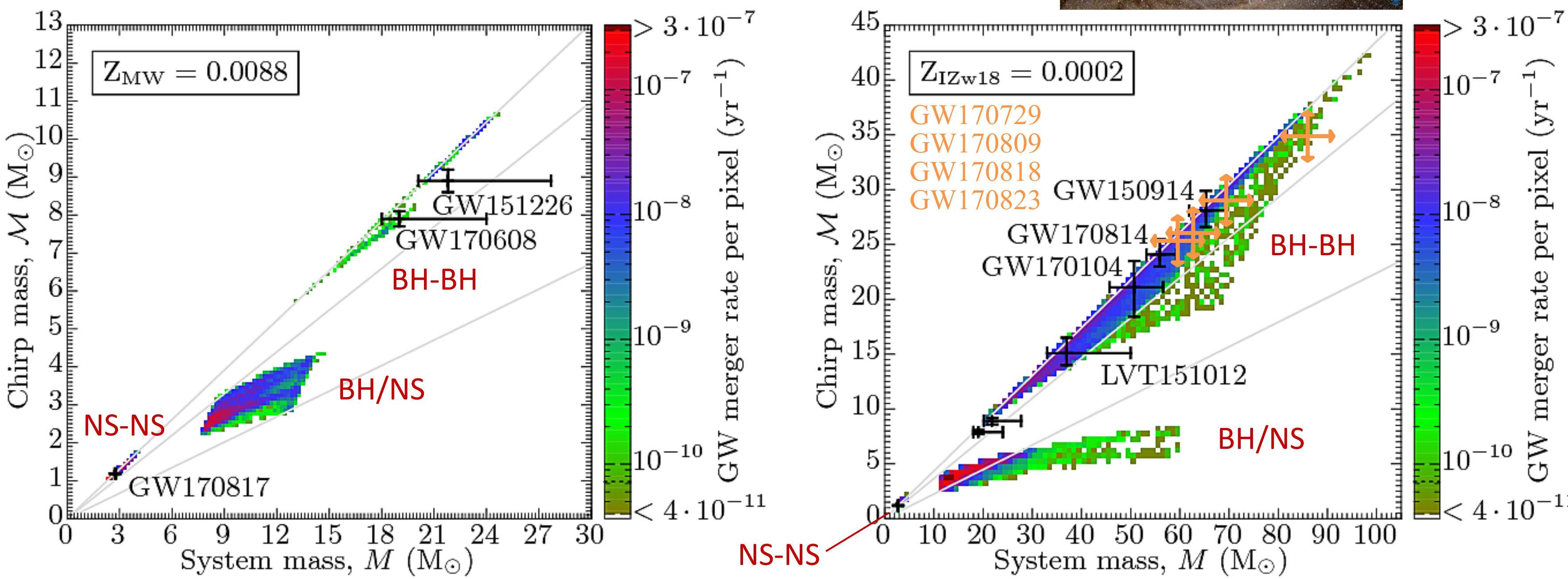

Kruckow et al. (2018), MNRAS

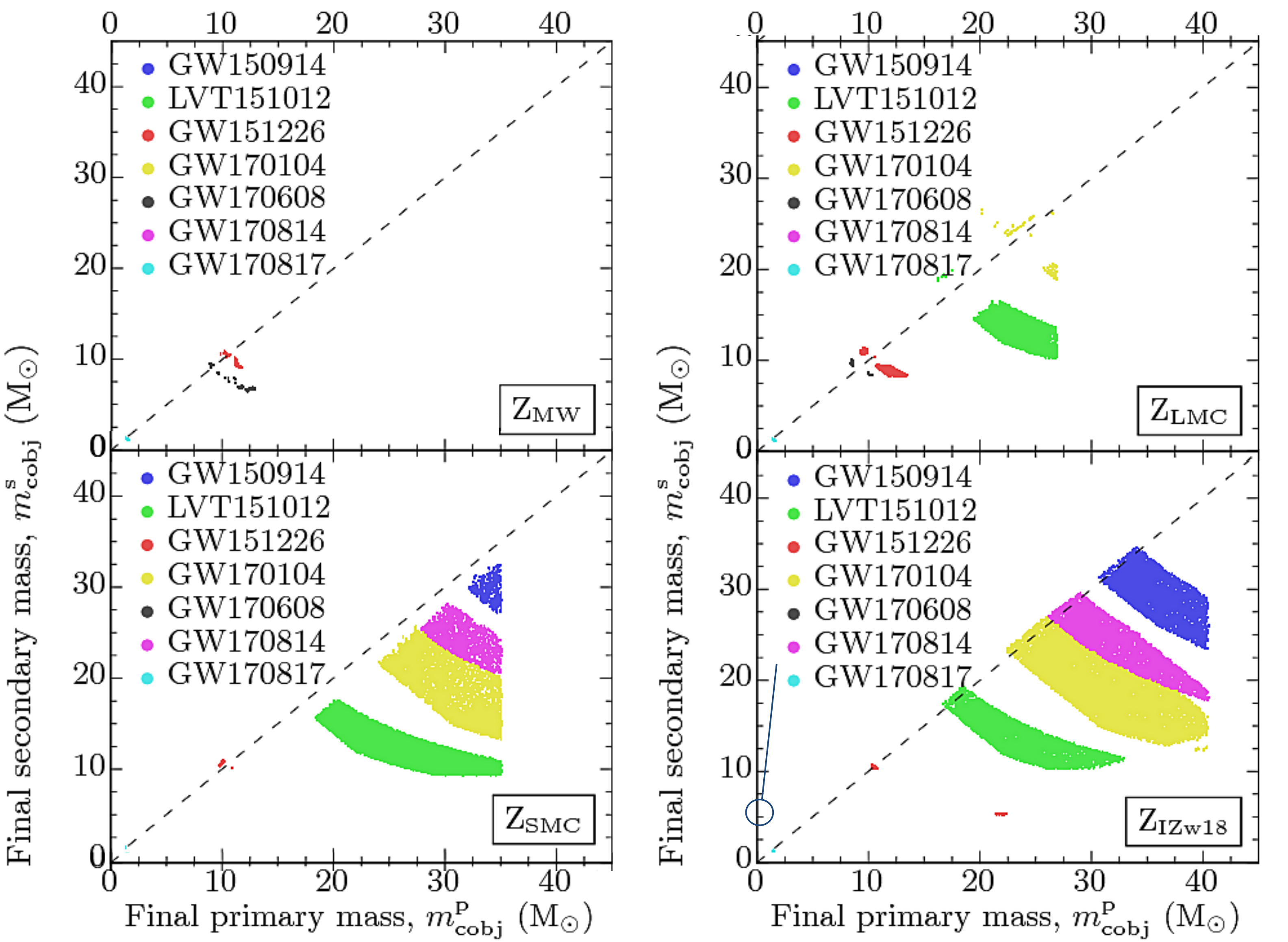

11* events in O1 and O2

10 BH+BH mergers
1 NS+NS merger

O3a

~ 50 events in O3a + 03b

	x	BH+BH mergers	23
?	y	NS+NS mergers	1(3)
	z	BH+NS mergers	2(4)
		mass gap	2(3)

- We predict ~10 times more detections of mixed BH/NS mergers compared to double NS mergers

Observational selection bias against?

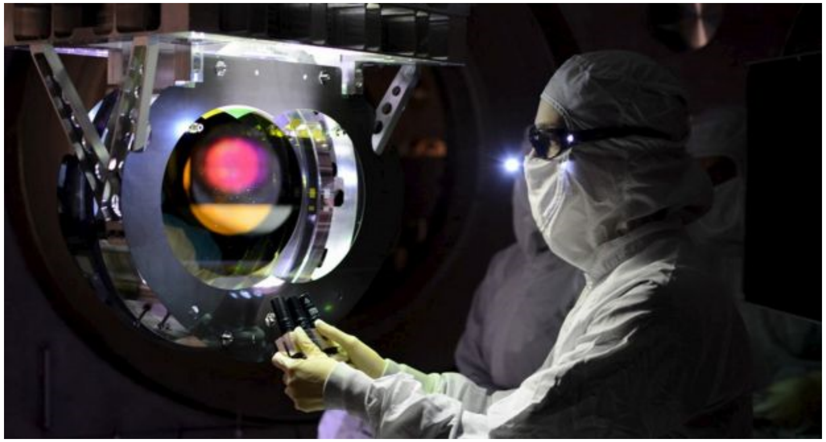

Notes on POP. SYNTHESIS

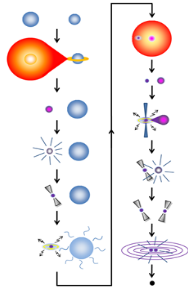

1. Reproduction of LIGO rates is no success criterion on its own
2. Can Galactic sources be reproduced? (properties of HMXBs, DNSs, etc.)
3. Is the input physics reasonable?
4. Is the evolution self consistent?
5. Watch out for papers that claim they can explain everything!

For the historical record Voss & Tauris (2003):

- Realistic CE binding energies
- Case BB RLO (evolved He-stars)
- Multi-component NS kick dist.

Table 6. The expected LIGO/VIRGO detection rates of compact mergers.

Systems	Galactic merger rate	LIGO I	LIGO II
NSNS	1.5×10^{-6} yr^{-1}	6.0×10^{-4} yr^{-1}	2.0 yr^{-1}
NSBH	8.4×10^{-8} yr^{-1}	1.7×10^{-4} yr^{-1}	0.6 yr^{-1}
BHNS	5.0×10^{-7} yr^{-1}	1.0×10^{-3} yr^{-1}	3.4 yr^{-1}
BHBH	9.7×10^{-6} yr^{-1}	2.5×10^{-1} yr^{-1}	840 yr^{-1}

300 Mpc

Chad Hanna's talk

O3a: ~1 per week
@ 120 Mpc

$52*(300/120)^3 = \underline{812\ \mathrm{yr}^{-1}}$

RECIPE

- Binary stellar evolution
- Population synthesis
  (input distributions and stellar grids)
- Galactic star formation rate
  (formation history of massive binaries)
- Galactic potentials
  (to probe location of mergers in host galaxies)
- Extrapolation to local Universe
  (scaling-law of galaxy number density)

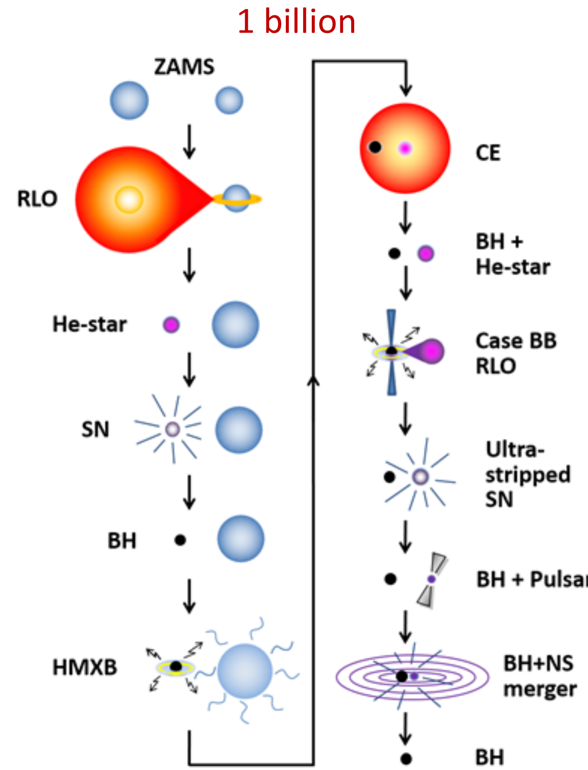

KICKS (2nd SN)

Conclusions Kicks (2nd SN)

Tauris, Langer & Podsiadlowski (2015); Tauris et al. (2017)

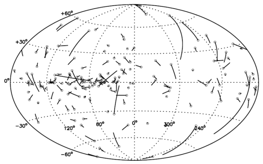

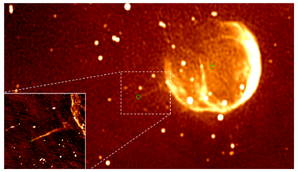

- Multi component kick distribution (e.g. GC sources, isolated pulsars, +1000 km/s)
- Kick magnitude depends on: mass of iron core; and also (less) on envelope mass
  (early discussion in Tauris & Bailes 1996)

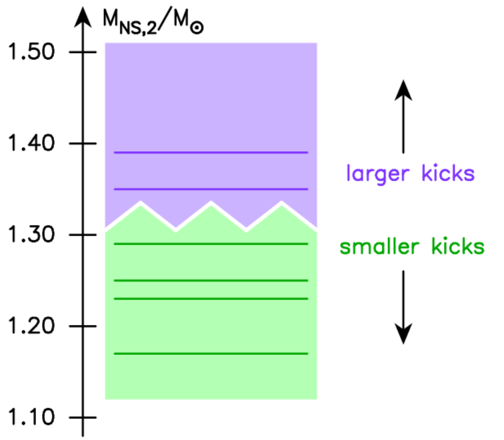

- All* DNS mergers undergo an ultra-stripped SN as 2nd SN
- Correlation between kick magnitude and NS mass
- Kicks may produce DNS merger times of < 1 Myr
  (sGRBs in star-forming regions!)

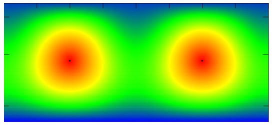

- Spin tossing occurs in 2 out of 2 known DNS systems where
  the young NS is observed. Also applies to double BH mergers?
  (→ misaligned spins from isolated binaries)

$$\chi_{eff} \equiv \frac{1}{M}\left(m_1\chi_1 + m_2\chi_2\right)$$

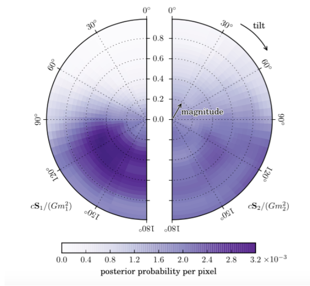

- No evidence for a preferred kick directions

NS+WD LISA SOURCES

Conclusions NS+WD LISA SOURCES

Tauris (2018), Phys.Rev.Lett.

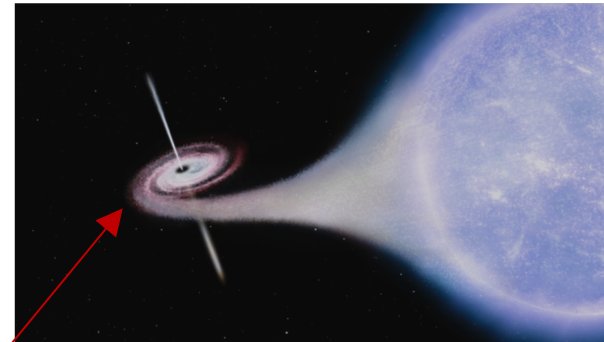

GW spectrum evolution with finite-temperature effects (specific entropy) of the WD donor

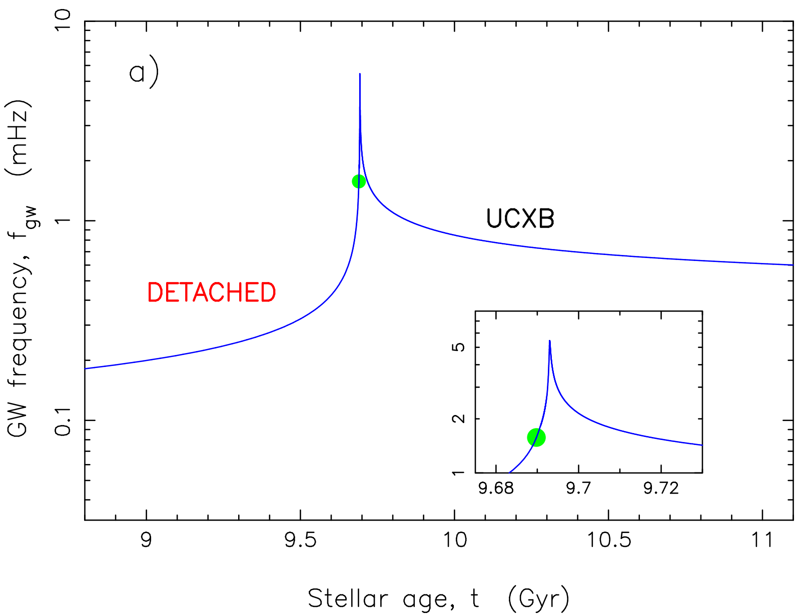

Determine the NS mass to a high accuracy (4%) via a new method

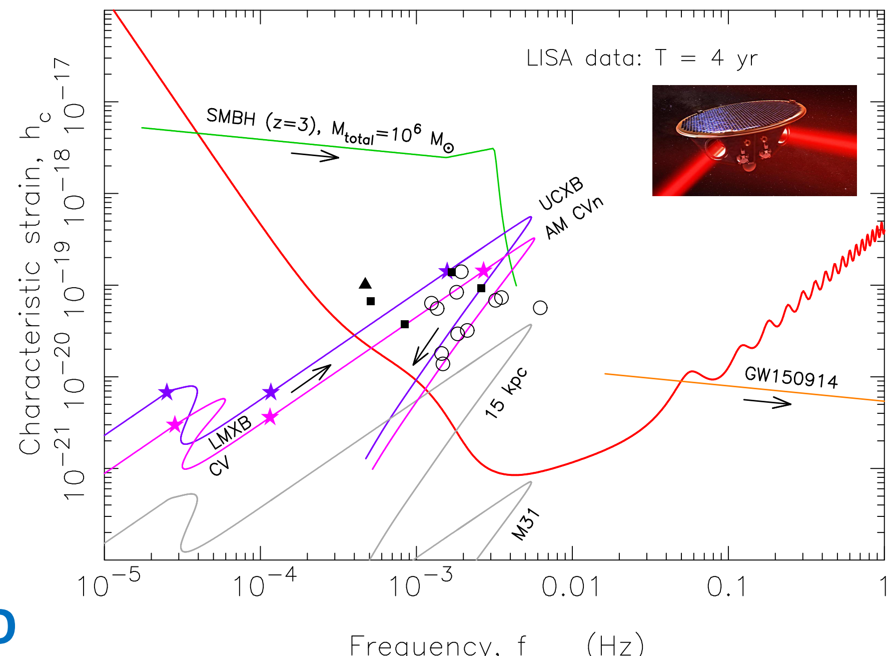

Dual-line spectroscopic GW source:

LIGO

$$I_{zz}\,\varepsilon = \sqrt{\frac{32}{80}}\;\pi^{-4/3} G^{2/3} f_{gw}^{-4/3} M_{chirp}^{5/3} \left(\frac{h_{spin}}{h_{orb}}\right)$$

LISA

My dream!

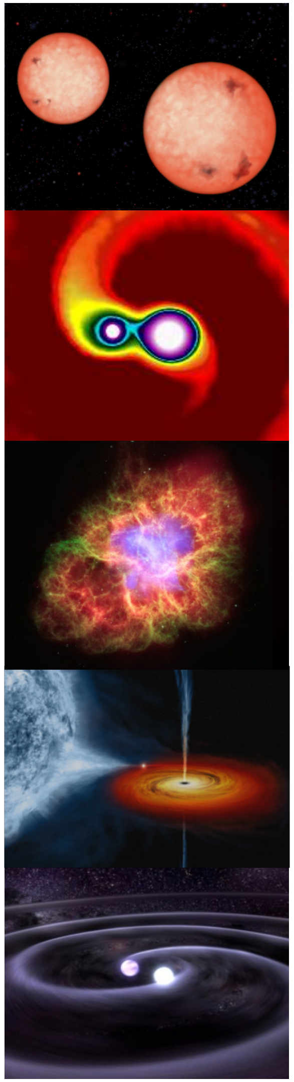

- We have a fairly good understanding of DNS formation in general.
  - ❖ Success: spins, amount of mass accreted, orbital parameters
  - ❖ Mediocre: masses, kicks
  - ❖ Failure: common envelope, B-fields, lowest mass NSs

- Strong **synergies** between
  - stellar evolution
  - X-ray binaries
  - SNe
  - GWs

- Future work
  - ➢ Formation and evolution of compact binary stars **self-consistently** …. until grav. collapse and apply these models as **realistic** SN input
  - ➢ Numerical modelling of **Galactic LISA sources** containing NSs


Thank you
11
基礎物理学研究所（湯川記念館）
Yukawa Institute for Theoretical Physics (Yukawa Hall)
SUPER DRY
Asahi
Glico
日商エステム
改源
CHINTAI
LOTTERIA
Ardent Beauty

KICKS (2nd SN)

Mon. Not. R. Astron. Soc. **342,** 1169–1184 (2003)

Galactic distribution of merging neutron stars and black holes – prospects for short gamma-ray burst progenitors and LIGO/VIRGO

R. Voss* and T. M. Tauris*

*Astronomical Observatory, Niels Bohr Institute, University of Copenhagen, DK-2100 Copenhagen Ø, Denmark

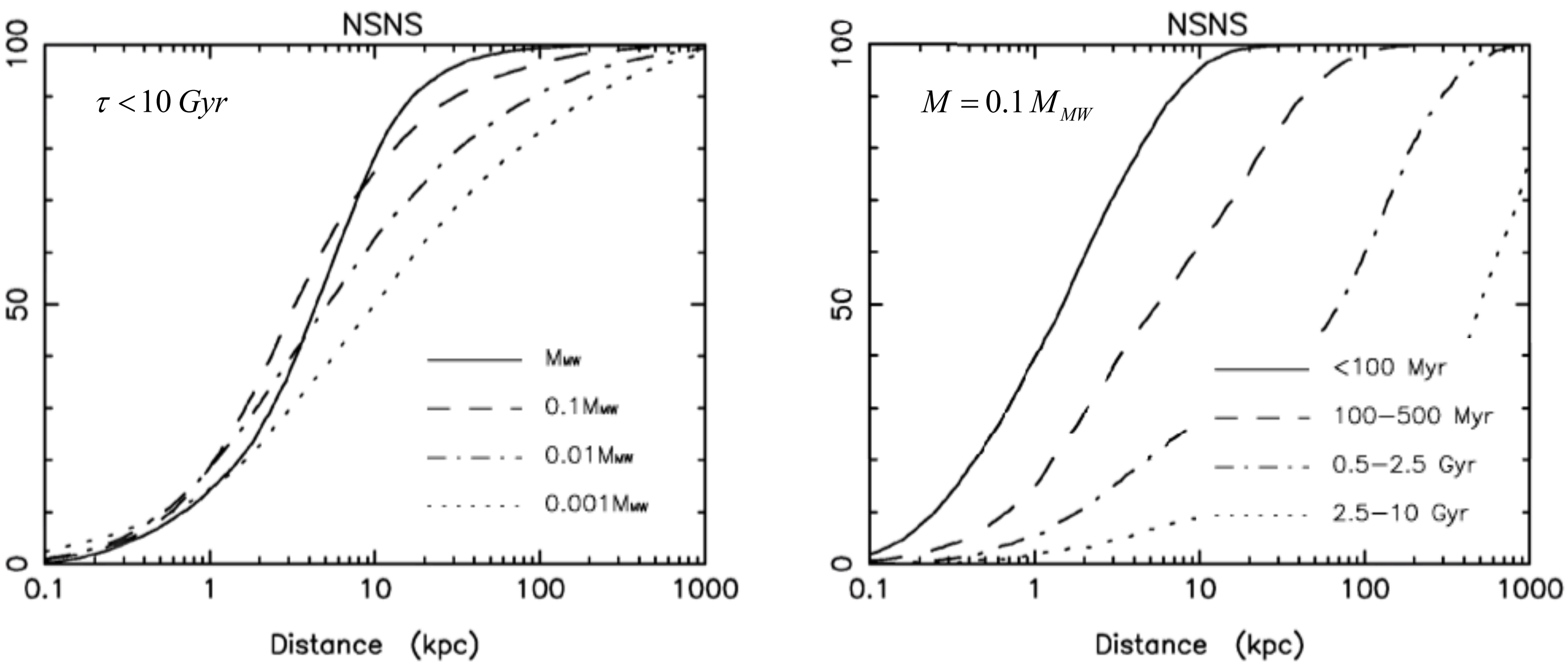

Voss & Tauris (2003), MNRAS

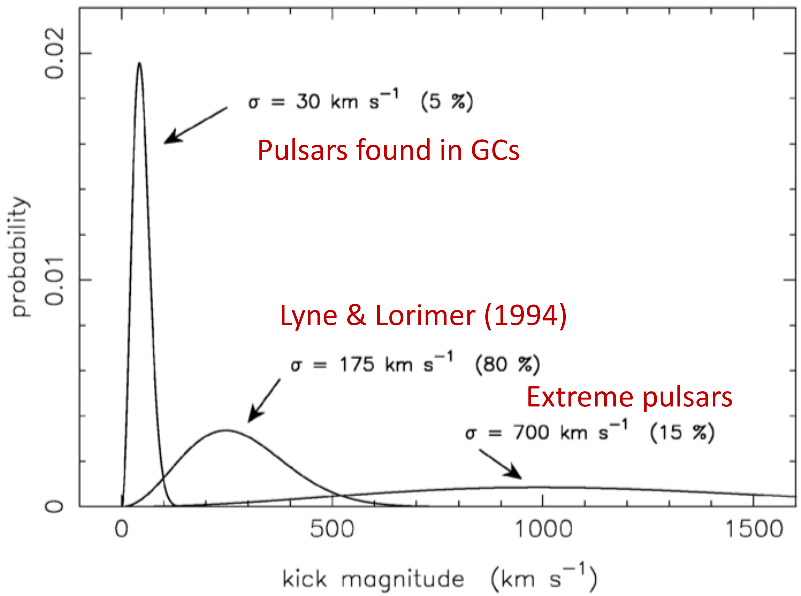

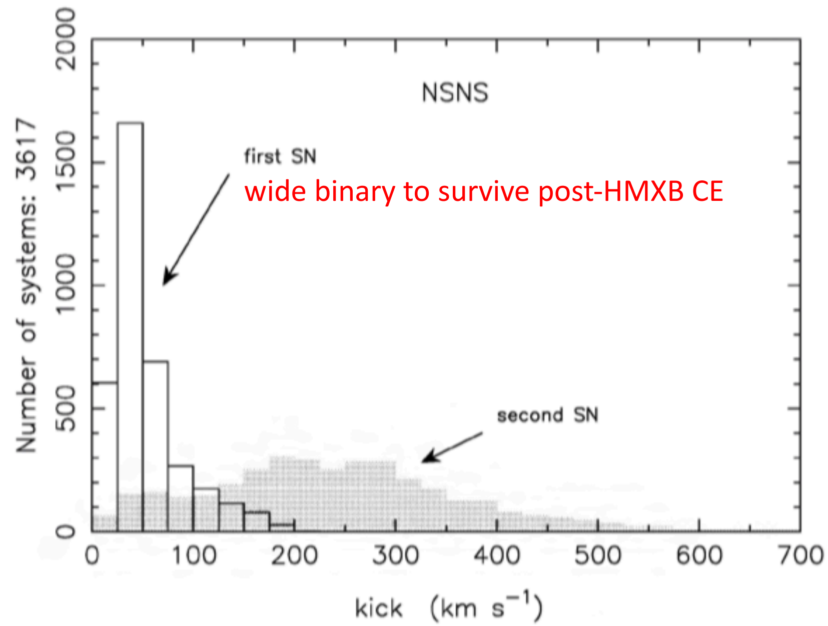

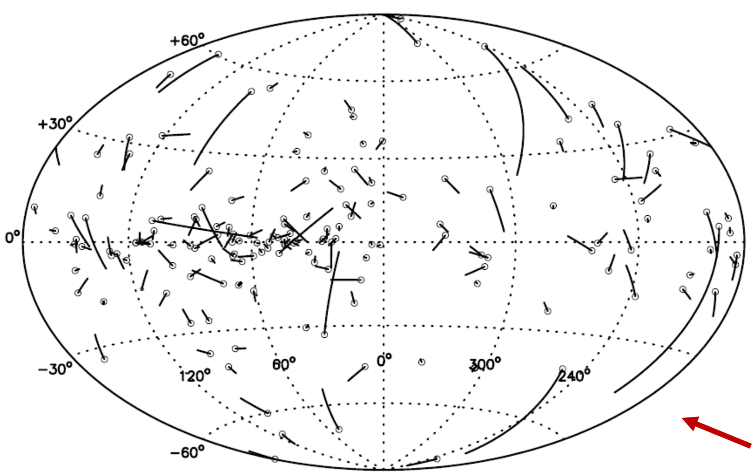

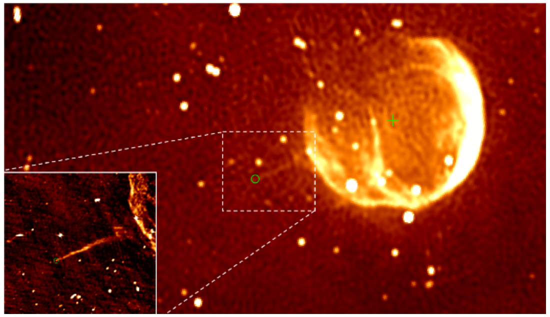

Radio proper motions show evidence for average 3D velocities of ~ 400 km s^{-1} (Lyne & Lorimer 1994; Hobbs et al. 2005).

Tauris et al. (2017), ApL

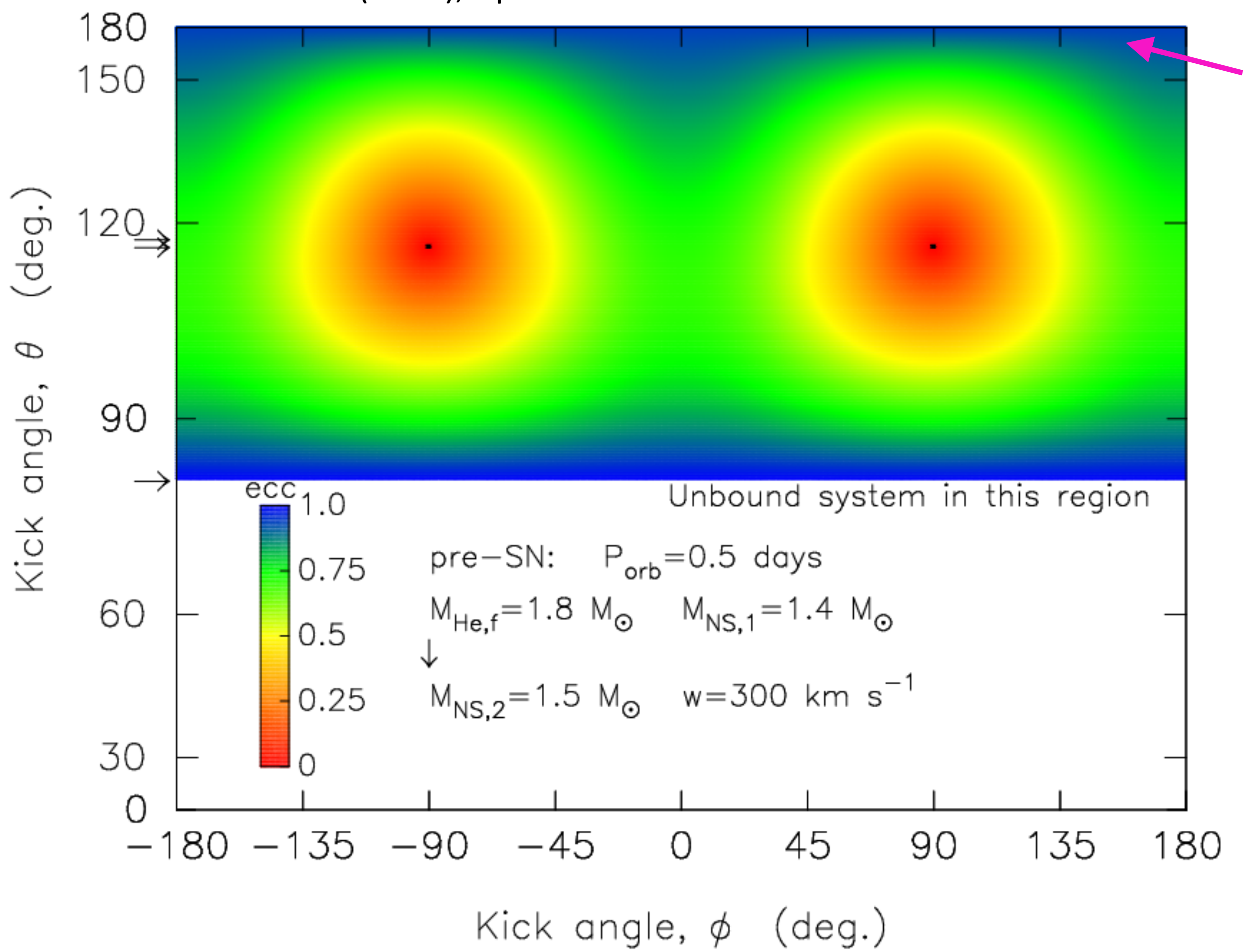

τ_{GW} < 1 Myr!
(short sGRB delay time)

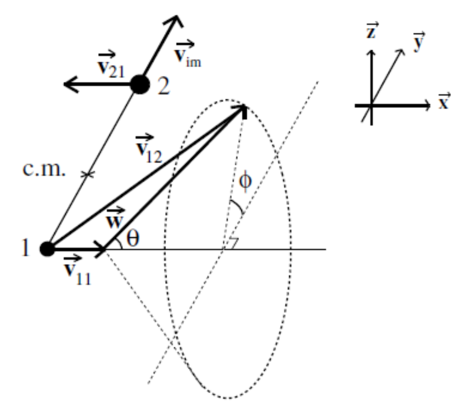

Consider the **kinematics** from the **2nd SN explosion**

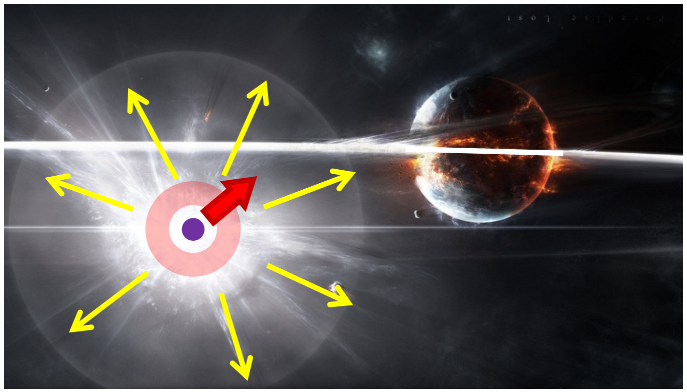

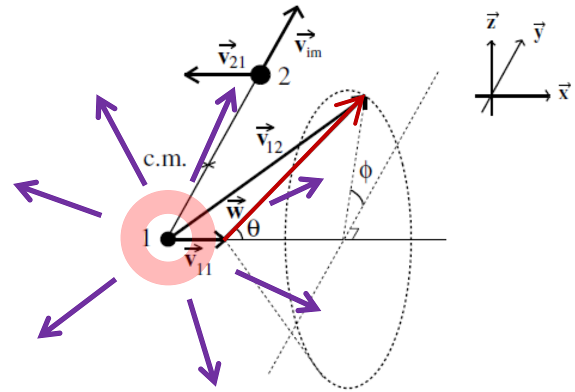

Our simulations take their basis in a <u>five dimensional phase space</u>.
The **input parameters** are:

- the pre-SN orbital period
- the final mass of the (stripped) exploding star
- the magnitude of the kick velocity imparted onto the newborn NS
- the two angles defining the direction of the kick velocity, θ and φ.

A <u>sixth and seventh input parameter</u> are the mass of the first-born NS and its misalignment angle.

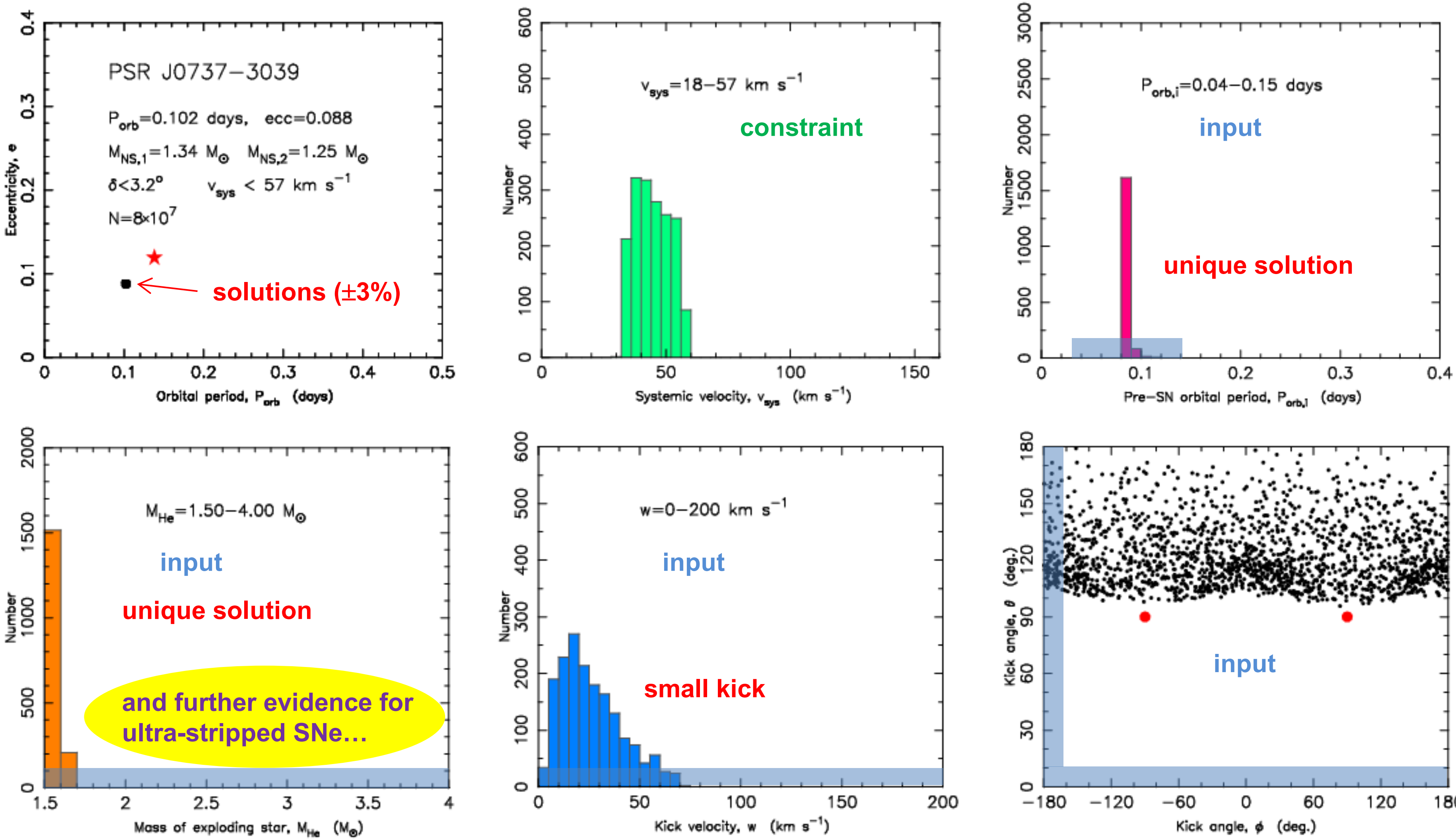

Tauris et al. (2017)

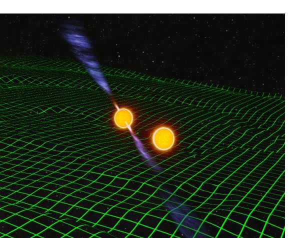

See also early analysis by Piran & Shaviv (2004; 2005) and Beniamini & Piran (2016)

★ Based on proper motion and distance measurements (Deller et al. 2009) combined with MC simulations of the 3rd velocity component and a Galactic potential.

Applying the constraint $v_{sys} < 57$ km s^{-1} provides an almost **unique solution** to the pre-SN progenitor binary of PSR J0737−3039. The pre-SN binary had an orbital period of $P_{orb,i}$ = 0.085±0.005 days and the mass of the (ultra-stripped) exploding star must have been $M_{He} = 1.56 \pm 0.06\ M_{\odot}$.

Piran & Shaviv (2005)

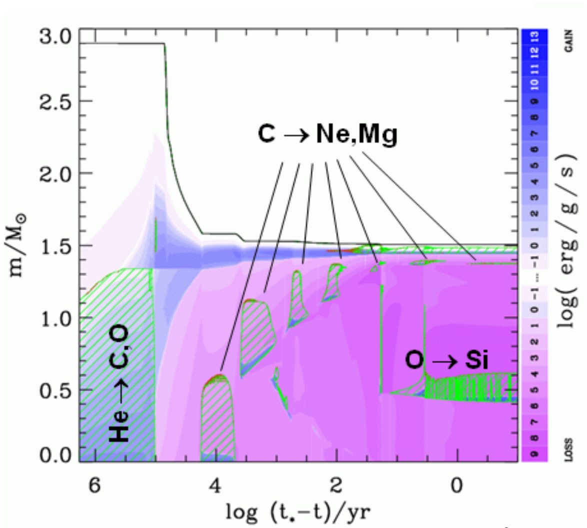

Interestingly enough, the very **first calculation** of a helium star–NS binary system leading to an **ultra-stripped SN** (Tauris et al. 2013) had pre-SN values of $P_{orb,i}$ = 0.070 days and $M_{He} = 1.50\ M_{\odot}$, and is thus **a solution** to the immediate **progenitor of PSR J0737−3039**.

Results for PSR B1913+16

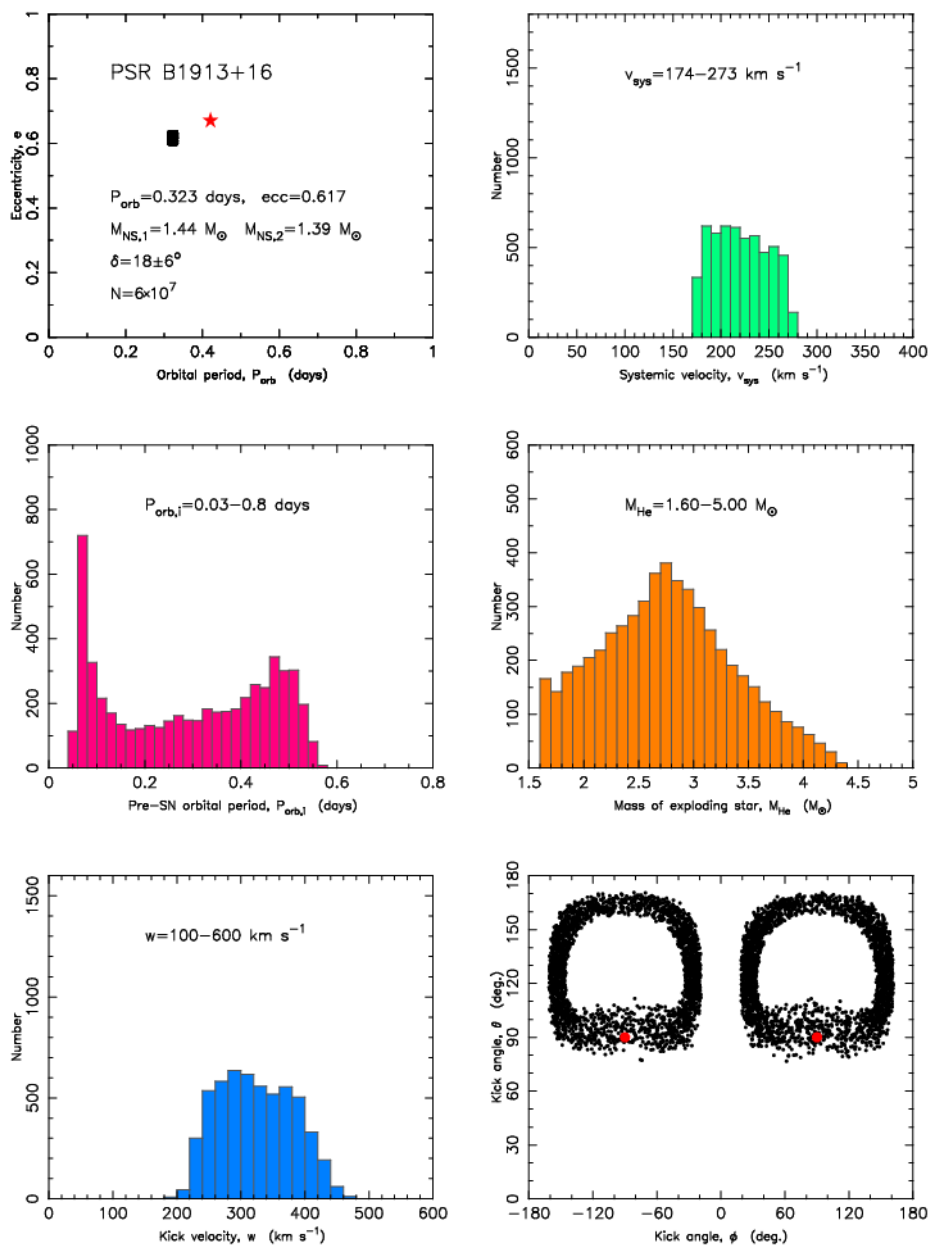

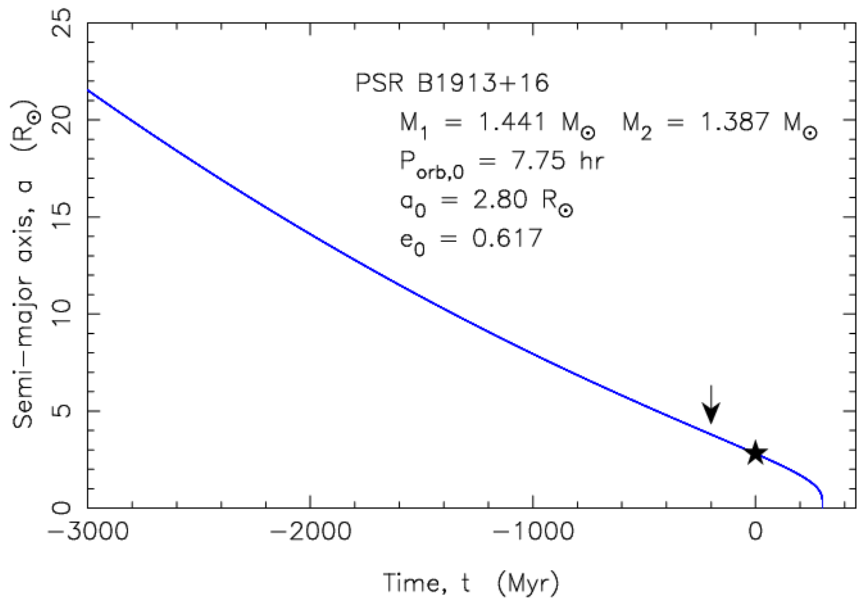

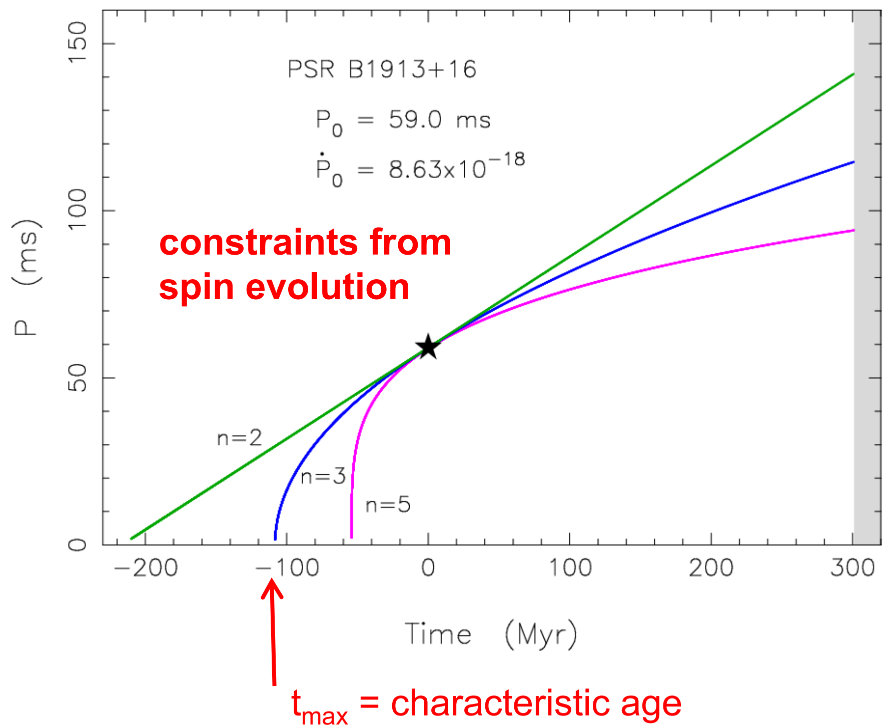

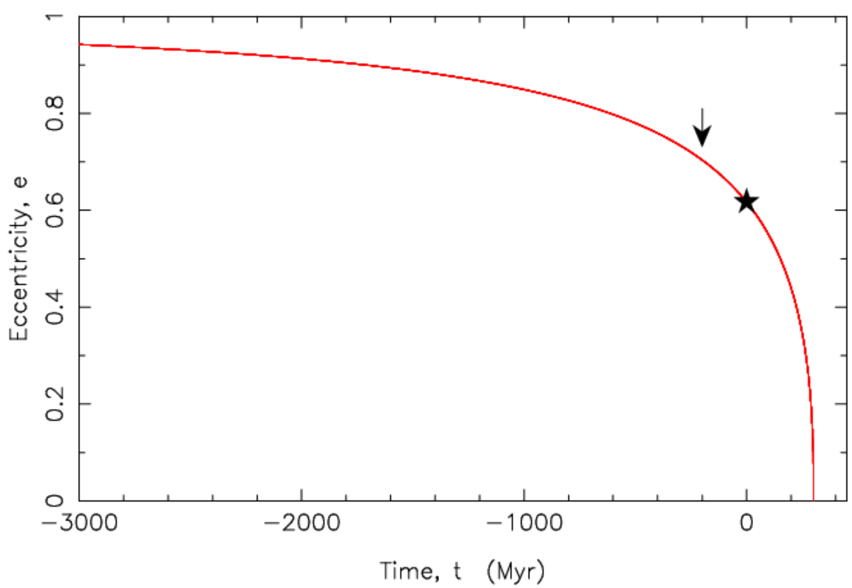

For **PSR 1913+16**, this yields upper limits of the post-SN parameters of a = 3.34 $R_\odot$ (corresponding to P_{orb} = 10.1 hr) and e = 0.670. This only leads to *very* marginal changes in the pre-SN solutions for this system.

Tauris, Langer & Podsiadlowski (2015), MNRAS

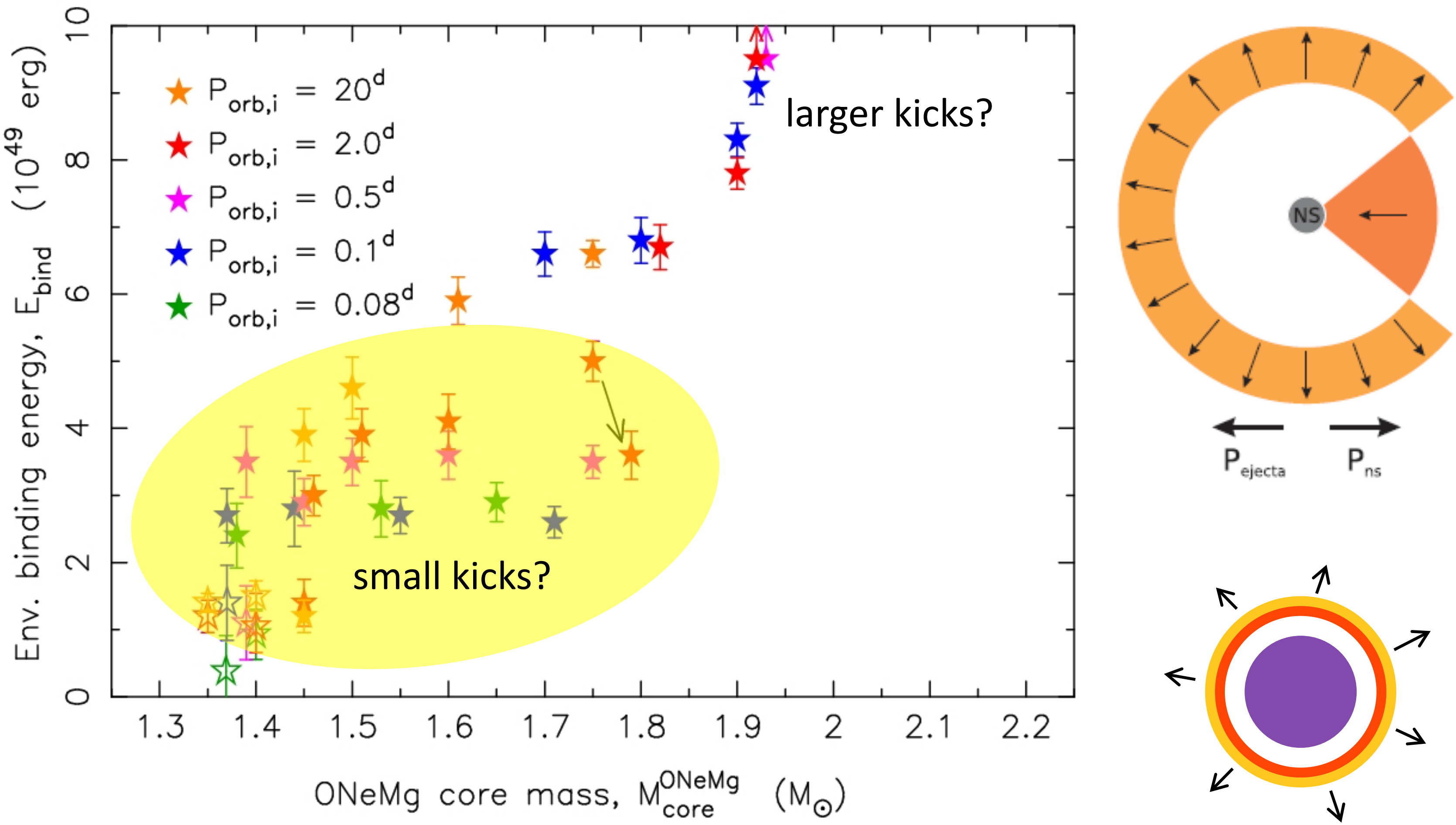

* Non-radial hydrodynamical instabilities, e.g. Standing Accretion Shock Instabilities (SASI) or neutrino driven convection bubbles (Janka 2012).

Theoretical kick magnitudes (following Janka 2017)

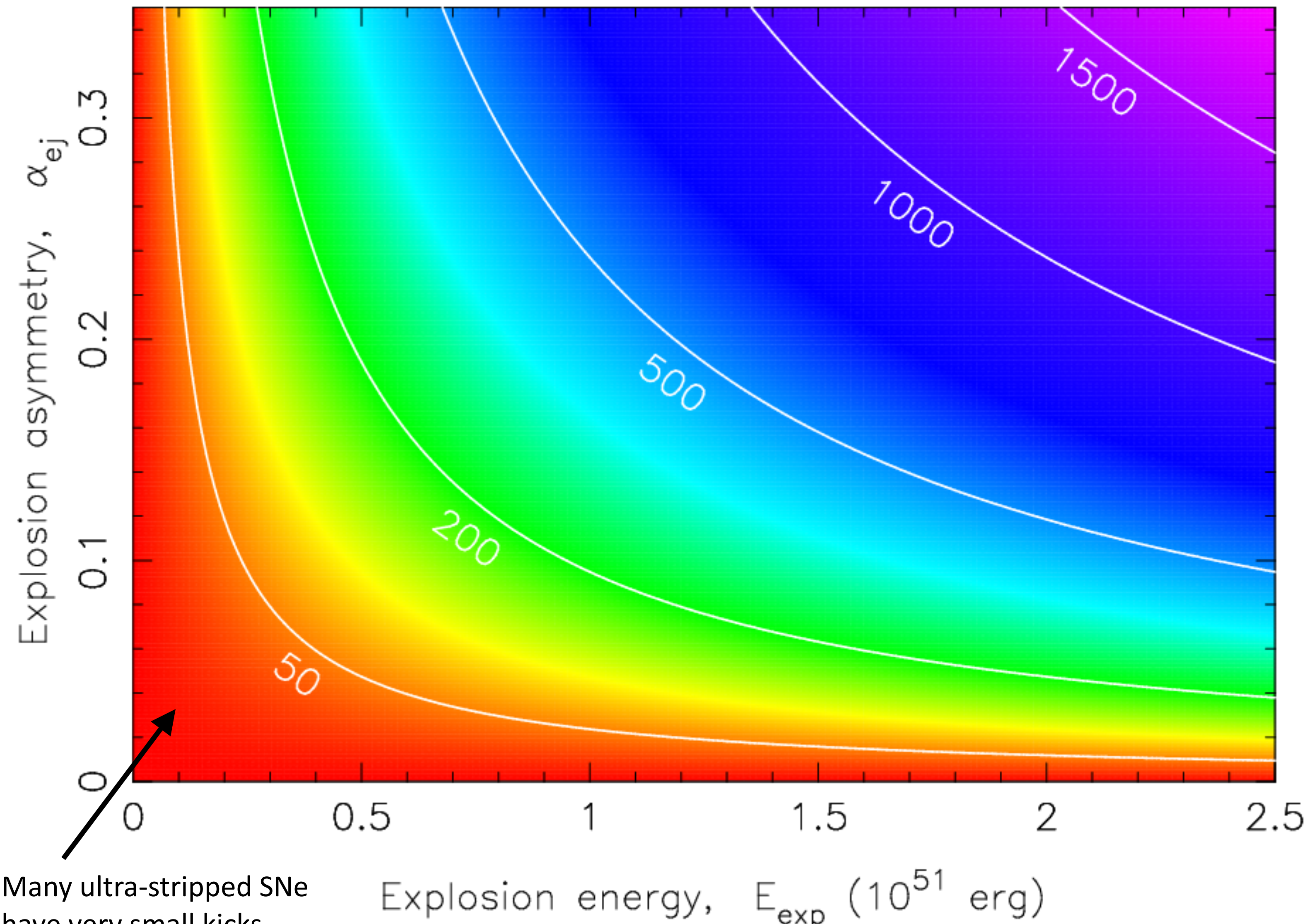

Many ultra-stripped SNe have very small kicks (although not all!)

Tauris et al.(2017), ApJ

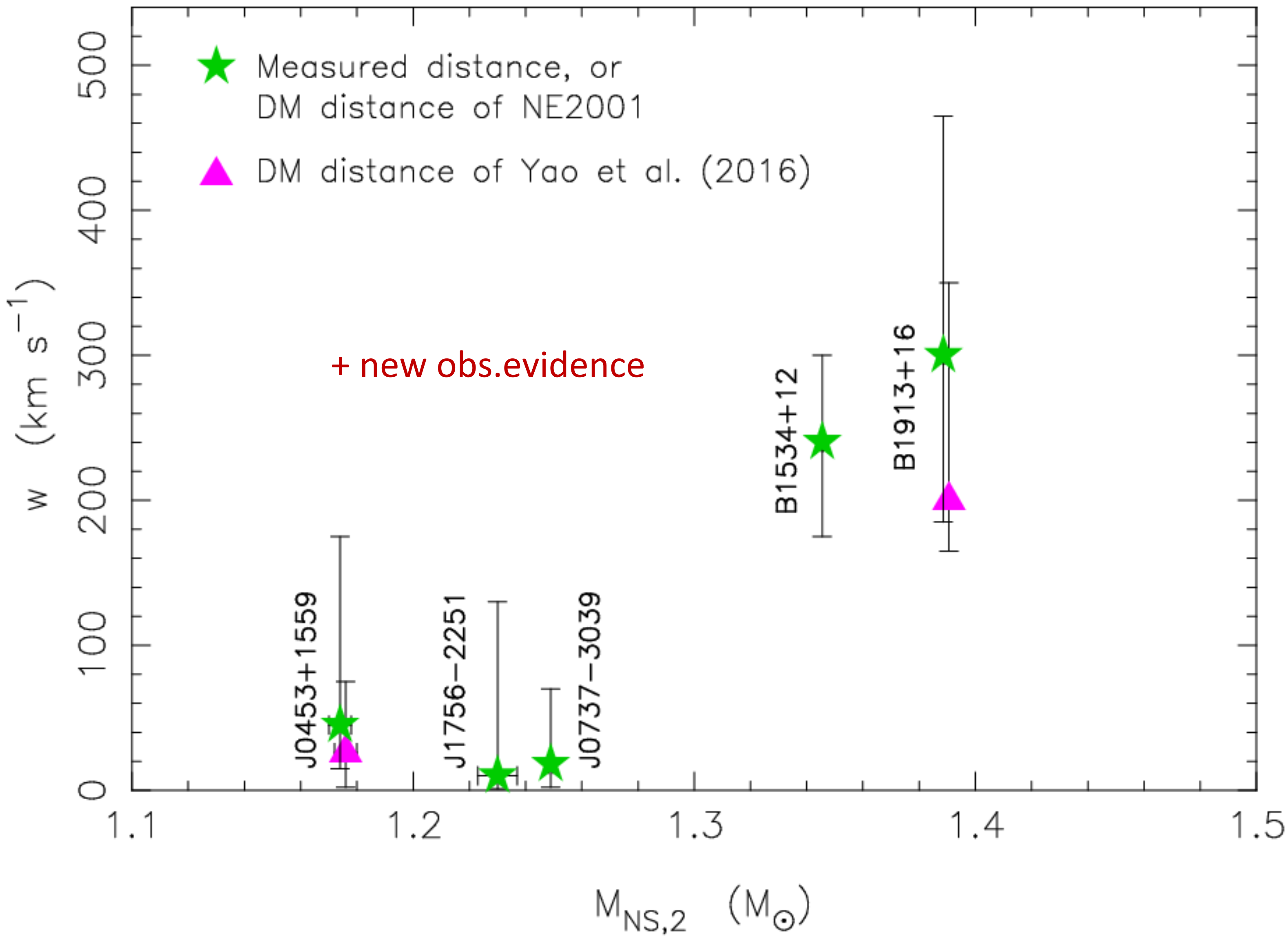

Kick – NS mass relation? Empirical evidence from current data

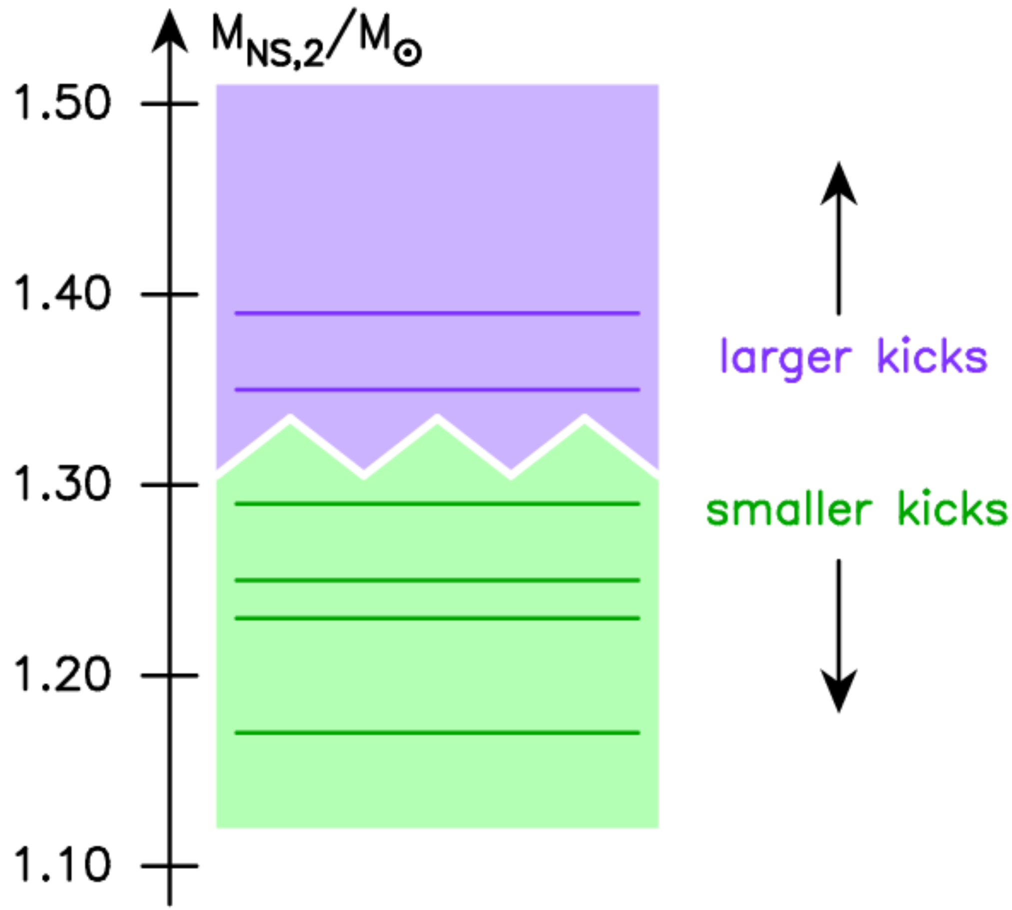

Kruckow+2018

arXiv:1801.05433

MNRAS (2018)

Progenitors of gravitational wave mergers: Binary evolution with the stellar grid based code ComBinE

Matthias U. Kruckow,[1*] Thomas M. Tauris,[2,1] Norbert Langer,[1,2] Michael Kramer,[2] Robert G. Izzard[3]

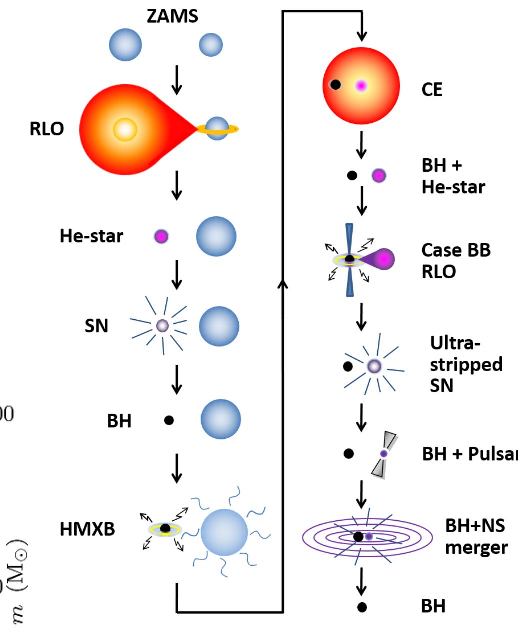

Population synthesis using Monte Carlo techniques:
Typically one billion binaries are evolved

Dense stellar grid* calculated with BEC

- age
- mass
- core mass
- radius
- luminosity
- effective temperature
- envelope structure parameter

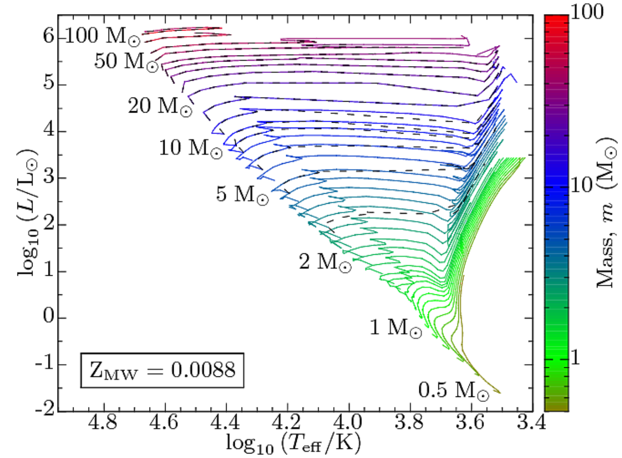

- semi-major axis (orbital period)
- eccentricity
- galactic position
- velocity

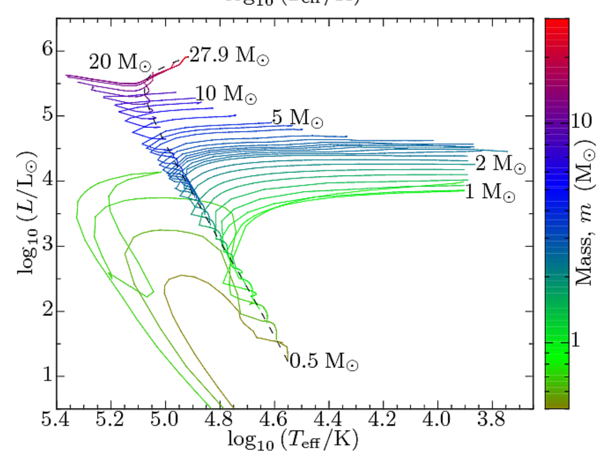

He-star (WR-star) tracks

Initial distribution functions
(M_1, M_2, a ,e, Z*, v_{rot}*)

Kruckow et al. (2018), MNRAS

GW merger rates	$Z_{\rm MW}$ = 0.0088	$Z_{\rm IZw18}$ = 0.0002
NS-NS	$2.98^{+0.15}_{-0.24}\times10^{-6}$ yr^{-1}	$2.82^{+0.16}_{-0.27}\times10^{-6}$ yr^{-1}
NS-BH	$0.00^{+0.00}_{-0.00}\times10^{0}$ yr^{-1}	$1.33^{+0.13}_{-0.22}\times10^{-9}$ yr^{-1}
BH-NS	$4.05^{+0.35}_{-0.59}\times10^{-6}$ yr^{-1}	$4.57^{+0.26}_{-0.37}\times10^{-6}$ yr^{-1}
BH-BH	$2.64^{+0.05}_{-0.07}\times10^{-7}$ yr^{-1}	$2.96^{+0.50}_{-0.55}\times10^{-6}$ yr^{-1}

$\sim$ 3 DNS mergers Myr^{-1} MWEG^{-1}

Table 5. Variations in DCO formation and merger rates for a MW-like galaxy caused by changing the values of selected key input parameters (columns 3 to 9). The default input parameters are listed in Table 2 and the resulting rates are shown in the second column. The binary types refer to the first and second compact objects formed. The pure uncertainties of Poissonian statistics are between 10^{-11} yr^{-1} and 10^{-8} yr^{-1}.

		α_{CE}	β_{min}	α_{RLO}	α_{th}	q_{limit}	α_{IMF}	$m^{p}_{max} = m^{s}_{max}$
	upper:	0.80	0.79	0.24	0.70	4.0	3	150 $M_\odot$
	lower:	0.20	0.50	0.15	0.30	1.5	2	80 $M_\odot$
Formation rates	**default**	α_{CE}	β_{min}	α_{RLO}	α_{th}	q_{limit}	α_{IMF}	$m^{p}_{max} = m^{s}_{max}$
NS-NS (yr^{-1})	6.81×10^{-6}	$^{+2.37}_{-1.72}\times10^{-6}$	$^{-0.63}_{+3.02}\times10^{-6}$	$^{-0.69}_{+1.06}\times10^{-6}$	$^{+0.35}_{-1.32}\times10^{-7}$	$^{+3.17}_{-1.01}\times10^{-6}$	$^{-0.33}_{+2.08}\times10^{-5}$	$^{-1.91}_{+1.05}\times10^{-8}$
NS-BH (yr^{-1})	5.49×10^{-9}	$^{+2.01}_{-0.04}\times10^{-8}$	$^{+1.20}_{-0.36}\times10^{-8}$	$^{+1.14}_{-0.50}\times10^{-8}$	$^{-0.77}_{-1.23}\times10^{-9}$	$^{+1.11}_{-0.05}\times10^{-7}$	$^{-0.35}_{+3.79}\times10^{-8}$	$^{-1.15}_{-1.69}\times10^{-9}$
BH-NS (yr^{-1})	1.49×10^{-5}	$^{+1.96}_{-3.26}\times10^{-6}$	$^{+0.17}_{-1.23}\times10^{-5}$	$^{+1.28}_{-2.73}\times10^{-6}$	$^{+1.05}_{-0.70}\times10^{-6}$	$^{+4.55}_{-1.28}\times10^{-5}$	$^{-0.10}_{+1.38}\times10^{-4}$	$^{+9.37}_{-9.15}\times10^{-7}$
BH-BH (yr^{-1})	2.27×10^{-6}	$^{+2.35}_{-0.30}\times10^{-6}$	$^{+1.06}_{-0.19}\times10^{-6}$	$^{+1.08}_{-0.28}\times10^{-6}$	$^{+2.88}_{-1.80}\times10^{-7}$	$^{+3.87}_{-0.02}\times10^{-5}$	$^{-0.16}_{+2.99}\times10^{-5}$	$^{+4.37}_{-1.11}\times10^{-6}$
GW merger rates	**default**	α_{CE}	β_{min}	α_{RLO}	α_{th}	q_{limit}	α_{IMF}	$m^{p}_{max} = m^{s}_{max}$
NS-NS (yr^{-1})	2.98×10^{-6}	$^{+7.75}_{-0.64}\times10^{-7}$	$^{-0.51}_{+2.71}\times10^{-6}$	$^{-5.67}_{+8.64}\times10^{-7}$	$^{-2.60}_{+1.47}\times10^{-7}$	$^{+0.85}_{-4.66}\times10^{-7}$	$^{-1.46}_{+9.68}\times10^{-6}$	$^{-3.11}_{-0.67}\times10^{-8}$
NS-BH (yr^{-1})	0.00×10^{0}	$^{+1.20}_{+0.01}\times10^{-8}$	$^{+2.58}_{+0.00}\times10^{-10}$	$^{+3.87}_{+0.00}\times10^{-10}$	$^{+1.94}_{+0.00}\times10^{-10}$	$^{+1.94}_{+0.00}\times10^{-9}$	$^{+0.00}_{+1.34}\times10^{-9}$	$^{+0.65}_{+1.93}\times10^{-10}$
BH-NS (yr^{-1})	4.05×10^{-6}	$^{+0.81}_{-2.09}\times10^{-6}$	$^{+0.25}_{-3.56}\times10^{-6}$	$^{+2.94}_{-7.65}\times10^{-7}$	$^{+4.25}_{-2.49}\times10^{-7}$	$^{+2.88}_{-2.73}\times10^{-6}$	$^{-0.26}_{+3.56}\times10^{-5}$	$^{+1.32}_{-1.61}\times10^{-7}$
BH-BH (yr^{-1})	2.64×10^{-7}	$^{+2.19}_{-0.25}\times10^{-6}$	$^{+0.01}_{+1.91}\times10^{-7}$	$^{+0.17}_{+4.45}\times10^{-8}$	$^{+3.11}_{-1.41}\times10^{-7}$	$^{+1.15}_{+0.10}\times10^{-6}$	$^{-0.19}_{+3.84}\times10^{-6}$	$^{+3.86}_{-1.96}\times10^{-7}$

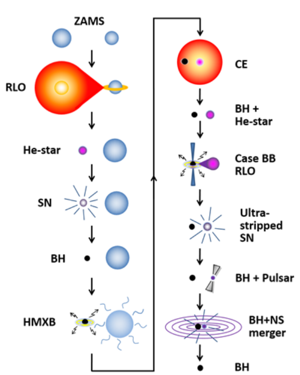

GW merger rates of a MW-like galaxy and their dependence on applied kicks and assumptions on EC SNe. The binary types ...e first and second compact objects formed.

GW merger rates	default	small kicks*	large EC SN kicks** $w_{ECSN} = w_{FeCCSN}$	small EC SN mass window*** $1.37\ M_\odot \le m^{ECSN}_{CO-core} < 1.38\ M_\odot$
NS-NS (yr^{-1})	2.98×10^{-6}	9.34×10^{-6}	1.54×10^{-6}	2.30×10^{-6}
NS-BH (yr^{-1})	0.00×10^{0}	1.94×10^{-10}	6.46×10^{-11}	1.29×10^{-10}
BH-NS (yr^{-1})	4.05×10^{-6}	7.59×10^{-6}	4.04×10^{-6}	4.04×10^{-6}
BH-BH (yr^{-1})	2.64×10^{-7}	3.05×10^{-7}	2.65×10^{-7}	2.66×10^{-7}

* half of all default kick magnitudes. ** similar to FeCC SNe, see Table 1. *** the default is $1.37\ M_\odot \le m^{ECSN}_{CO-core} < 1.435\ M_\odot$.

Heavy r-process elements: Beniamini et al. (2016): $\underline{5.0\text{–}20.0\times10^{-4}}$ per CC SN.

Our default and "optimistic" estimates of a DNS merger rate = 3.0–14.0 Myr^{-1} MWEG.
Combined with a Galactic CC SN rate of about 0.01 yr^{-1}
→ translates into a relative merger rate of about $\underline{3.0\text{–}14.0\times10^{-4}}$ per CC SN.

sGRBs: Wanderman & Piran (2015): $\underline{2.2\text{–}6.4\ \mathbf{f^{-1}}\ \mathrm{yr}^{-1}\ \mathrm{Gpc}^{-3}}$
where f^{-1} is a beaming factor in the range $1 < f^{-1} < 100$.

sGRB are expected from both DNS and mixed NS/BH mergers,
adding our simulated merger-rate densities we get $\underline{25\text{–}86\ \mathrm{yr}^{-1}\ \mathrm{Gpc}^{-3}}$.
These numbers agree for $\underline{f^{-1} = 4\text{–}40}$ (Metzger & Berger 2012; Fong et al. 2015).

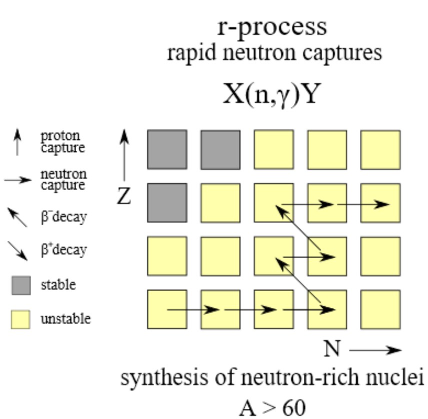

BH-BH:

LIGO/Virgo: 12–213 yr^{-1} Gpc^{-3} (Abbott et al. 2017a)

We find: 0.6–35 yr^{-1} Gpc^{-3}

(depending on metallicity and galaxy-density scaling)

Our rate is sensitive to CE physics (factor 10↑ if using α_{CE}=0.8 vs α_{CE}=0.5).

NS-NS:

LIGO/Virgo: 1540 (+3200 -1220) yr^{-1} Gpc^{-3} (Abbott et al. 2017c)

We find: 10–35 (10–400)* yr^{-1} Gpc^{-3} (optimizing all input physics incl.* smaller kicks)

BH-NS: should be detected more often than NS-NS by a factor 10!

We expect detections in O3 or O4.

local Universe

Z_{MW}	$\langle M^{2.5} \rangle$	$R_{z=0}$	R_D	R_{cSFR}	$R_{D,cSFR}$
NS-NS	1.36 $M_\odot^{2.5}$	9.85×10^{0} yr^{-1} Gpc^{-3}	0.28 yr^{-1}	3.47×10^{1} yr^{-1} Gpc^{-3}	0.98 yr^{-1}
NS-BH	20.0 $M_\odot^{2.5}$	0.00×10^{0} yr^{-1} Gpc^{-3}	0.00 yr^{-1}	0.00×10^{0} yr^{-1} Gpc^{-3}	0.00 yr^{-1}
BH-NS	15.7 $M_\odot^{2.5}$	1.80×10^{1} yr^{-1} Gpc^{-3}	5.88 yr^{-1}	4.72×10^{1} yr^{-1} Gpc^{-3}	15.43 yr^{-1}
BH-BH	233 $M_\odot^{2.5}$	6.01×10^{-1} yr^{-1} Gpc^{-3}	2.92 yr^{-1}	3.08×10^{0} yr^{-1} Gpc^{-3}	14.95 yr^{-1}
Z_{IZw18}	$\langle M^{2.5} \rangle$	$R_{z=0}$	R_D	R_{cSFR}	$R_{D,cSFR}$
NS-NS	1.27 $M_\odot^{2.5}$	1.00×10^{1} yr^{-1} Gpc^{-3}	0.27 yr^{-1}	3.28×10^{1} yr^{-1} Gpc^{-3}	0.87 yr^{-1}
NS-BH	32.3 $M_\odot^{2.5}$	6.61×10^{-3} yr^{-1} Gpc^{-3}	0.00 yr^{-1}	1.55×10^{-2} yr^{-1} Gpc^{-3}	0.01 yr^{-1}
BH-NS	35.5 $M_\odot^{2.5}$	1.54×10^{1} yr^{-1} Gpc^{-3}	11.40 yr^{-1}	5.32×10^{1} yr^{-1} Gpc^{-3}	39.34 yr^{-1}
BH-BH	1720 $M_\odot^{2.5}$	1.68×10^{1} yr^{-1} Gpc^{-3}	603.02 yr^{-1}	3.45×10^{1} yr^{-1} Gpc^{-3}	1235.27 yr^{-1}
optimistic	$\langle M^{2.5} \rangle$	$R_{z=0}$	R_D	R_{cSFR}	$R_{D,cSFR}$
NS-NS	1.31 $M_\odot^{2.5}$	7.09×10^{1} yr^{-1} Gpc^{-3}	1.94 yr^{-1}	1.59×10^{2} yr^{-1} Gpc^{-3}	4.37 yr^{-1}
NS-BH	19.4 $M_\odot^{2.5}$	0.00×10^{0} yr^{-1} Gpc^{-3}	0.00 yr^{-1}	0.00×10^{0} yr^{-1} Gpc^{-3}	0.00 yr^{-1}
BH-NS	21.9 $M_\odot^{2.5}$	1.34×10^{1} yr^{-1} Gpc^{-3}	6.11 yr^{-1}	2.44×10^{1} yr^{-1} Gpc^{-3}	11.17 yr^{-1}
BH-BH	275 $M_\odot^{2.5}$	4.34×10^{1} yr^{-1} Gpc^{-3}	248.34 yr^{-1}	1.09×10^{2} yr^{-1} Gpc^{-3}	623.03 yr^{-1}

NS+WD LISA SOURCES

LISA
~2034

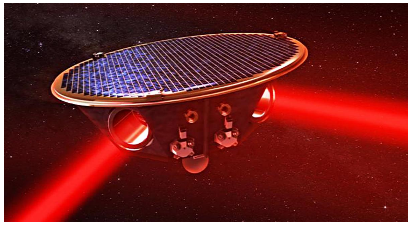

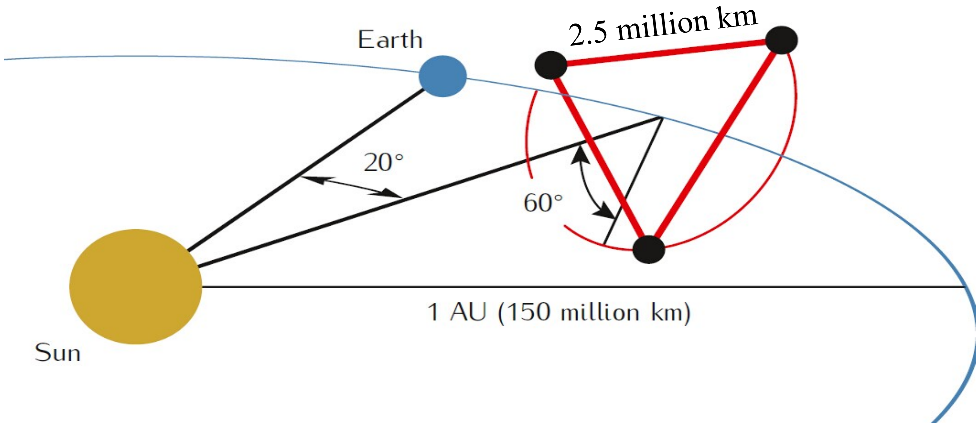

3G
~ ?

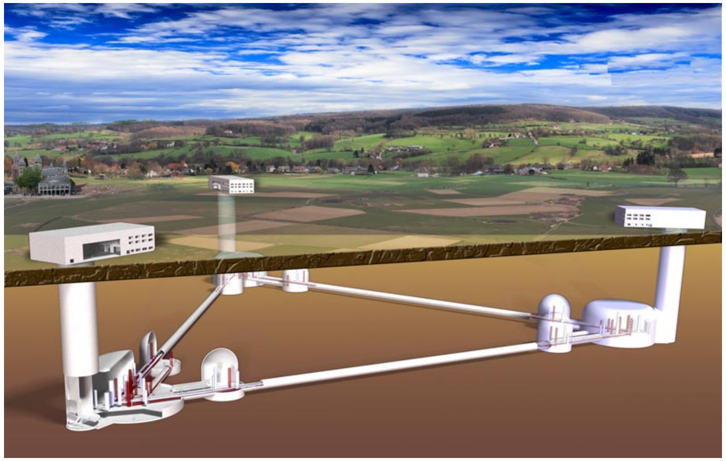

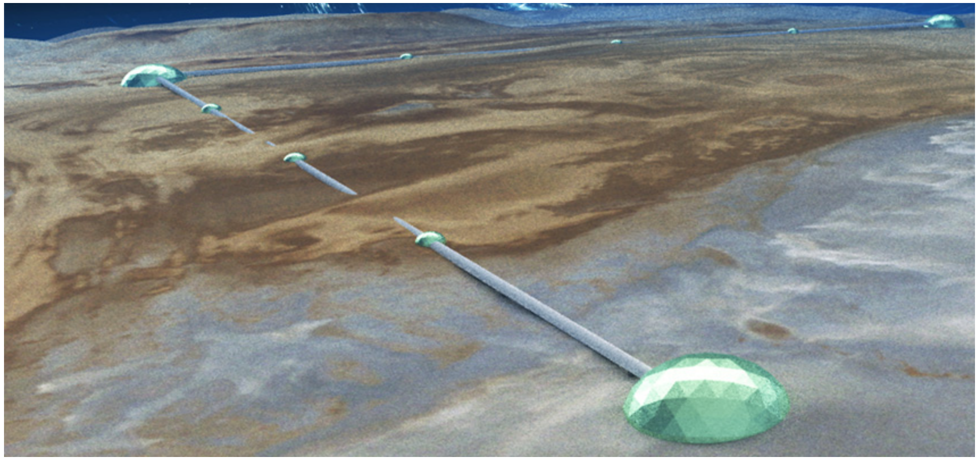

EINSTEIN TELESCOPE

COSMIC EXPLORER

Ask for 3 detectors
(~ 1 billion € each)

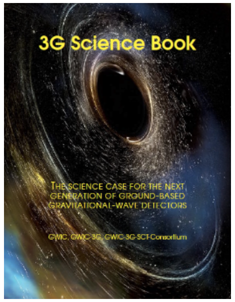

- Detect all BH-BH mergers out to z~20
- Detect the BH seeds evolving into SMBHs
- Possibly detect primordial BHs
- Determine the NS EoS to extreme precision
- etc.

The space-born observatory **LISA** (2034)
will detect thousands of resolvable **Galactic GW sources**
(besides millions of signals below the confusion limit)

WD, NS, BH

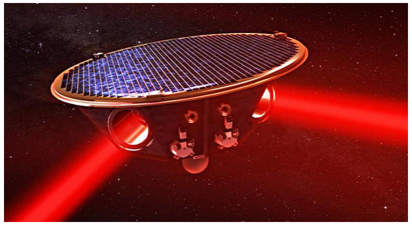

Sessana (2016)

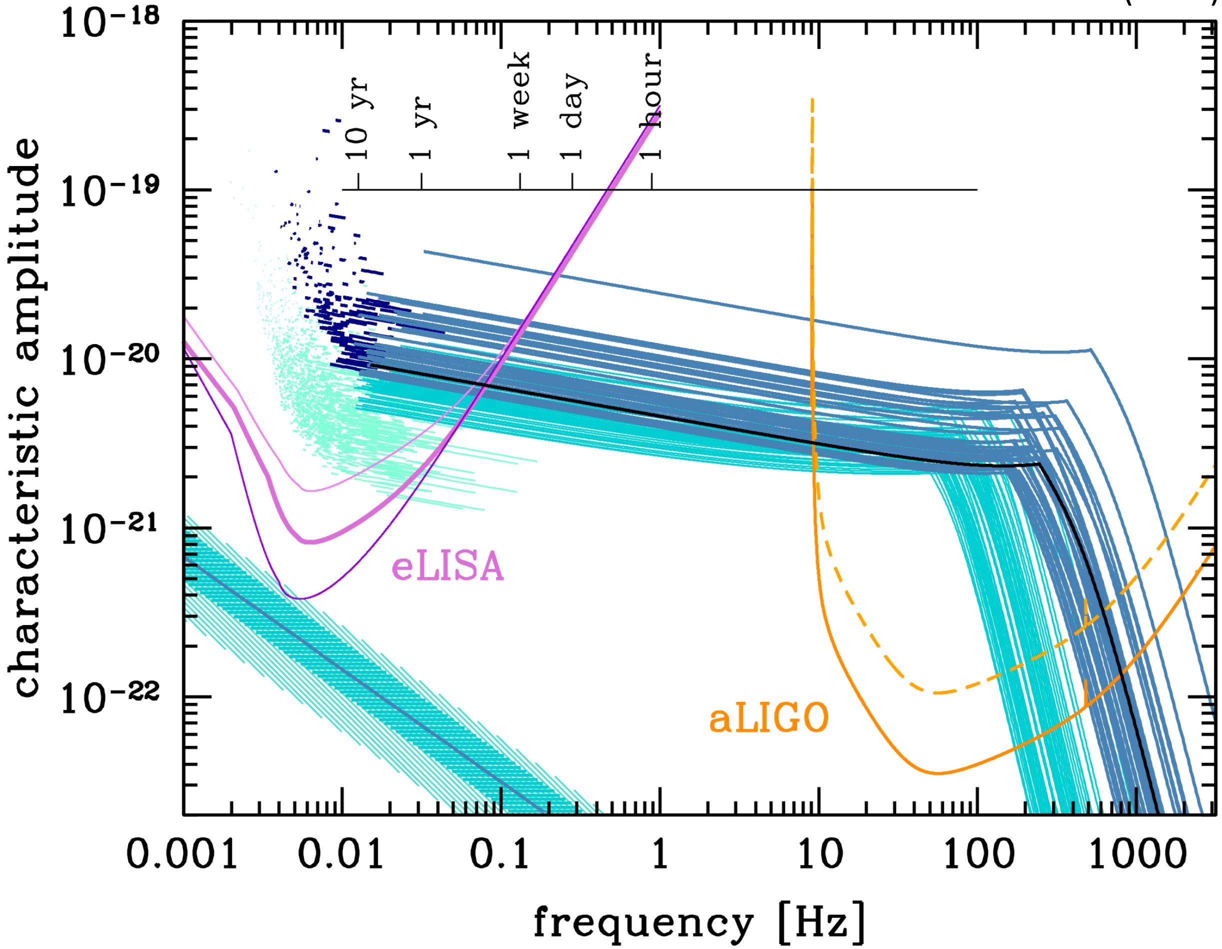

First calculations of stable mass transfer from a WD to a NS

(Sengar, Tauris, Langer & Istrate 2017), MNRAS Letters

Tauris (2018), PRL

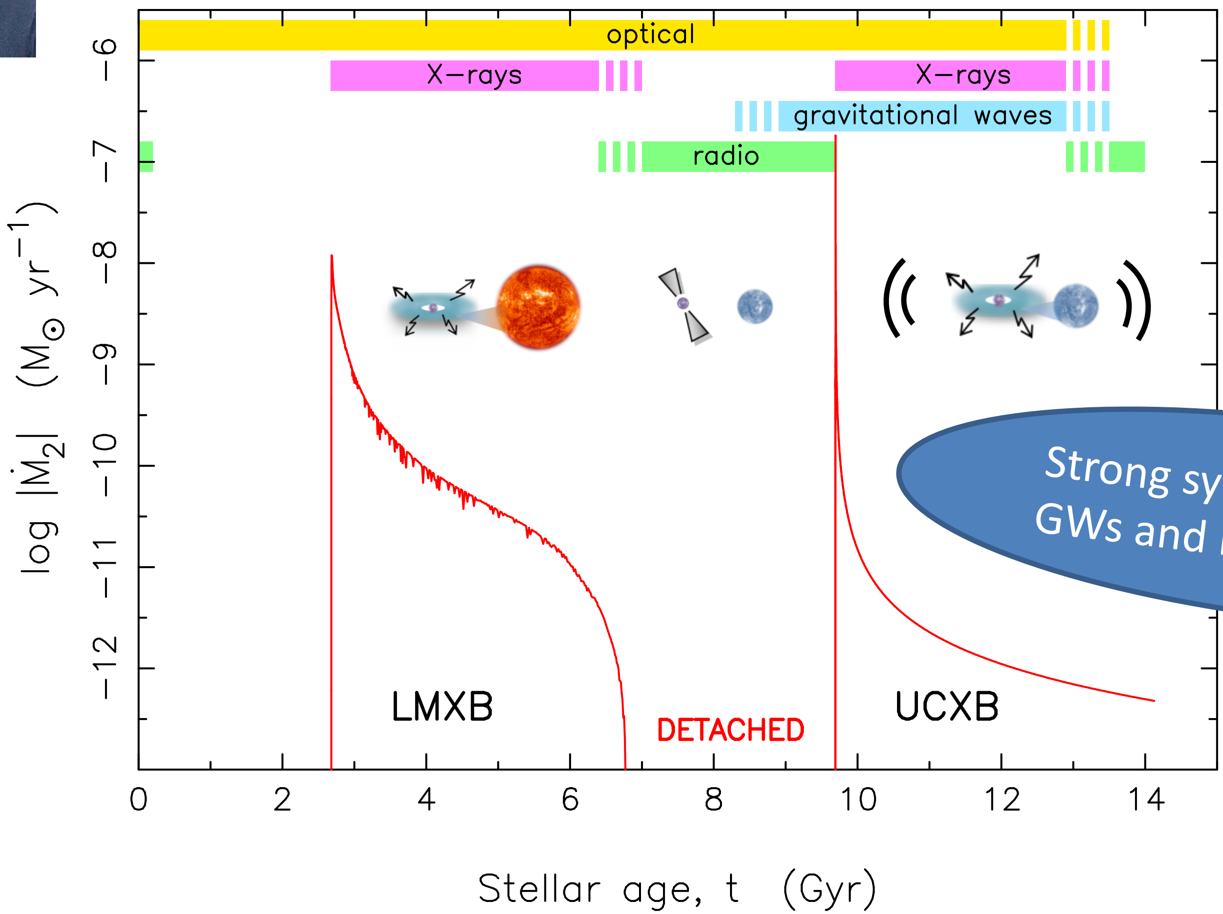

Strong synergies between GWs and EM observations

Tauris (2018), PRL

GW spectrum evolution

with finite-temperature effects (specific entropy) of the WD donor

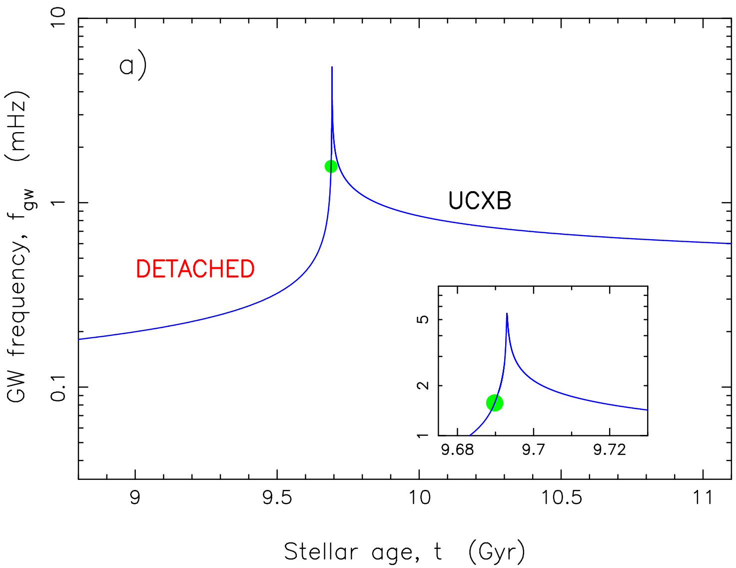

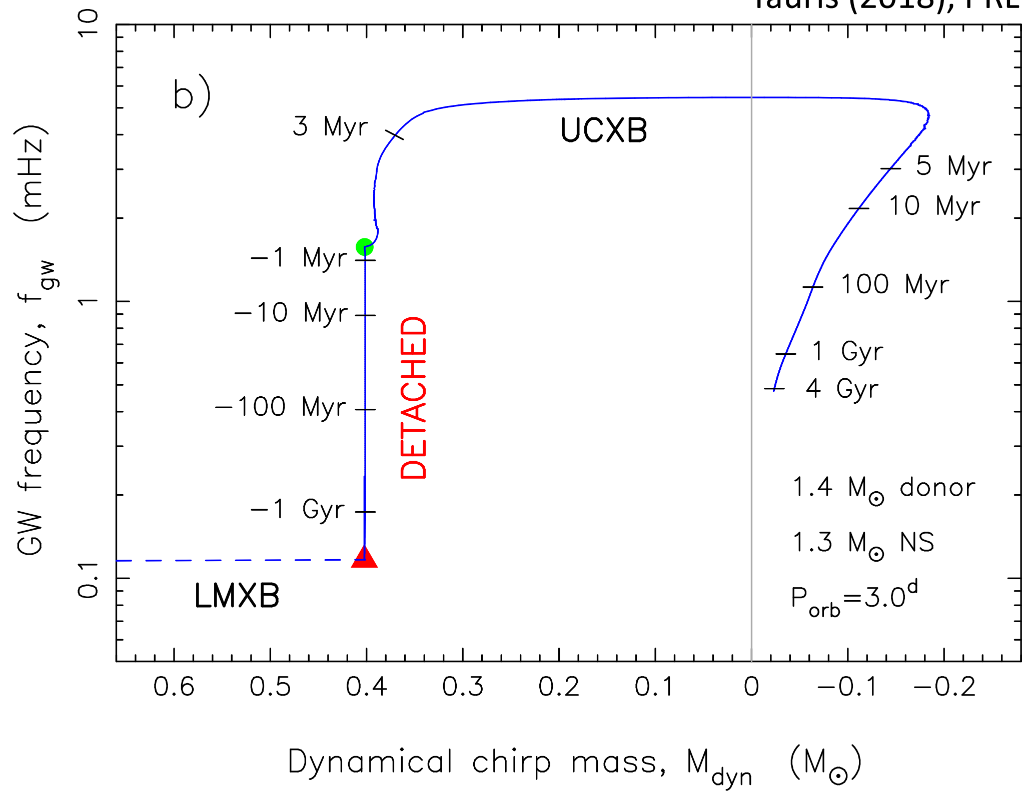

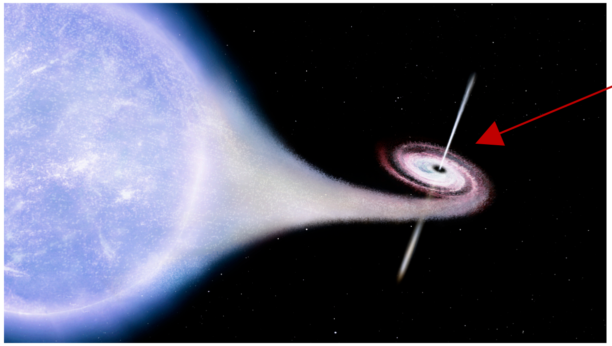

Determine NS the mass to a high accuracy via a new method

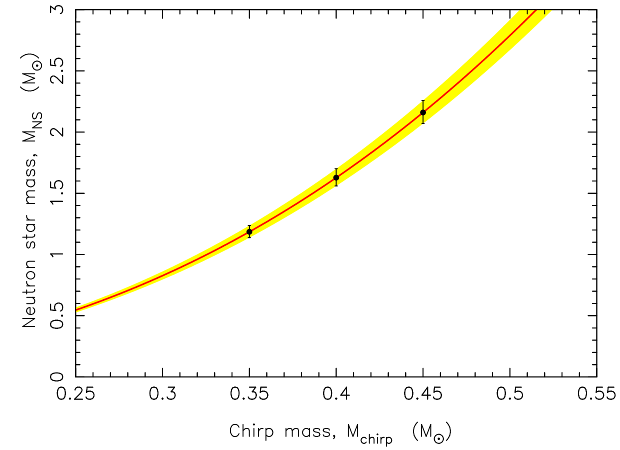

Tauris (2018), PRL

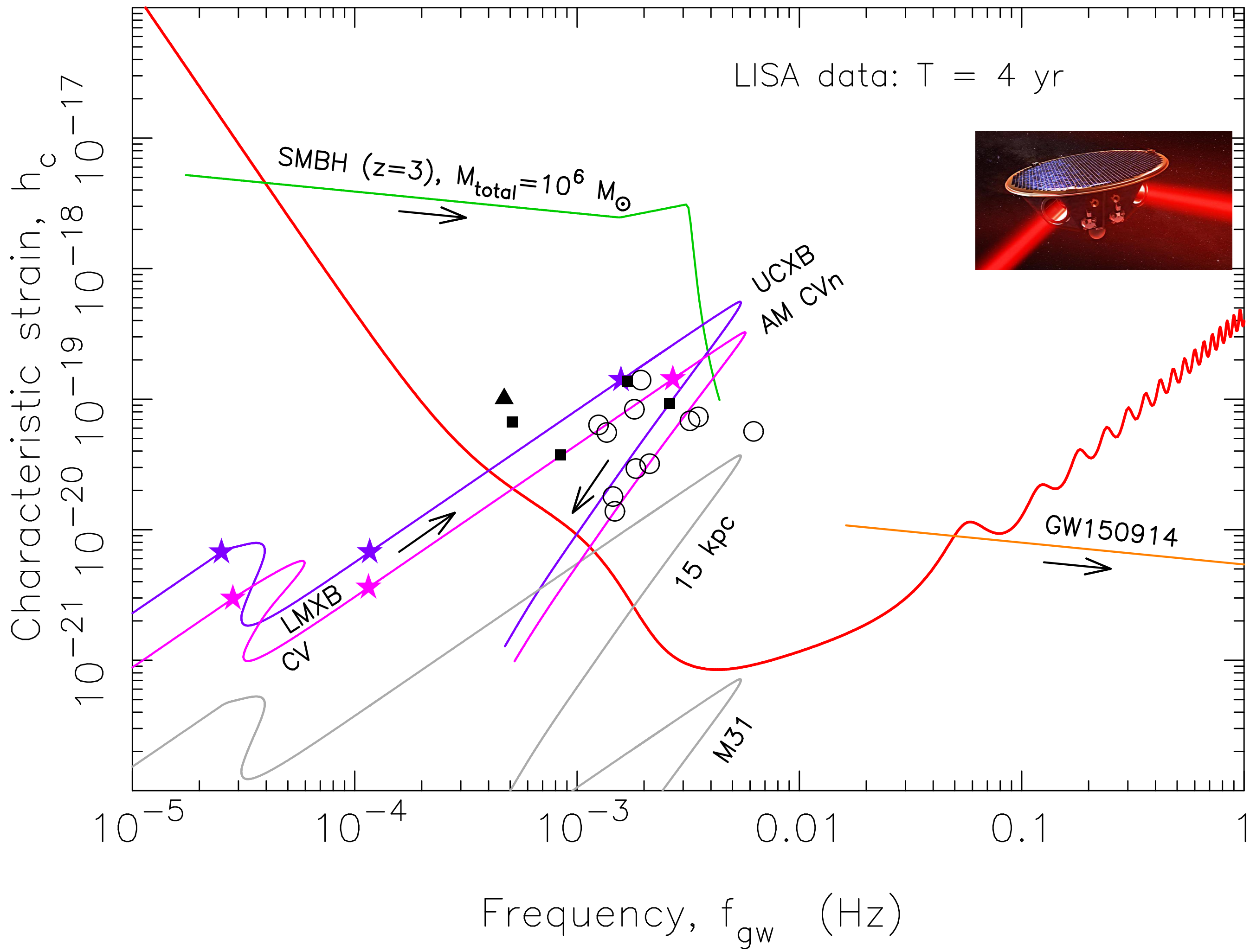

$$h_c \approx \sqrt{N_{cycles}}\,\sqrt{2}\,h_0 = \sqrt{2 f_{gw} T_{obs}}\,h_0 \qquad h_0 = \sqrt{\frac{32}{80}}\,\frac{\pi^{2/3} G^{5/3} f_{gw}^{2/3} M_{chirp}^{5/3}}{c^4\, d_L}$$

Discovery of a ***dual-line*** GW binary

Tauris (2018), PRL

$$I_{zz}\,\varepsilon = \sqrt{\frac{32}{80}}\;\pi^{-4/3} G^{2/3} f_{gw}^{-4/3} M_{chirp}^{5/3} \left(\frac{h_{spin}}{h_{orb}} \right)$$

LIGO

LISA

Independent on the distance to the binary